

**CHARACTERIZATION
OF GLUCOSE STARVATION TRIGGERED
TRANSCRIPTIONAL MEMORY**



Dissertation
DER FAKULTÄT FÜR BIOLOGIE
DER LUDWIG-MAXIMILIANS-UNIVERSITÄT
MÜNCHEN

Jessica A. Pellegrino

February 2020

Research Completed at the Helmholtz Center Munich

German Research Center for Environment and Health (GmbH)

Institute of Functional Epigenetics

Date of Submission: February 18th, 2020

First Examiner: Prof. Dr. Robert Schneider

Second Examiner: Prof. Dr. John Parsch

Date of Oral Examination: September 17th, 2020

Eidesstattliche Erklärung

Ich versichere hiermit an Eides statt, dass die vorliegende Dissertation von mir selbstständig und ohne unerlaubte Hilfe angefertigt ist.

Erklärung

Hiermit erkläre ich, dass die Dissertation nicht ganz oder in wesentlichen Teilen einer anderen Prüfungskommission vorgelegt worden ist.

Ich erkläre weiter, dass ich mich anderweitig einer Doktorprüfung ohne Erfolg nicht unterzogen habe.

Jessica A. Pellegrino

München, February 2020

Summary

In order for cells to maintain their intended state, such as a neuron, skin or immune cell, they must express certain genes while repressing others. In addition to maintaining cellular identity, cells must sense and react to environmental changes. This transcriptional memory can arise from a response to a repeated stimulus, for example nutrient deprivation, when a cell “remembers” the challenge and adapts its reaction to cope with it. Our research aims to determine if glucose starvation can convey transcriptional memory in human liver cells and how this memory is maintained in repeated starvation responses.

Using the human hepatocarcinoma cell line, Huh7, we observe an increase in gene expression in response to subsequent glucose starvations. Using RNA-Seq, we identify 65 memory genes that show an increased expression in response to subsequent glucose starvations including PCK2, CHAC1, ASNS, SHMT2 and others. We observe enrichment of the transcription factor ATF4 at promoters of these memory genes in a starvation dependent manner by ChIP-Seq. The memory genes similarly exhibit a starvation dependent enrichment of histone marks H3K27ac, H3K9ac, and RNA Polymerase II serine 5, in addition to variable DNA-accessibility as measured by ATAC-Seq.

Zusammenfassung

Charakterisierung des durch Glukoseentzug erzeugt transkriptionelles Gedächtnis.

Damit Zellen, wie z.B. ein Neuron, eine Haut- oder Immunzelle, ihren beabsichtigten Zustand beibehalten können, müssen sie bestimmte Gene exprimieren und andere unterdrücken. Zusätzlich zur Aufrechterhaltung der zellulären Identität müssen die Zellen Veränderungen der Umwelt wahrnehmen und darauf reagieren. Dieses transkriptionelle Gedächtnis kann aus einer Reaktion auf einen wiederholten Reiz, zum Beispiel auf Nährstoffmangel, entstehen, wenn sich eine Zelle an die Herausforderung "erinnert" und ihre Reaktion darauf anpasst, um sie zu bewältigen. Unsere Forschung zielt darauf ab zu bestimmen, ob der Glukoseentzug das transkriptionelle Gedächtnis in menschlichen Leberzellen übertragen kann und wie dieses Gedächtnis bei wiederholten Entzugsreaktionen aufrechterhalten wird.

Mit Hilfe der menschlichen Hepatokarzinom-Zelllinie Huh7, beobachten wir eine Zunahme der Genexpression als Reaktion auf spätere Glukosentzugreaktionen. Mittels RNA-Seq, haben wir 65 sogenannte Gedächtnisgene identifiziert, die erhöhte Expression als Reaktion auf wiederkehrenden Glukoseentzug zeigen, darunter PCK2, CHAC1, ASNS, SHMT2 und andere. Die Gedächtnisgene zeigen eine Anreicherung des Transkriptionsfaktors ATF4 an den Genpromotoren, die abhängig vom Glukoseentzug ist. Die Gedächtnisgene zeigen auch eine vom Glukoseentzug abhängige Anreicherung der Histon-Marker H3K27ac, H3K9ac und RNA-Polymerase-II-Serin 5, zusätzlich zur veränderten DNA-Zugänglichkeit, die durch ATAC-Seq bestimmt wird.

Table of Contents

Summary	4
Zusammenfassung	5
Table of Contents	6
1 Introduction:	10
1.1 Epigenetic Regulation	11
1.2 Chromatin Structure and Histone Modifications	11
1.2.1 Histone Modifying Enzymes	13
1.2.2 Transcriptional Machinery and Transcription Factors	14
1.2.3 Enhancers	15
1.3 Transcriptional Memory and Epigenetic Inheritance	15
1.3.1 Mechanisms of Epigenetic Memory	16
1.3.1.1 DNA Methylation	16
1.3.1.2 Polycomb Group Proteins	17
1.3.1.3 Immune Memory	17
1.3.1.4 Histone Variants	19
1.3.1.5 Mitotic Bookmarking	19
1.3.2 Additional Examples of Memory	20
1.3.2.1 Yeast	20
1.3.2.2 Plants	20
1.3.2.3 <i>C. elegans</i>	21
1.3.2.4 <i>Drosophila</i>	21
1.4 Glucose Response	22
1.4.1 Exposure to High Glucose	22
1.4.2 Exposure to Low Glucose	23
1.4.2.1 Liver Metabolism and Gluconeogenesis	23
1.4.3 Cancer Cell Metabolism	24

1.4.4	UPR Response to Nutrient Stress _____	25
1.4.5	ATF4-Mediated Transcriptional Response to Stress _____	26
Hypothesis _____		28
Aims _____		28
2	Results _____	28
Aim I: Establish a Transcriptional Memory System and Candidate Genes _____		28
2.1.1	Kinetics of Glucose Starvation in Huh7 cells and Identification of Memory Genes _____	28
2.1.2	Determination of Candidate Memory Genes Using Literature Review and qPCR Screening. _____	33
2.1.3	RNA-Sequencing on 3x Glucose Starvation to Screen for Memory Genes. _____	37
Aim II: Characterization of Memory Gene Classifications _____		42
2.1.4	Pathway Analysis _____	42
2.1.5	Transcription Factor Motifs _____	43
2.1.6	Autophagy and Circadian Rhythm _____	45
2.1.7	Cell Cycle _____	46
2.2	Primary Liver Hepatocyte Cell Response to Glucose Starvation _____	48
2.3	ATF4 is Necessary for the Expression of a Subset of Memory Genes. _____	50
2.3.1	ATF4 Expression in Response to Starvation _____	50
2.3.2	siRNA Knockdown of ATF4 _____	52
2.3.3	ATF4 Inhibitor ISRIB _____	53
2.3.4	Gene Expression Kinetics for ATF4 Responsive Memory Genes _____	54
2.3.5	Endoplasmic Reticulum (ER) Stress Effect on Memory _____	55
Aim III: Investigate the Mechanism Responsible for Transcriptional Memory _____		57
2.3.6	The Role of Transcription Factor CEBPG on the Expression of Memory Genes _____	57
2.3.7	The Behavior of Pre-spliced, Nascent RNA During Glucose Starvation _____	58
2.3.8	Mass Spectrometry of Histone Modifications _____	59
2.3.9	Modulation of Epigenetic Modifications by Small Molecules to Perturb Memory. _____	60
2.3.10	Chromatin Immunoprecipitation to Profile Behavior at Memory Genes _____	63
2.3.10.1	ChIP qPCR Optimization _____	63

2.3.10.2	ChIP- Seq Time Course	64
2.3.10.3	The Role of Enhancers in Memory Gene Regulation	68
2.3.11	DNA Accessibility During Glucose Starvation by ATAC-Seq	70
3	Discussion	72
3.1	Notable Topics Concerning Memory Experimental Model	72
3.1.1	RNA Transcript Accumulation	72
3.1.2	Huh7 Cells have Incomplete Gluconeogenesis Machinery	73
3.1.3	Correlating Memory Genes to Cell Cycle	73
3.1.4	Additional Models for Studying Memory	73
3.1.5	The Absence of Memory in our Experiments	74
3.2	Starvation Response and Memory	75
3.2.1	The Role PEPCK in Cancer Cells	75
3.2.2	Memory Genes Regulating Acetyl-CoA	76
3.2.3	The Role of Amino Acid Metabolism in Memory	77
3.2.4	The Role of ATF4 in Memory	79
3.3	Possible Mechanisms of Memory	79
3.3.1	Role of DNA Methylation	79
3.3.2	Role of Histone Modifications in Memory	80
3.3.2.1	Data Analysis Strategy and Limitations	80
3.3.2.2	Enhancers	81
3.4	Future Outlook	81
4	Materials and Methods	83
4.1	Cell Culture	83
4.1.1	Cell Line Culture	83
4.1.2	Primary Hepatocyte Culture	83
4.1.3	siRNA Knockdown	84
4.2	Transcription	84
4.2.1	RNA Extraction	84

4.2.2	cDNA Synthesis	84
4.2.3	qPCR- Quantitative Real Time PCR	85
4.3	Fluidigm BioMark and Singular Single Cell qPCR	85
4.4	RNA-Seq	85
4.5	Protein	86
4.5.1	Protein Extraction	86
4.5.2	RIPA Extraction	86
4.5.3	Western Blot	87
4.5.4	Fixation of Cells and Immunofluorescence	87
4.6	Chromatin Immunoprecipitation (ChIP)	88
4.6.1	ChIP Seq Library Preparation	90
4.7	ATAC seq	92
Materials		96
4.8	Antibodies	96
4.9	Consumables	97
4.10	Buffers	101
4.11	Primers	104
4.11.1	Human Expression Primers	104
4.11.2	Mouse Expression Primers	106
4.11.3	Human ChIP Primers	107
4.11.4	ATAC-Seq Primers	108
Abbreviations		110
Bibliography		114
Appendix		127
	Acknowledgements	127

1 Introduction:

In order for cells to maintain their intended state, for example as a neuron, a skin cell or an immune cell, they must maintain expression of certain genes, while repressing others. Cells also need to sense and react to changes in their environment while maintaining and remembering their cellular identity. So called transcriptional memory can result from these responses to environmental stimuli, when a cell “remembers” that a gene had been on or off before and is thereby able to adapt its reaction to a repeated stimulus. Some examples of environmental challenges linked to transcriptional memory are e.g., temperature, nutrients, oxygen availability, biochemical composition, mechanical forces or other stressors. The concept that cells can remember epigenetic states is reported in multiple organisms (D'Urso and Brickner 2017). Many incidences of transcriptional memory have been described in *Drosophila* (Francis and Kingston 2001), yeast (Brickner 2009; Kundu and Peterson 2009), and mammals (Foster, Hargreaves, and Medzhitov 2007; Medzhitov 2007) (Natoli and Ostuni 2019). A transcriptional memory that is controlled by epigenetic mechanisms is referred to as epigenetic memory. In some cases, the terms transcriptional memory and epigenetic memory are used as synonyms, although this is not always applicable.

My research aims to identify a novel model of transcriptional memory in mammalian cells and investigate its mechanism, namely within an epigenetic framework. I hypothesize that cellular stress, resulting from a lack of glucose in human liver hepatocarcinoma cells, will trigger the expression of a specific set of genes which will then respond to an additional glucose starvation in an adaptive manner. In my research, I have identified a subset of glucose starvation responsive genes in the hepatocarcinoma cell line, Huh7, that exhibit a higher level of expression in a second, and sometimes a third, round of glucose starvations. These genes, I call “memory genes,” consist of 65 genes whose

expression is significantly higher in a second exposure to glucose starvation conditions, while their expression returns to basal levels when refed with glucose. Upon analysis of this group of memory genes, I observed an overrepresentation of the transcription factor ATF4, as well as distinct enrichment patterns of histone modifications at these genes. In conclusion, I have comprehensively characterized a set of glucose starvation responsive memory genes.

1.1 Epigenetic Regulation

For organisms, the ability to sense and react to their environments is essential for the survival and propagation of the individual, as well as the population in general. This response results in the expression of genes and often these responses must be maintained, and, in some cases, passed on to offspring. When the mechanism of this maintenance is not transmitted by changes in DNA, it is regarded as epigenetically regulated. In his landmark publications in 1942, Conrad Waddington argued that adaptive responses of an organism to an environmental stimulus cannot be conveyed by solely genetic mutation, but rather that an adaptive response can occur that “mimics the response well enough to enjoy a selective advantage” (Waddington 1942), consequently coining the term “epigenetics” (Waddington 2012). Over the past twenty years, the scope of our knowledge in the field of epigenetics has vastly expanded (Allis et al. 2015) providing insight, on a cellular level, to how organisms transduce genetic information without changing their DNA sequence (Allis and Jenuwein 2016).

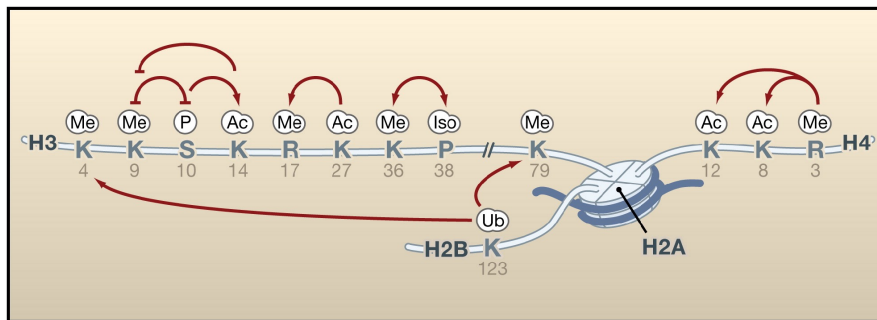
1.2 Chromatin Structure and Histone Modifications

The compaction of the approximately 2 meter long length of DNA within the cell's nucleus is carried out by folding of the genomic DNA, packaged around a nucleosomal core

particle, in a structure collectively referred to as chromatin. (Jenuwein and Allis 2001). The nucleosome consists of an octamer of core histones made up of two of each H3, H4, H2A, and H2B histones, around which the DNA is coiled, as well as an H1 linker histone. Protruding from the nucleosome are histone tails, which are charged amino-terminal tails that are exposed and subject to posttranslational modifications (PTMs) including lysine and arginine methylation, lysine acetylation, serine phosphorylation, and ubiquitination (Turner 2002). The information stored in the combination of these modifications of the histone tails serves as an epigenetic marking system, coined the “histone code” (Jenuwein and Allis 2001), that regulates the behavior of genomic material. Histone modifications can also result in a change in the net charge of nucleosomes that can loosen DNA-histone interactions, as well as having a direct influence on higher order chromatin structure, resulting in a disruption in DNA compaction (Li, Carey, and Workman 2007).

While the most well studied of the histone modifications are located at the amino-terminal tails, modifications on the globular domains of histones, which form the core of the nucleosome (Lawrence, Daujat, and Schneider 2016), also occur. While these globular domain modifications have gained importance in recent years, we will focus on modifications on lysines of the H3 tail, namely acetylation of lysine 9 (H3K9ac) and lysine 27 (H3K27ac) and mono- and di-methylation of lysine 4 (H3K4me1/me3) and lysine 27 (H3K27me3). The histone marks H3K9ac, H3K27ac, and H3K4me1/me3 are classified as active histone marks because their enrichment correlates in an increase in gene expression while H3K27me3 is considered as a repressive mark. (Li, Carey, and Workman 2007). In addition to acetylation and methylation on lysines of H3, histone modifications can also include acetylation and methylation on other histones, as well as phosphorylation and ubiquitination (Figure 1). Several additional acylations have been recently uncovered such as propionylation, butyrylation, crotonylation, succinylation, and lacylation (Barnes,

English, and Cowley 2019) (Zhang et al. 2019). Another distinct feature of histone regulation is the existence of histone variants that are protein isoforms of canonical histones. These variants can replace canonical histones to cause specialized outcomes to affect cellular processes (Venkatesh and Workman 2015).



Chromatin Modifications	Residues Modified	Functions Regulated
Acetylation	K-ac	Transcription, Repair, Replication, Condensation
Methylation (lysines)	K-me1 K-me2 K-me3	Transcription, Repair
Methylation (arginines)	R-me1 R-me2a R-me2s	Transcription
Phosphorylation	S-ph T-ph	Transcription, Repair, Condensation
Ubiquitylation	K-ub	Transcription, Repair
Sumoylation	K-su	Transcription
ADP ribosylation	E-ar	Transcription
Deimination	R > Cit	Transcription
Proline Isomerization	P-cis > P-trans	Transcription

Figure 1: Overview of Common Histone Modifications.

Adapted from Kouzarides, T. 2007. Chromatin modifications and their function, Cell, 128: 693-705.

1.2.1 Histone Modifying Enzymes

The next step in the investigation of the histone “code” is to understand how histone modifications are deposited on histone tails. The regulation of these post translational modifications is accomplished by specific enzyme classes responsible for either depositing histone marks or removing them, so-called histone “readers” or “erasers”. Histone acetyltransferases and methyltransferases are the enzymes responsible for depositing acetyl or methyl marks, respectively, while deacetylases and demethylases

remove them. (Kouzarides 2007) (Berger 2002). The discovery and understanding of the role of these enzymes in cellular processes has been critical, as many of these enzymes are members of protein complexes, thus the inclusion of a histone modifying component within these complexes provides an entirely new insight into the role of a complexes.

1.2.2 Transcriptional Machinery and Transcription Factors

The transcription of RNA from a DNA template is a fundamental event in the function of a cell. Transcription in eukaryotes is carried out by the enzyme RNA polymerase II (RNA Pol II). Along with elements called transcription factors (TFs) that recognize common promoter sequences, respond to regulatory factors and conformational changes, RNA Pol II can initiate gene transcription in a controlled manner. RNA Pol II mediated transcription involves the assembly of the pre-initiation complex (PIC), activation of the PIC, initiation, promoter clearance, elongation and finally, termination. (Roeder 1996) (Hahn 2004). Transcriptional initiation occurs after RNA Pol II is recruited to the gene promoter and the initiation factor, TFIIF, which phosphorylates serine 5 (S5) on the C-terminal domain (CTD) of RNA Pol II. In order for RNA Pol II to be released and transcriptional elongation to occur, serine 2 (S2) needs to be phosphorylated by P-TEFb, allowing for the transcriptional of the DNA template. (Sims, Belotserkovskaya, and Reinberg 2004)

Transcription factors (TF) are essential for the regulation of gene expression, as they exert control over the specification of cell types and developmental patterning, as well as pathway control. By definition, TFs regulate gene transcription through binding of DNA in a sequence specific manner (Lambert et al. 2018). These sequence specific domains are referred to as motifs, consisting of a short sequence of DNA at which a particular TF preferentially binds to. (Lambert et al. 2018) The variety of ways TF motifs regulate gene

expression is vast, including the combinatorial binding of TFs, context specific TF binding, feedback loops, and additional mechanisms, creating a connectivity within regulatory networks (Gerstein et al. 2012) that is still being uncovered as more experimental and data mining techniques are developed to address these unknowns.

1.2.3 Enhancers

In order for transcription to proceed, RNA Pol II machinery must be assembled at the transcription start site (TSS), though additional regulatory DNA elements called enhancers. Enhancers are often required to improve transcription levels and can be located further from the TSS (Catarino and Stark 2018). Enhancer sequences are short DNA motifs at which transcription factors can bind, that recruit co-activator and co-repressors which regulate enhancer activity. These enhancer regions are typically nucleosome-free regions that contain a characteristic histone modification signature, notably enrichment of H3K4me1 and H3K27ac (Shlyueva, Stampfel, and Stark 2014). Enhancer function has been implicated in models of epigenetic memory in non-dividing cells, specifically in the memory of stimulus responsive genes in repeated macrophage stimulation. Enhancers were observed to remain in a poised state, even during the removal of the stimulation, allowing for a faster and stronger response upon restimulation, as marked by enrichment of specific histone modifications and TFs (Ostuni et al. 2013).

1.3 Transcriptional Memory and Epigenetic Inheritance

Heritable changes in gene expression or behavior that are induced by a previously encountered stimulus have been regarded as epigenetic memory, in contrast to a more dynamic regulation of gene expression (D'Urso and Brickner 2014). Epigenetic memory

has also been described as a mechanism by which cellular identity is maintained through successive cells cycles during development and differentiation (Kim and Costello 2017). Furthermore, epigenetic memory can be expanded to include epigenetic inheritance across generations, also referred to as trans- or inter-generational inheritance, whereby a phenotype is generated in response to a stimulus in the parental generation and that response mechanism is propagated to the offspring, in absence of the initial stimulus, and independent to a change in the DNA sequence (Campos, Stafford, and Reinberg 2014). The ability of epigenetic memory to communicate information to newly divided cells or to the next generation offspring is a seemingly quick process in contrast to the more complex mechanism and irreversible means to convey information through a change in the DNA sequence.

1.3.1 Mechanisms of Epigenetic Memory

1.3.1.1 DNA Methylation

A well categorized mechanism of epigenetic memory is through DNA methylation, especially in stem cells and cancer cells. DNA methylation is a stable epigenetic mark that can be inherited through multiple cell divisions that mediated by DNA methyltransferase enzymes (DMNTs). DNA methylation mainly occurs at CpG rich sites, though not exclusively (Bird 2002). While DNA hypermethylation of tumor suppressor genes causes their repression in cancer cells (Ohm et al. 2007), conversely, hypomethylation of the cancer genome is observed in many cancer cell types (Kim and Costello 2017). Furthermore, DNA methylation has been described to play an important role in maintaining cell type specificity after differentiation, as it can also act as a barrier to cellular reprogramming (Kim and Costello 2017). Interesting new research performed on induced pluripotent stem (iPS) cells reported that iPS cells retained a transcriptional memory of their cell line of origin, resulting in expression of somatic genes that could be

partially explained by incomplete promoter DNA methylation (Tian et al. 2016). These findings highlight the persistence of DNA methylation as a mechanism of epigenetic memory.

1.3.1.2 Polycomb Group Proteins

Polycomb group proteins (PcG) have also been confirmed to play a role in epigenetic memory in mammals, namely in development. It has been shown that components of the Polycomb repressive complex 1 (PRC1) that are derived from maternal genomes are transferred to the paternal genome after fertilization in early embryos. This transfer of proteins points to a direct effect from maternal heterochromatin on the silencing of genes in the zygote (Puschendorf et al. 2008) (Daxinger and Whitelaw 2012). The Polycomb repressive complex 2 (PRC2) has been shown to regulate paternal repression of imprinted gene domain in extra-embryonic tissue through acquisition of H3K27me3 and H3K9me. In cancer cells, PRC2 regulates an H3K27me3 mediated repression of tumor suppressive genes in conjunction with DNA hypermethylation, observed in embryonic cancer cells and maintained in adult cancer cells (Ohm et al. 2007).

1.3.1.3 Immune Memory

The immune system in mammals displays a wide variety of memory mechanisms to respond to challenges. In their review of immune memory response, Natoli and Ostuni delineate between immunological adaptation and immune memory (Figure 2).

	Adaption	Memory
Reversibility	Yes	No
Persistence	Short term or long term	long term
Specificity	No	Yes
Mechanisms	Receptor signaling/recycling	DNA sequence alterations
	Chromatin/histone modification	Epigenetic modifications (DNA methylation)
	Metabolic reprogramming	Self-sustaining feedback loops
	TF occupancy/distribution	Induction of long-lived mediators
Target cells	Innate, adaptive immune cells Adaptive immune cells Non-immune cells	Adaptive immune cells

Figure 2: Properties of Adaptation and memory in Immune System
Adapted from Natoli, G. and R. Ostuni 2019. "Adaptation and memory in immune responses." *Nat Immunol* 20(7): 783-792.

They describe immune memory as an ability to remember a first encounter and mount a more rapid and stronger second response, as a result of irreversible changes on the DNA sequence accompanied with self-sustaining feedback loops and additional epigenetic regulations. Whereas an immunological adaption refers to when an environmental stimulus influences future responses to the same, or another, stimulus. Notably, such adaptations are reversible, however the adaptive response may persistent over long periods of time or multiple stimulus exposures (Natoli and Ostuni 2019). An adaptive immune response to lipopolysaccharide (LPS) stimulation in macrophages, during which an initial challenge of LPS induces a robust genes expression program and is proceeded with a challenge of a second LPS stimulation. A subset of the responsive genes expresses more rapidly and at a higher level, and are thus designated “tolerized” to denote their increased tolerance to transcription (Foster, Hargreaves, and Medzhitov 2007). Macrophages and fibroblasts pretreated with interferon- γ (IFN- γ) acquire an adaptive memory exhibited by a faster and increased level in expression in a second exposure to IFN- γ . The memory can be attributed to a faster and greater recruitment of RNA Pol II and phospho-STAT1, as well as an acquisition of histone H3K36me3 and variant H3.3 enrichment (Kamada et al. 2018), revealing a clear epigenetic regulation of the memory response.

1.3.1.4 **Histone Variants**

Epigenetic memory mediated by histone variant H3.3 has also been described in experiments utilizing nuclear transfer (NT) to transplant a nucleus from endoderm cells into enucleated eggs to trace the expression of the endoderm specific marker *edd* in the resulting embryos. This endoderm specific marker was expressed in non-endoderm cells in the embryo, demonstrating an epigenetic memory for the endoderm lineage. The memory was maintained by an association of the histone variant H3.3 to the promoters of genes that exhibited a memory, i.e., active gene expression, (Ng and Gurdon 2008) thus marking the memory genes with H3.3

1.3.1.5 **Mitotic Bookmarking**

Finally, the recent discovery of mitotic bookmarking as a means of conveying transcriptional memory via advancements of experimental techniques has demonstrated that despite the assumption that most genes are transcriptionally silent during mitosis, there is, in fact, a low level of transcription occurring. Data suggests that promoter architecture is permissive in mitotic chromatin which allows for the low level of transcription and a more open chromatin state at promoters thereby creating a state of transcriptional readiness to allow for a robust re-expression of genes at mitotic exit, maintaining the memory of transcription through mitosis. Researchers have postulated that a retained enrichment of H3K27ac during mitosis might serve to bookmark memory genes during mitosis (Palozola, Lerner, and Zaret 2019).

1.3.2 Additional Examples of Memory

1.3.2.1 Yeast

Transcriptional memory is a type of memory that conveys a response to environmental stimuli through mitotically heritable changes which modify a cell's responsiveness to the same stimulus in subsequent exposures to that stimuli, resulting in a more rapid or robust transcriptional response (D'Urso and Brickner 2014). A well characterized example of transcriptional memory occurs in budding yeast, *Saccharomyces cerevisiae*, in response to differences in nutrient sources on the GAL network of genes. Genes in the GAL network robustly respond to the present of galactose as the carbon source during growth, whereas GAL genes are repressed in the presence of glucose. When yeast cells are previously exposed to galactose, switched to glucose media for repression, and then re-exposed to galactose, they display a reinduction memory in which GAL genes induce more quickly upon re-exposure to galactose (Stockwell, Landry, and Rifkin 2015). The ATP-dependent chromatin remodeler, SWI/SNF has been shown to be essential for transcriptional memory in experiments with short term repression of one hour (Kundu and Peterson 2009.)

1.3.2.2 Plants

Several examples of epigenetic memory exists in *Arabidopsis* plants, namely in response to stress (Lamke and Baurle 2017). Vernalization is a process during which plants remember cold temperatures and respond by flowering earlier. Vernalization results in changes in H3K9 and H3K27 methylation on the FLC gene locus, mediated by cold-activated polycomb group complexes and non-coding RNAs, which allow the plant to remember that it has been exposed to cold (Bastow et al. 2004). Similarly, the stress of recurring dehydration in *Arabidopsis* results in an increase in the rate of transcription of stress-induced genes that return to basal levels of transcription in watered conditions,

though in these conditions enrichment of H3K4me3 and RNA Pol II S5 remains high. The stalling of RNA Pol II on stress-induced genes indicates the genes are primed for robust transcription under repeated dehydration conditions (Ding, Fromm, and Avramova 2012).

1.3.2.3 *C. elegans*

Mitochondrial stress results in a transcriptional memory in *C. elegans* by causing changes in chromatin structures through H3K9me2 histones marks, traditionally associated with gene silencing through the activity of its methyltransferase met-2 and the lin-65 cofactor which allow for an opening up of the chromatin to allow the binding of stress responsive factors to bind. This stress response is retained in the into adulthood (Tian et al. 2016) . In addition to histone marks, epigenetic memory transmitted by small RNAs has been shown to be transgenerationally inherited over several generation in *C. elegans* in response to a starvation induced developmental arrest and results in an increased lifespan of the offspring of the starved animals. (Rechavi et al. 2014)

1.3.2.4 *Drosophila*

In *Drosophila*, heat shock or osmotic stress induces a stress responsive phosphorylation of dATF-2 which disrupts heterochromatin. This disruption of heterochromatin is transmitted to the next generations, which retains this defective chromatin state (Seong et al. 2011) and is described as an epigenetic memory. Another well-known mechanism of epigenetic memory involves Polycomb-group proteins (PcG) which establish and maintain gene silencing and trithorax (trxG) group proteins which reverse gene silencing and activate gene expression (Schuettengruber et al. 2009). PcG genes have been described in their role in silencing of Hox genes during development,

along with the role *trxG* proteins have in maintaining Hox expression (Bantignies and Cavalli 2006). Besides these roles in gene regulation during development, PcG and *trxG* proteins have been reported to be involved in response to toxic stress through a reduction in PcG gene expression which results in the de-repression of regulators. This modified response phenotype is epigenetically inherited in subsequent generations of flies (Stern et al. 2012).

1.4 Glucose Response

1.4.1 Exposure to High Glucose

Recently, the concept of metabolic memory has gained traction due to increasing evidence that environmental factors associated with nutrient availability, such as hyperglycemia during diabetes, can result in misregulation of gene expression mediated by epigenetic mechanisms. Metabolic memory has been reported in cells exposed to high glucose. These cells experience a disrupted response in gene expression, which persists long after the hyperglycemic challenge is removed (Reddy, Zhang, and Natarajan 2015). Research has shown that when adipocytes are exposed to high glucose conditions, they upregulate a subset of inflammatory response genes whose promoter methylation patterns are altered to render those genes less repressed, suggesting that high glucose creates an epigenetic priming phenotype for these inflammatory response genes which leads to increased transcriptional response when challenged with high glucose conditions (Ronningen et al. 2015).

1.4.2 Exposure to Low Glucose

1.4.2.1 Liver Metabolism and Gluconeogenesis

Similarly, low glucose conditions in liver cells induces a robust transcriptional response. In mammalian livers, glucose enters the liver and is used to synthesize glycogen in the fed state in a process called glycolysis, while during periods of short term fasting, glycogen is used to generate glucose through glycogenolysis. However, during prolonged fasting, glycogen is depleted and the hepatocytes in the liver synthesize glucose utilizing the biosynthetic intermediates lactate, glycerol, amino acids, and pyruvate, which can be synthesized in the liver or delivered in the blood from other sources (Rui 2014). The key step in gluconeogenesis is the enzyme phosphoenolpyruvate carboxylase (PEPCK) converting oxaloacetate (OAA) to phosphoenolpyruvate (PEP). Before this can occur, mitochondrial OAA must become cytosolic by either conversion to PEP by mitochondrial phosphoenolpyruvate carboxylase (PEPCK-M), transamination of aspartate, or reduction of malate (Stark and Kibbey 2014) (Yang, Kalhan, and Hanson 2009). There are two isoforms for PEPCK, distinguished by their area of activity, cytosolic PEPCK-C (PCK1) and mitochondrial PEPCK-M (PCK2). Recent research has suggested that PEPCK-M can work alone, or with PEPCK-C, to improve gluconeogenic potential (Mendez-Lucas et al. 2013). Next, cytoplasmic OAA is converted to PEP by cytoplasmic phosphoenolpyruvate carboxylase (PEPCK-C) and after several biochemical reactions is converted into fructose 1,6-bisphosphate (F1,6P) which is then dephosphorylated by fructose 1,6 bisphosphatase (FBPase) to generate fructose-6-phosphate (F6P). F6P is converted to glucose-6-phosphate (G6P) then dephosphorylated to generate glucose (Rui 2014) (Fig 3). Liver metabolism is a highly regulated process and numerous transcription factors and coactivators, including CREBH, FOXO1, ChREBP, SREBP, PGC-1 α , CRTC2, and CBP/p300, have been

reported to control the expression of the enzymes and genes mediating its regulation (Oh et al. 2013).

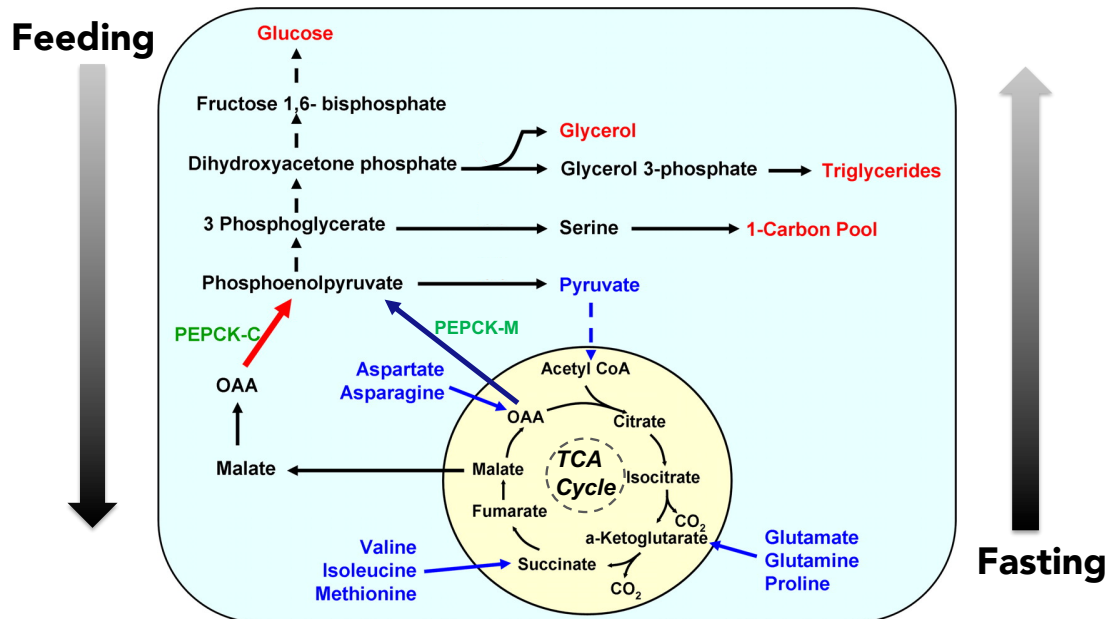


Figure 3 : Biosynthetic Pathway of Gluconeogenesis during Fasting in the Liver
Adapted from Yang, J., et al. 2009. "What is the metabolic role of phosphoenolpyruvate carboxykinase?" J BiolChem 284 (40): 27025-27029.

1.4.3 Cancer Cell Metabolism

It is well known that cancer cells have adapted to thrive in nutrient challenged conditions (Mayers and Vander Heiden 2015). Cancer cell metabolism is highly influenced by the availability of various fuel sources such as glucose, amino acids, fatty acids, acetate, and oxygen (DeNicola and Cantley 2015), resulting in the ability of cancer cells to adapt, overcome, and flourish in response to difficult conditions such as glucose deprivation. Recently, it has been shown that in some cancer cell types, including lung and colon, that PCK1 is not highly expressed, however PCK2 is expressed at elevated levels (Leithner et al. 2015; Vincent et al. 2015). This research has proposed that PCK2 is utilizing a portion of the gluconeogenic machinery to utilize tricarboxylic acid (TCA)-derived molecules to

generate fuel in low glucose conditions (Balsa-Martinez and Puigserver 2015), partially explaining the observed increase of PCK2 expression in many cancer cell types. Increased levels of PCK2 expression in prostate cancer cells is associated with more aggressive tumors and research has shown that PCK2 expression increases tumor initiation in cultured prostate cells by reduced production of citrate and acetyl CoA, thus lowering TCA cycle activity, suggesting “PCK2 is critical for the metabolic switch in tumor initiation” (Zhao et al. 2017). PCK2 expression is also elevated in MCF7 breast cancer cells during ER stress conditions and amino acid limitation, and has been shown to be mediated by transcription factor ATF4 through ATF4 recruitment to a consensus amino acid response element (AARE) sequence on the PCK2 promoter. This AARE sequence is also observed in other ATF4 mediated genes (Mendez-Lucas et al. 2014).

1.4.4 UPR Response to Nutrient Stress

The transcription factor ATF4 plays a major role in the endoplasmic reticulum's (ER) response to stress. Disruption of the homeostasis of the ER leads to ER stress, and subsequently activates the unfolded protein response (UPR) program to re-establish normal function in the ER. Stressors include hypoxia, amino acid deprivation, and glucose starvation, all of which activate one or more of the 3 branches of the UPR response pathway (Corazzari et al. 2017) (Fig 4 (Hetz et al. 2011)).

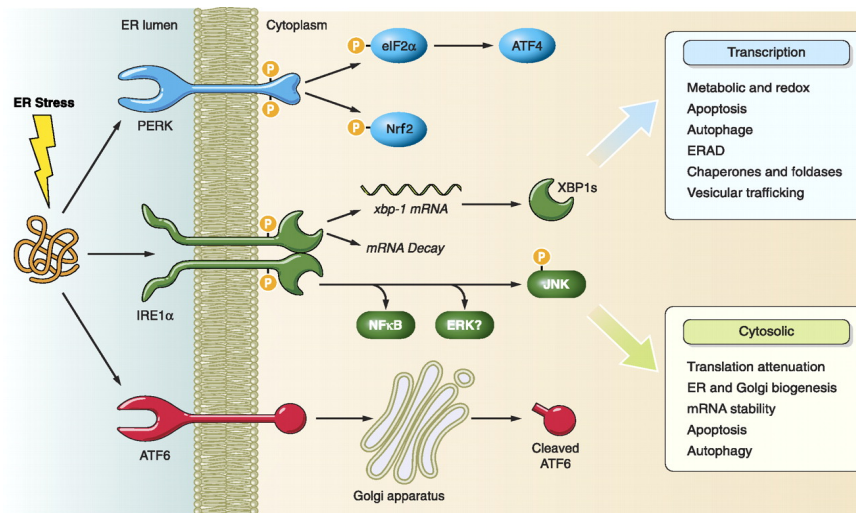


Figure 4: The unfolded protein response (UPR): Accumulation of misfolded proteins at the ER activate the UPR program.

Taken from Hetz, C., et al. 2011. "The unfolded protein response: integrating stress signals through the stress sensor IRE1 α ." *Physiol Rev* 91(4): 1219-1243.

Glucose starvation activates the PERK-eIF2 α -ATF4 branch of the UPR pathway in tumors (Wang and Kaufman 2014), cancer cell lines (Mendez-Lucas et al. 2014), and during gluconeogenesis (Rui 2014). Simply put, upon ER stress, PERK activates the phosphorylation of eIF2 α (eukaryotic initiation factor 2 α) which results in a decrease in translation of most mRNAs with select exceptions, notably ATF4 (Wang and Kaufman 2014). The increased translation of ATF4 is mediated by alternative reading frames (Lu, Harding, and Ron 2004). ATF4 then enters the nucleus to activate ER stress response genes to promote cell survival or activate apoptosis, depending on the kinetics of gene activation (Baird and Wek 2012).

1.4.5 ATF4-Mediated Transcriptional Response to Stress

Recently, a large scale multi-omics approach was used to characterize the effect of ER stress on ATF4 mediated gene expression in the reprogramming of cellular metabolism. Through analysis of the transcriptome, proteome, and metabolome of ER stressed HeLa cells, ATF4 was shown to induce the expression of cytoprotective genes

which led to a rewiring of cellular metabolism resulting in the synthesis of key metabolites, namely serine (Quiros et al. 2017). The heterodimerization of ATF4 with another TF, CEBPG, has been implicated in glutathione biosynthesis dysregulation. In response to oxidative stress, mouse embryonic fibroblasts (MEFs) express ATF4 stress responsive genes. When MEFs from CEBPG knockout mice were exposed to oxidative stress, there was a decrease in the expression genes specific for glutathione metabolism, though not other ATF4 stress-responsive genes, proposing the requirement of both ATF4 and CEBPG for their expression (Huggins et al. 2015), further fine-tuning ATF4 mediated gene regulation. Currently, new implications for the role of ATF4 in stress-induced responses are being uncovered in numerous biological contexts and with countless biological outcomes. Consequently, the clear role ATF4 plays in cancer cell metabolism in response to stresses (Wortel et al. 2017), such as glucose deprivation, makes ATF4 an intriguing member of our cast of transcriptional memory genes and interactors.

Hypothesis

Transcriptional memory can be triggered by nutrient deprivation, specifically glucose starvation, in mammalian cells leading to an adaptive response of the effected genes in future instances of the same nutrient deprivation.

Aims

The goal of my research project was to determine whether a transcriptional memory can be triggered by glucose starvation in mammalian cells. The first aim was to determine a suitable human cell line that is responsive to glucose starvation and evaluate whether the response to a second starvation results in an adaptive transcriptional outcome, hence a transcriptional memory. The second aim was to characterize this memory using next-generation sequencing techniques. The final aim was to gain insight into the underlying mechanism of glucose starvation mediated memory.

2 Results

Aim I: Establish a Transcriptional Memory System and Candidate

Genes

2.1.1 Kinetics of Glucose Starvation in Huh7 cells and Identification of Memory

Genes

We chose two human liver immortalized cell lines, Huh7 and HepG2, to test for transcriptional memory. The first experiment for both cell lines was to confirm optimum growth conditions based on published results and then to establish the kinetics for induction for our model system. To investigate glucose starvation conditions and kinetics,

we performed a time course comparing cells grown in optimal media conditions to cells grown in the same media in the absence of glucose over the course of 48 hours (Fig 1). Time points at 1, 2, 4, 8, 12, 18, 24, 36, and 48 hours were collected for RNA extraction and cDNA synthesis. Meanwhile, we compiled a list of relevant genes from literature searches to include genes involved in the gluconeogenic pathway for enzymes (G6PC, glucose-6-phosphatase; FBP1 Fructose-1,6-bisphosphatase; PC, pyruvate carboxylase; ALDOB, Aldolase B; KHK, Fructokinase; PCK1, Cytoplasmic Phosphoenolpyruvate Carboxylase; PCK2, Mitochondrial Phosphoenolpyruvate Carboxylase) and transcription factors (CREBH and FOXO1).

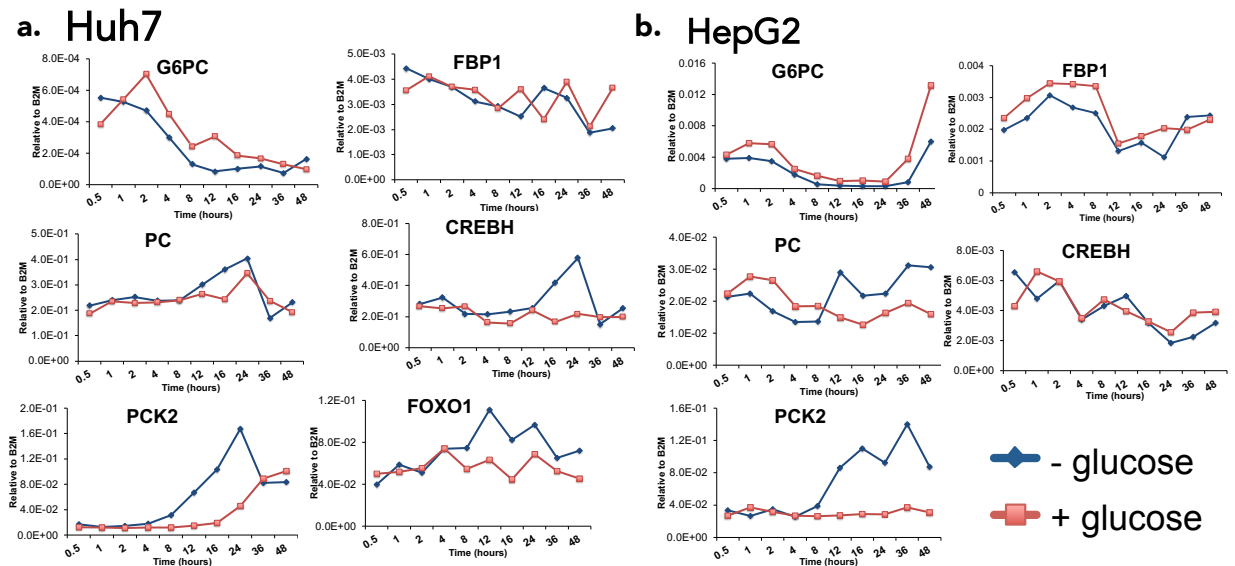


Figure 1: Time Course to investigate gene expression in response to glucose starvation. qPCR results for a) Huh7 and b) HepG2 cells in glucose containing, +glucose and glucose starved conditions, - glucose, expression data is normalized to control gene B2M, pilot experiment (n=1)

The genes that exhibited the strongest response to glucose starvation were PCK2 and CREBH, with maximum induction at the 18 or 24 hour time point (Fig 1a and 1b). While both cell lines showed a response to glucose starvation, HepG2 showed markedly lower expression of PC, ALDOB, CREBH and higher expression in KHK. As our goal was to study a model more closely following a gluconeogenic phenotype, we chose to focus on Huh7 cells for all subsequent experiments, focusing on PCK2 expression for establishing

our model. This cell line was established from a hepatocyte derived cellular carcinoma cell line that was originally taken from a liver tumor in a 57-year-old Japanese male (Nakabayashi et al. 1982).

Once we confirmed PCK2 as our model gene, we next determined when PCK2 returned to its baseline level of gene expression. This was accomplished by starving the cells for 24 hours then re-feeding the cells with Dulbecco's Modified Eagle's Media (DMEM) containing 25 mM glucose and collecting cells at the previously mentioned time points for RNA, cDNA and qPCR focusing on the expression of PCK2 and CREBH (Fig 2). Gene expression for PCK2 began to decrease at 2 hours and was back to basal levels between 18 and 24 hours. While PCK2 expression returns to its basal level at 18 hours, we have chosen 24 hours refeeding time, to allow for the cells to recover from the starvation and for some flexibility in the timing of other possible memory genes that have yet to be determined.

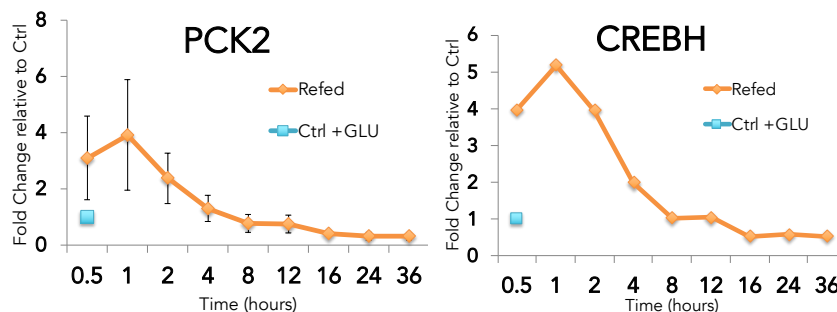


Figure 2: Refeeding Time Course to determine basal level of PCK2 (n=3, error bars-standard deviation) and CREBH (n=1) gene expression after glucose starvation. Expression levels are calculated as fold change relative to Huh7 cells grown exclusively in glucose containing media (Ctrl +GLU).

In order to assess whether PCK2 exhibited a transcriptional memory after repeated glucose starvation, we starved the Huh7 cells of glucose for 24 hours, re-fed them for 24 hours with glucose then performed a second round of glucose starvation. During this second round of starvation, we took RNA at time points at 2, 4, 8, 12, 24, and 36 hours post re-feeding (Fig 3). Since transcriptional memory has been described as an adaptative

response to a stimulus, whether it be a faster or slower transcriptional response or a higher or lower level of transcription in comparison to the initial response, we were interested in analyzing both the timing and level of expression in a second induction. In the 24 hour re-feeding and re-starve experiment, we observed higher PCK2 expression in the second starvation versus the first starvation (Fig 8a), though we did not observe faster induction in gene expression in the second starvation compared to the first. Thus, we will focus our memory model on a higher gene expression in subsequent inductions.

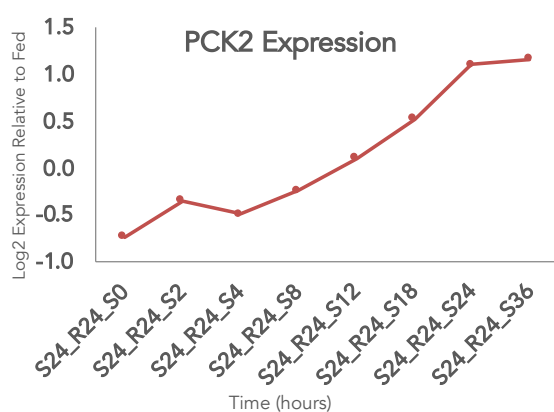


Figure 3: Second Starvation Time Course to determine kinetics of PCK2 gene expression after a second glucose starvation (S). Expression levels are calculated as Log2 expression relative to fed (R) condition.

Next, we wanted to confirm that we were using the optimal culture conditions to investigate cancer cell metabolism. Since cancer cells and primary cell often require different culture conditions for propagation, we tested several conditions. For our preliminary studies with Huh7 cells, the cells were grown and re-fed in 25mM glucose containing DMEM with 10% Fetal Bovine Serum (FBS), penicillin/streptomycin (pen/strep), and supplemented with L-Glutamine, sodium pyruvate (NaPyr), and nonessential amino acids (NEAA), then starved with Glucose-free DMEM, 10% FBS, pen/strep, and L-glutamine. To determine how the nutrient composition of the cell culture media may affect our target gene response, we tested different formulations of media, specifically investigating whether the cells are using other sources of fuel such as pyruvate or glutamine. First, we tested the 24 hours starve/24 hour fed/24 hour starve time course with a lower glucose concentration of 11mM, closer to a physiological “fed state” (Mayers

and Vander Heiden 2015), as a 25mM glucose concentration of glucose is considered “high glucose.” We observed little difference between 11mM glucose conditions and 25 mM glucose containing DMEM (Fig 4a). Next, we removed the sodium pyruvate in the 11mM glucose culture conditions and also saw little change when these cells were starved, therefore confirming 25mM glucose DMEM as our culture conditions (Fig 4b). We then wanted to determine if the sodium pyruvate and nonessential amino acid supplementation greatly affected gene expression and found it did not. To investigate whether composition of the glucose free DMEM starvation media affected gene expression, we tested media with no L-glutamine and NaPyr, and glucose-free DMEM with the addition of NEAA (Fig 4c). The non-essential amino acids include L-alanine, L-asparagine, L-aspartic acid, L-glycine, L-serine, L-proline and L-glutamic acid and have been reported to play a role in many biological processes such as biosynthesis of macromolecules and post translation and epigenetic modifications, notably in cancer (Choi and Coloff 2019) therefore they could have an effect on Huh7 cells. Neither condition showed a marked difference from the original culture conditions of glucose-free DMEM with L-glutamine and pen/strep. We continued our experiments with our preliminary culture conditions, as listed above.

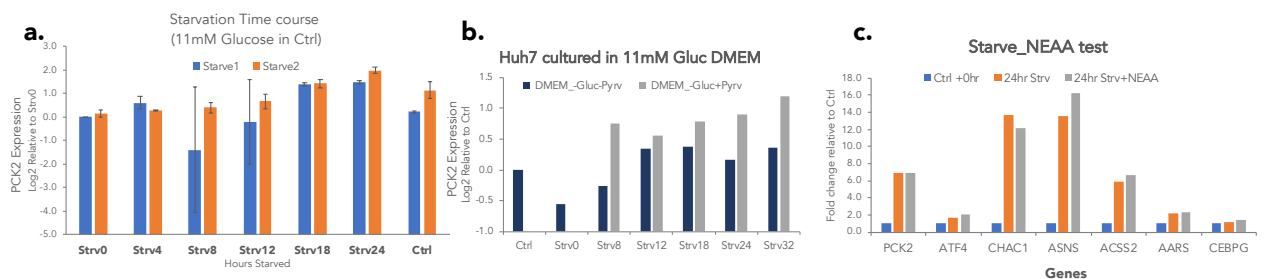


Figure 4: Cell Culture Condition Optimization. Huh7 cells were grown in DMEM with (a.) 11mM glucose (n=3, error bars are standard deviation) or (b.) 11mM glucose with or without sodium pyruvate supplemented in starved and fed conditions to look at the effect on PCK2 expression, Log2 fold change relative to Starve 0 time point. (c.) Cells were grown in the presence or absence of supplemented non-essential amino acid (NEAA) in starved condition and gene expression was measured as fold change relative to Control (Ctrl) for each gene.

starvation time course, we searched for genes that responded to glucose starvation. We also utilized the BioMark's ability to test 96 genes against 96 samples to determine which of the control genes ACTB, B2M, HPRT1, and TUBB show the least variation across glucose deprived time points. We observe B2M had the least variable expression (Fig 5a), therefore we can continue to use it as our control gene for our starvation experiments. Of the 96 genes we tested, we found several genes that respond to glucose starvation in Huh7 cells (Fig5b).

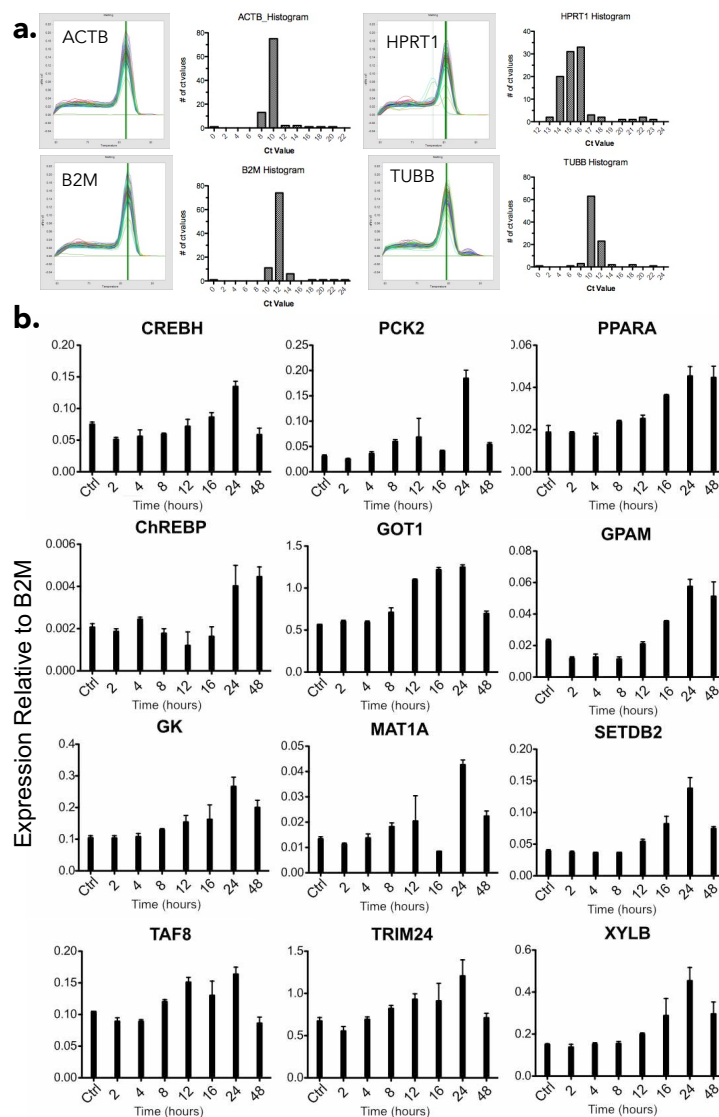


Figure 5: Fluidigm BioMark qPCR screening for candidate genes.

(a) Control genes were examined for uniform expression distribution across conditions and qPCR melt curve behavior.

(b) Glucose starved responsive genes determined by increased expression from control 2 hour glucose fed and glucose starved from 2 to 48 hours (error bars are technical replicates, n=3).

For next experiment with the BioMark, we wanted to determine when these genes returned to their baseline level of gene expression. This was accomplished by starving the cells for 24 hours then re-feeding the cells with glucose containing media and collecting cells at 12, 18, 24, 36 or 48 hours and subsequently (Fig 6). Of the 96 candidate genes, several genes showed their highest expression at 24 hours with a decrease of expression following glucose feeding.

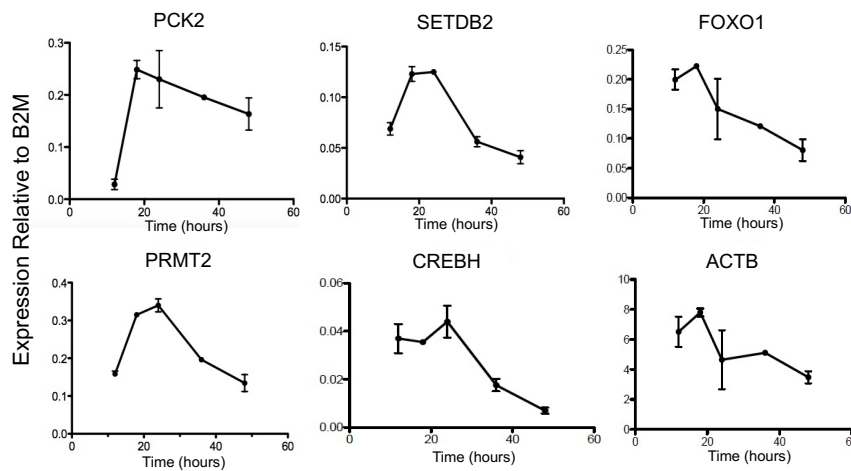


Figure 6: Fluidigm BioMark qPCR refeeding time course. Expression of genes in the re-fed condition, post 24 hour glucose starve, plotted expression relative to B2M

Next, we were interested in investigating how much heterogeneity exists in our population of cells during glucose starvation. We performed a single cell qPCR Fluidigm assay starving cells of glucose for 24 hours, then collecting and sorting them using the Fluidigm Singular microfluidic cell sorting system. We then used the BioMark, to run qPCR on our single cells for the 96 genes we previously tested in the BioMark. Generally speaking, we observed very few genes that showed differential expression in individual cells, represented in the first line of the violin plots (Fig 7). The majority of genes showed a uniform expression across starved cells, expressly PCK2.

Violin Plot of Gene Expression By the Order of PCA Gene Scores

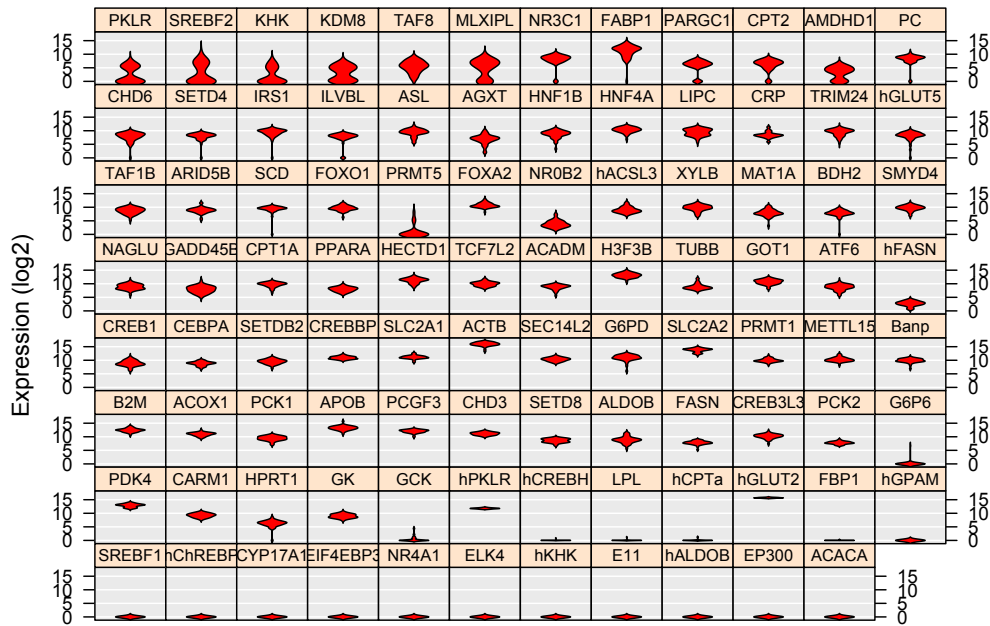


Figure 7: Single Cell qPCR 24 hour starvation. Expression of genes after 24 hour glucose starvation, sorted from highest to lowest heterogeneity by Principle Component Analysis (PCA) as determined by distribution of Log2 expression in single cells

We subsequently confirmed PCK2 memory by qPCR on the RNA level and by Western blot on the protein level. Additional starvation experiments were performed to determine the persistence of this PCK2 transcriptional memory (Fig 8a). Next, we tested whether a third starvation displayed an even higher PCK2 expression compared with the first and second starvation and we found an increase in transcription in the third starvation (Fig 8b), though not in additional starvations (Fig 8c).

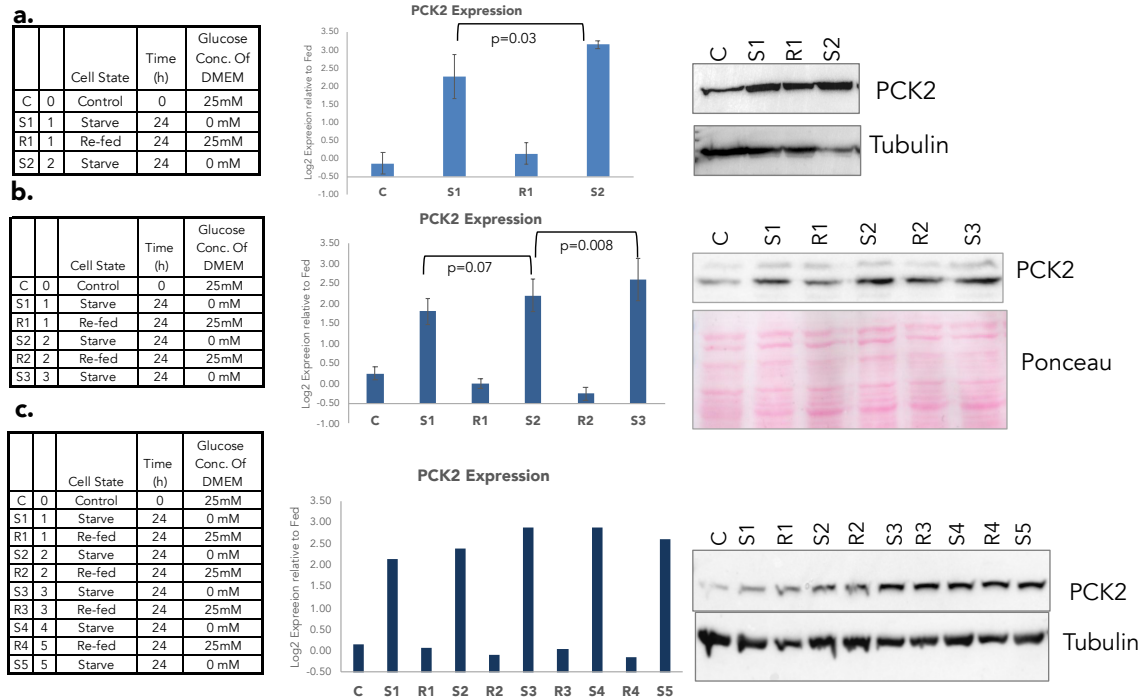


Figure 8: PCK2 gene has memory in up to 3 starvations. PCK2 exhibit an increase in gene expression and protein level by Western Blot after (a) 2 glucose starvations (n=4) and (b) 3 glucose starvation (n=4). PCK2 does not continue to increase at 4 and 5 starvations. Expression is plotted as Log₂ fold change relative to average fed states, error bar in (a) and (b) represent standard deviation.

2.1.3 RNA-Sequencing on 3x Glucose Starvation to Screen for Memory Genes.

In order to identify additional memory genes using an unbiased approach, we performed a large scale RNA-Seq experiment in Huh7 cells, for 3 starvation cycles, in triplicate. Our preliminary analysis of the RNA-Seq experiment defined memory genes as those whose expression increased at least 2 fold in the first starvation, returned to baseline expression in re-fed conditions, then in the second starvation increased at least 1.5-fold when compared to the first starvation. We validated these hits using qPCR and observed several of these genes, though not all, had an increased expression in the third starvation. Some interesting genes from our initial analysis included ASNS, CHAC1, INHBE, SLC7A11, DDIT3, CTH, ACSS2, MTHFD2, STC2, PSAT1, GPT2, TRIB3, and ATF4. A preliminary assessment of genes that exhibited the above definition of memory were related to cancer metabolism and endoplasmic reticulum stress.

To more thoroughly analyze the gene expression results, I collaborated with bioinformaticians in the lab who used the R/Bioconductor software package Limma (Ritchie et al. 2015) for differential gene analysis to calculate the Log₂ fold change, abs (Log₂(FC)). We then defined specific criteria to determine whether a gene has memory, utilizing a classification tree to describe the behavior of the genes across the starvation time course experiment (Fig 9a). First, we defined the criteria for a memory. The top decision node consists of all genes with a normalized expression value greater than 10 reads, normalized by gene length, in averaged control time points, which we denote as *** (all genes). This node is split into 3 branches, which we refer to as the Starvation layer consisting of U** (Up- a significant increase of expression in response to the first starvation), N** (No response- no significant response), and D** (Down- a significant decrease in expression after starve). We define a significant response in the Starvation layer as a Log₂ fold change of 0.5 between control and the first starvation. Each of the U**, N**, and D** nodes branches into 3 additional nodes, however for simplicity, I will only describe the branches from the U**, as these are where we find our genes of interest, however, for N** and D** the descriptions follow the same pattern.

In order to find genes that show a transcriptional memory, we focused to the branch below the starvation layer, designated as the M1 layer (first memory). Since our definition of memory (Fig 9b) is an increased expression level in starve 2 as compared to starve 1, the Log₂ fold change between these conditions must be 0.3 (Fig 9b). The resulting nodes are defined as UU*, UN*, and UD*, with UU* containing the genes with transcriptional memory. As previously described, our memory experiments continue with a third starvation. To designate these genes, we proceed to define our M2 layer, containing UUU, UUN, and UUD, using the same Log₂ fold change of 0.3 to denote significance.

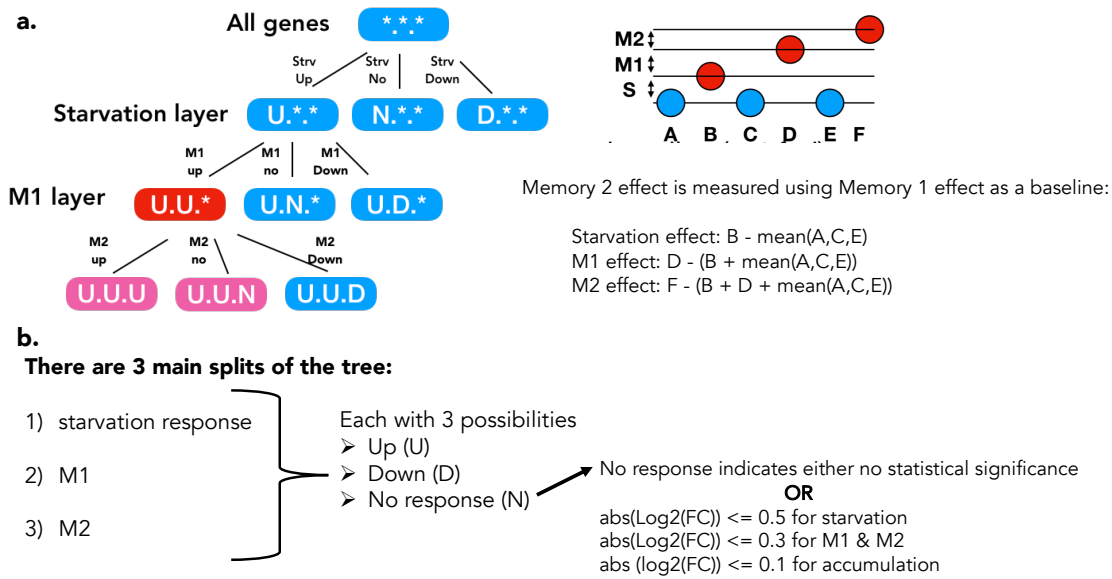


Figure 9: Classification Tree for Memory gene analysis of RNA-Seq. (a) Schematic representing the decision tree for memory classification (b) Definition of memory by fold change .

After the complete analysis of all branches across our time points, we end up with 26 terminal nodes (Fig 10). For the purpose of further discussion, we have designated the UU* branches which include the terminal nodes UUN and UUD, that display a first memory, and UUU that displays a first and second memory. Other important classifications include the NNN node which denotes genes that do not respond to glucose starvation and more important, the UNN group which includes the genes that respond to starvation but do not show a significant increase in expression in the second and third starvation, therefore do not exhibit memory. We will refer to the UNN group as the oscillating genes and use them as a control group to further characterize our memory genes.

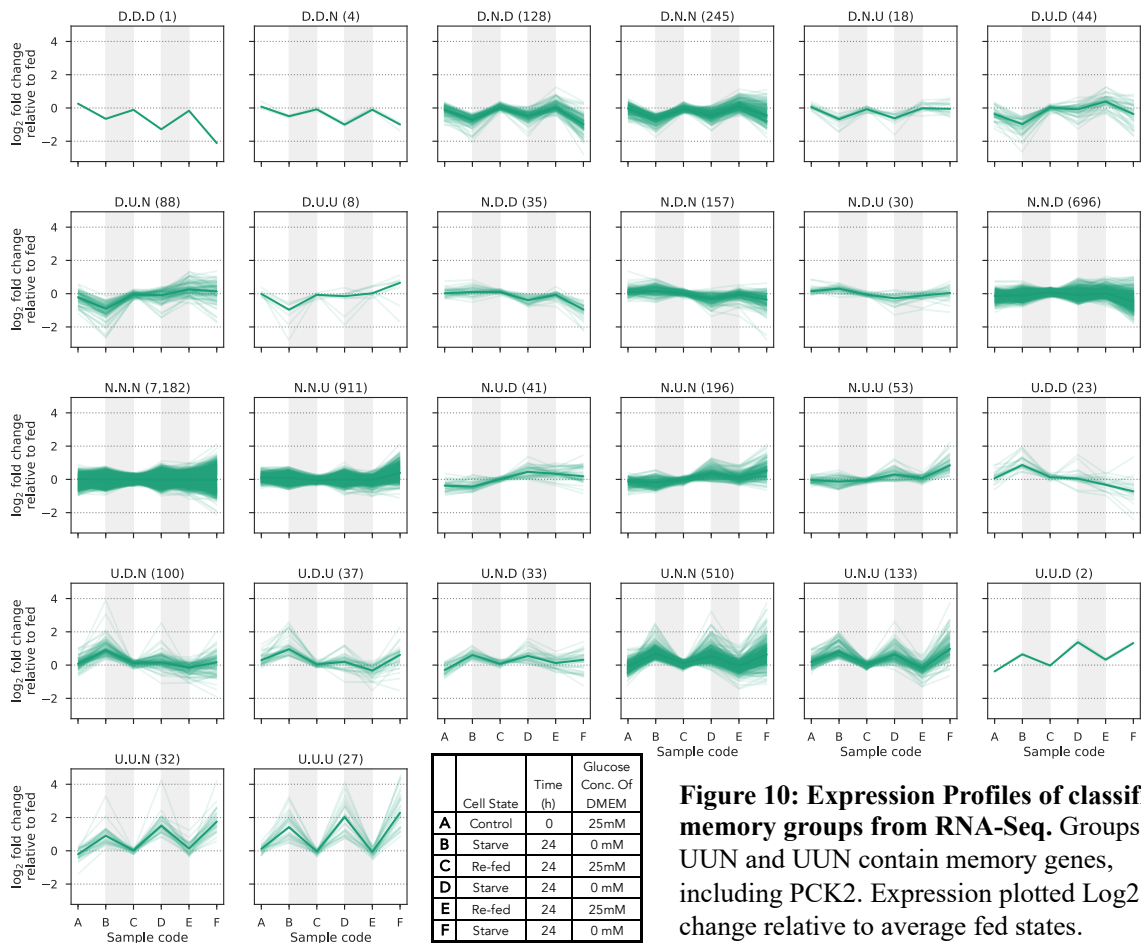


Figure 10: Expression Profiles of classified memory groups from RNA-Seq. Groups UUN and UUN contain memory genes, including PCK2. Expression plotted Log2 fold change relative to average fed states.

In addition to using the level of gene expression and its Log2 fold change when calculating memory, we must take into account that the expression difference is not due to an accumulation of transcripts over the time course. Therefore, we took special care to include a “accumulation effect” to ensure that the gene expression of the memory genes returns to the baseline expression in the fed state. In our model for describing the accumulation effect, we assume that accumulation would increase linearly over time for a gene, therefore if we plot the expression of a gene each for time point, we can plot an accumulation trend line (Fig 11). If the slope of this trend line is significantly non-zero, then we have an accumulation effect, either up or down.

Accumulation Trend Line

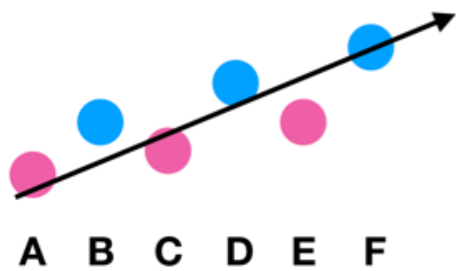


Figure 11: Model of Accumulation Effect:

Genes whose expression fall along the trend line are said to have an accumulation effect, however the accumulation effect does not play a significant role in the majority of memory genes.

Our analysis showed for the majority of the memory genes, accumulation is not an issue. Of the 31 genes in the UUU group, there are 9 genes with a down and 2 genes with an up accumulation effect, while of the 34 genes in the UUN/UUD groups there are 16 genes with an up and 2 with a down accumulation effect (Table 2). Of the 75 memory genes we named in our initial fold change analysis of our time course, we see 42 of these genes in the classification tree model for transcriptional memory. The memory gene PCK2 falls into the UUU group, showing an up accumulation effect however this accumulation effect was not observed in the multiple biological replicate qPCR experiments to optimize and confirm our transcriptional memory experimental design.

Branch	Gene name	Accumulation response
U.U.U	SLC3A2	No response
	XPOT	
	SHMT2	
	CEBPG	
	WARS	
	SNTB1	
	TRIB3	
	GRPEL2	
	DDIT3	
	SLC1A4	
	TUBE1	
	STC2	
	INHBE	
	CTH	
	SLC6A9	
	ADM2	
	ALDH1L2	
	ASNSP1	
	RP11-42O15.3	
	PCK2	Up
SLC17A2	Down	
GARS		
MTHFD2		
SARS		
ASNS		
MTHFD1L		
SLC7A1		
SLC7A11		
EREG		
ZFP69B		
ULBP1		

Branch	Gene name	Accumulation response
U.U.N	ACLY	No response
	AARS	
	PSAT1	
	MARS	
	ATF4	
	PHGDH	
	CARS	
	EIF4EBP1	
	LIPG	
	RHBDD1	
	SH2B3	
	LPIN1	
	JDP2	
	SLCO2A1	
	CBS	
	CHAC1	
	SLC43A1	
	ACSS2	
	GPT2	
	F7	
MTHFR		
SESN2		
SLC38A3		
UNC5B		
SNAI3-AS1		
ADGRD1		
UNC93A		
RP11-660L16.2	Down	
GLI1		
ENHO	Down	
YARS		
RP1-228H13.5	Up	
DHCR7		
U.U.D	ALDOC	

Table 2: Classification of Memory Genes and Accumulation Effect:
Memory genes are classified by group and accumulation effect

Aim II: Characterization of Memory Gene Classifications

2.1.4 Pathway Analysis

Using the Reactome Knowledgebase (Bijay et al. 2020, Fabregat et al. 2018), we performed a pathway analysis on the memory genes in the UUU/UUN/UUD groups (Fig 12a) and compared it with results from the UNN oscillating genes (Fig 12b). The top hits for our memory genes include PERK regulation, tRNA aminoacylation, ATF4 activation of endoplasmic reticulum (ER) response, amino acid transport, unfolded protein response (UPR), and metabolic processes such as serine biosynthesis and amino acid biosynthesis. The pathways for the oscillating genes included downstream signal transduction, signaling by VEGF and PDGF, and other ambiguous biological pathways.

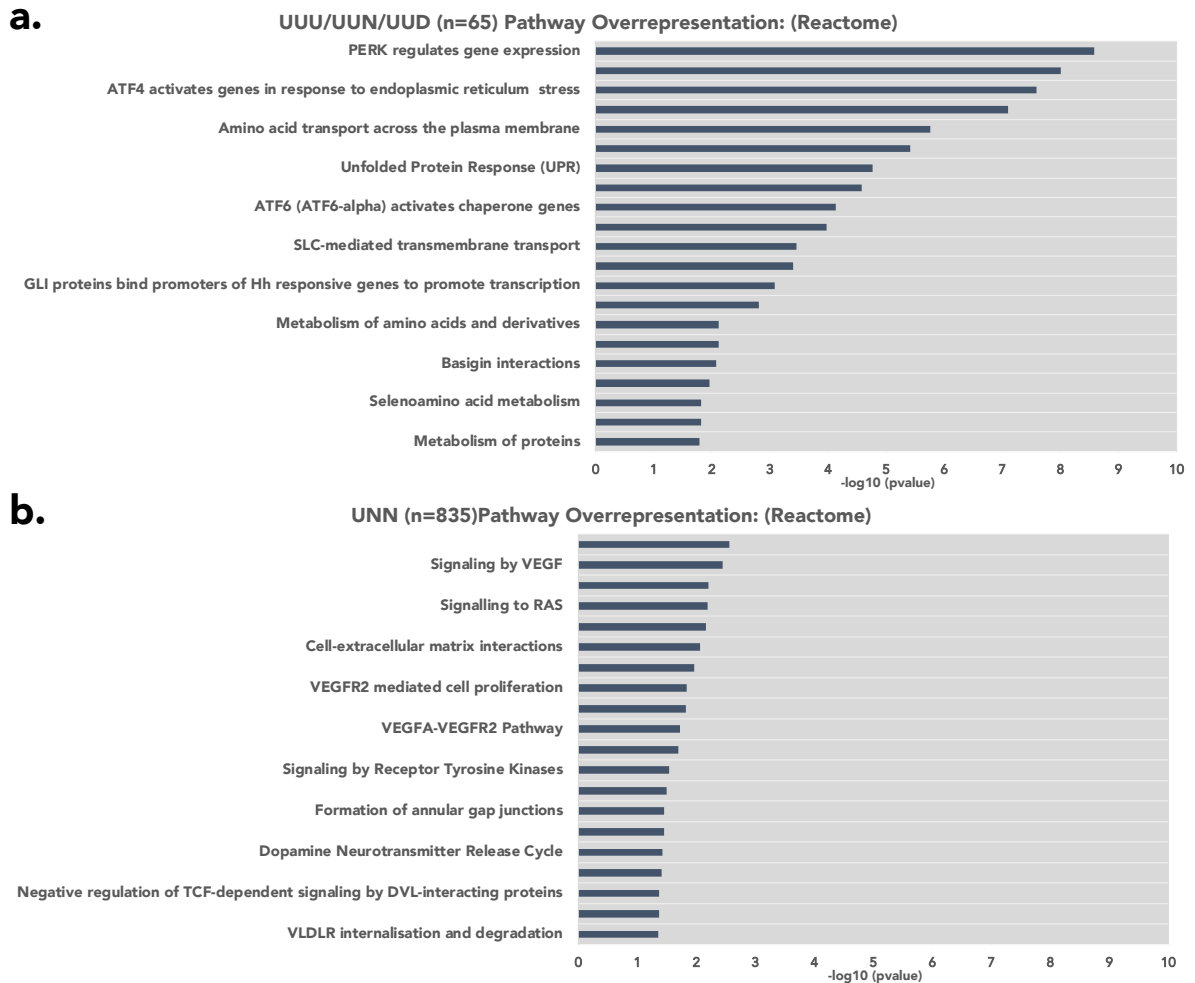


Figure 12: Pathway Analysis: Reactome Knowledgebase Pathway Analysis for (a) Memory Genes in groups UUU/UUN/UUD (b) Oscillating genes in group UNN, plotted as $-\log_{10}$ p-value.

2.1.5 Transcription Factor Motifs

To further characterize our memory genes, we analyzed transcription factor (TF) binding site overrepresentation in our RNA-Seq data. To do this we took regions -1500 base pairs (bp) upstream and +500 bp downstream from the canonical promoters of our genes as based on established criteria. We used FIMO (Grant, Bailey, and Noble 2011) to scan these canonical promoter sequences. For the transcription factor motif analysis, we used the motifs from JASPAR (Khan et al. 2018). The goal of this transcription factor analysis was to detect which TF motifs are overrepresented in our different classifications, e.g., terminal nodes or branches, of our RNA-Seq data. For our analysis, we selected n genes (genes from a particular classification like UUU) out of N genes (all the genes we observed in the dataset),

2.1.6 Autophagy and Circadian Rhythm

In addition to determining candidate memory genes, we can also use the RNA-Seq data to investigate if glucose starvation had an effect other regulatory cellular processes such as cell cycle regulation, autophagy, circadian rhythm, as well as determining whether our liver cancer cells are undergoing gluconeogenesis. In the preliminary optimization experiments, we investigated the 24 hour glucose starvation would trigger an autophagy response by checking at the gene expression of select autophagy responsive genes at control and 24 hour time points then following the refeeding with glucose. In these preliminary experiments, we did not detect a major autophagy response to glucose starvation or refeeding (Fig 14a). Using our expression data from the 3x starvation RNA-Seq data, we are able to further show that autophagy is not triggered by our starvation time course (Fig 14b) as determined by the expression of autophagy associated genes (Fig 14c) (Seok et al. 2014).

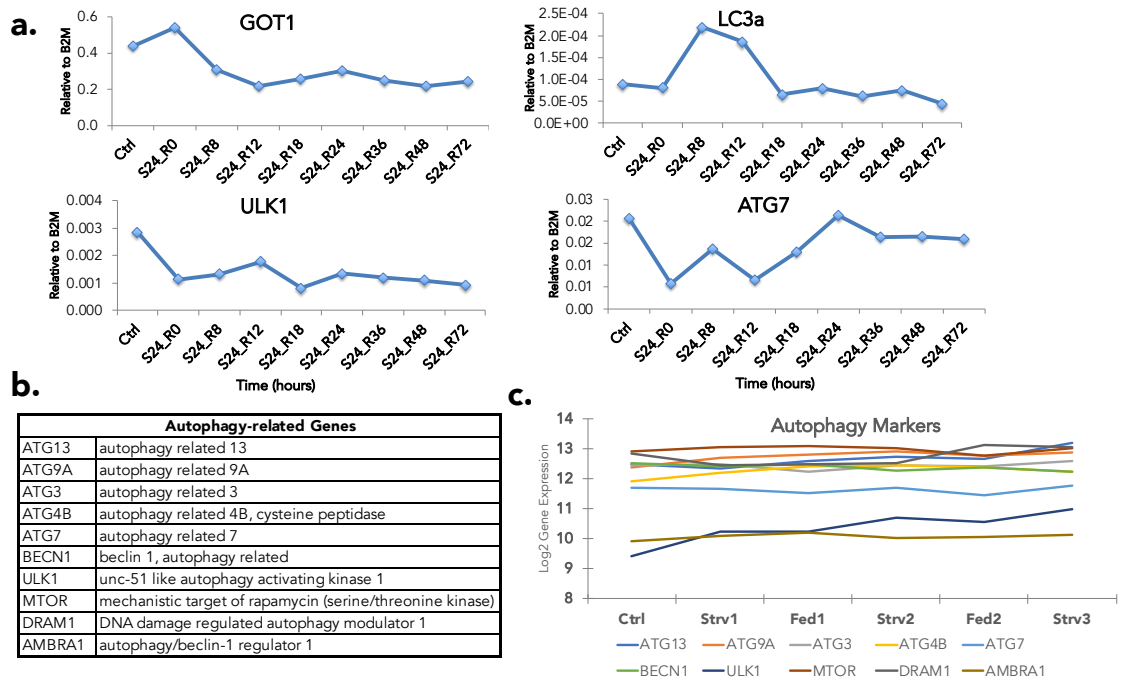


Figure 14: Autophagy markers are not affected by 24 hour glucose starvation: qPCR for autophagy marker do not show a response to 24 hour glucose starving or refeeding (a) qPCR analysis of autophagy markers (b) in repeated starvation time course, expression relative to B2M (c) RNA-Seq analysis do not show a specific response in a 3x starvation memory time course, Log₂ gene expression relative to fed.

Another biological process that is often disrupted by starving/feeding experiments is circadian rhythm. Using the literature (Savvidis and Koutsilieris 2012) (Longo and Panda 2016), we compiled a list of genes that are circadian markers and did not see a noteworthy pattern with them in response to our time course (Fig 15).

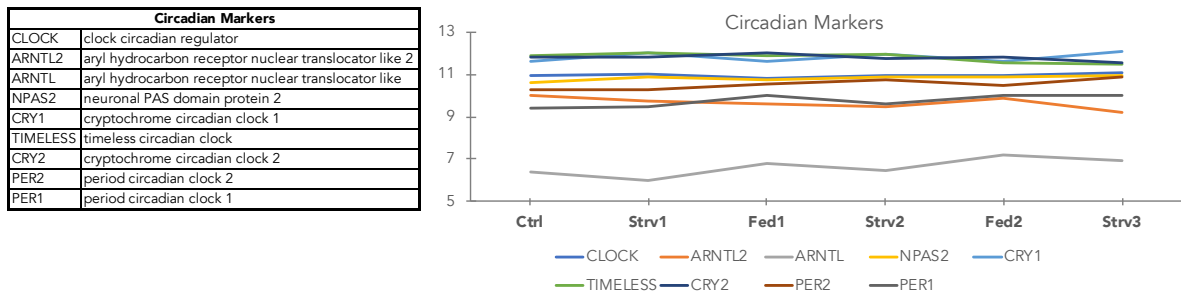


Figure 15: Circadian Rhythm markers are not affected by glucose starvation: RNA-Seq analysis of circadian markers do not show a response in a 3x starvation memory time course, Log2 gene expression relative to fed

2.1.7 Cell Cycle

Cell cycle is one of the most, if not the most, important regulatory networks that must be examined when challenging cells with a stimulus. It is essential to understand how glucose starvation and subsequent refeeding affect the cell cycle thereby determining whether our memory is cell cycle dependent. We used the Cyclebase human database (Santos, Wernersson, and Jensen 2015) feature called “Peaktime” which categorizes the expression of proteins that are cell cycle markers into their respective phases, i.e. G1, G1/S, S, G2, G2/M and M. We then mapped the genes in the Peaktime database to our RNA-Seq database (Fig 16). Only one gene present in the UUU group, SLC17A2, shows a profile relevant to cell cycle M phase, while the other genes of interest are found in non-periodic genes (genes that may affect cell cycle when knocked down) or in the non-affected (N/A) group.

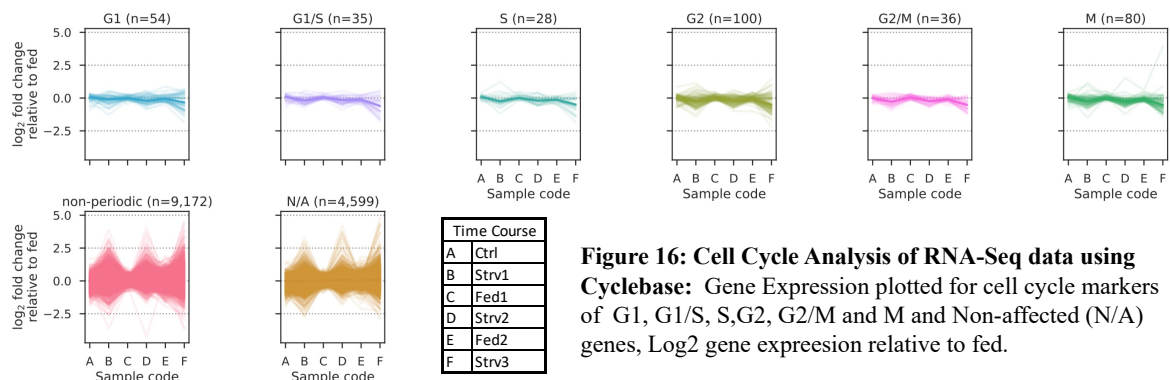


Figure 16: Cell Cycle Analysis of RNA-Seq data using Cyclebase: Gene Expression plotted for cell cycle markers of G1, G1/S, S, G2, G2/M and M and Non-affected (N/A) genes, Log2 gene expression relative to fed.

To further investigate cell cycle regulation, we wanted to look at cell cycle synchronization over our starve/feed time course and if we see an increase synchronization in any specific cell cycle-phase marker. Our assumption is that the variance of expression levels for our three technical replicates would be lower for more synchronized cells. However, while we do observe some reduced variance in our first starve (B), first fed (C) and second starve (D), the variance once again increases in the second fed (E) and third starve (F) (Fig 17). We would expect a decreasing variance with each subsequent time point. We can conclude that there is not a clear cell cycle correlation between the 3x glucose starvation time course and the memory genes in groups UUU and UUN.

Variance of Cell Cycle Markers

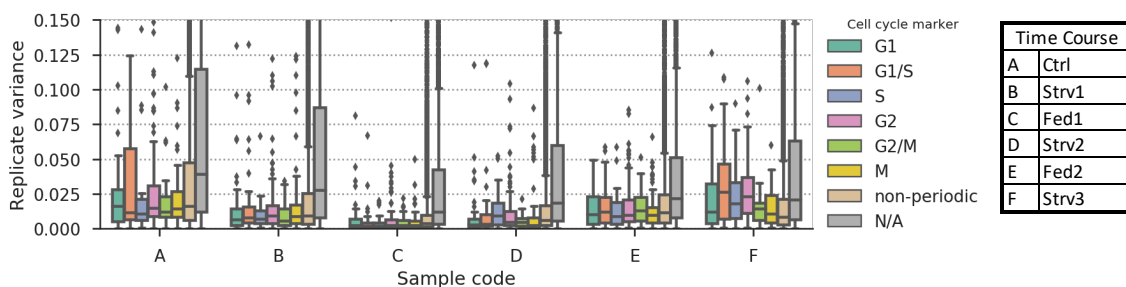


Figure 17: Synchronization of Cell Cycle Markers across time points: The replicate variance for triplicates from RNA-Seq is plotted for expression of different cell cycle marker genes groups. We do not observe a clear cell cycle synchronization across our 3x glucose starvation time course

2.2 Primary Liver Hepatocyte Cell Response to Glucose Starvation

Surprisingly, very few gluconeogenic genes came up in our memory and oscillating gene groups. In light of these results, we began to question how similar our Huh7 cells behave to primary hepatocytes. We tested primary mouse hepatocytes from wildtype C57Bl6 mice, isolated by collaborators and we subjected them to our starvation time course to investigate mRNA transcript levels after glucose starvation. We performed qPCR for the memory genes *Pck2*, *Acss2*, and *Ddit3* and surprisingly no clear memory expression emerged, though for *Pck2* and *Ddit3* we observed a similar increase of expression at the second starve despite the fact that we saw no gene induction in the first starve (Fig 18). The expression of *Foxo1*, a transcription factor involved in gluconeogenesis, did not show a response to glucose starvation. The genes responsible for the gluconeogenic enzymes phosphoenolpyruvate (*Pck1*), pyruvate carboxylase (*Pcx*), pyruvate kinase (*Pklr*), and glutamic pyruvate transaminase 2 (*Gpt2*) also did not show an increase in expression in response to starvation, *Pck1*, *Pcx* and *Pklr* even showing a slight decrease in starved and fed conditions when compared to control.

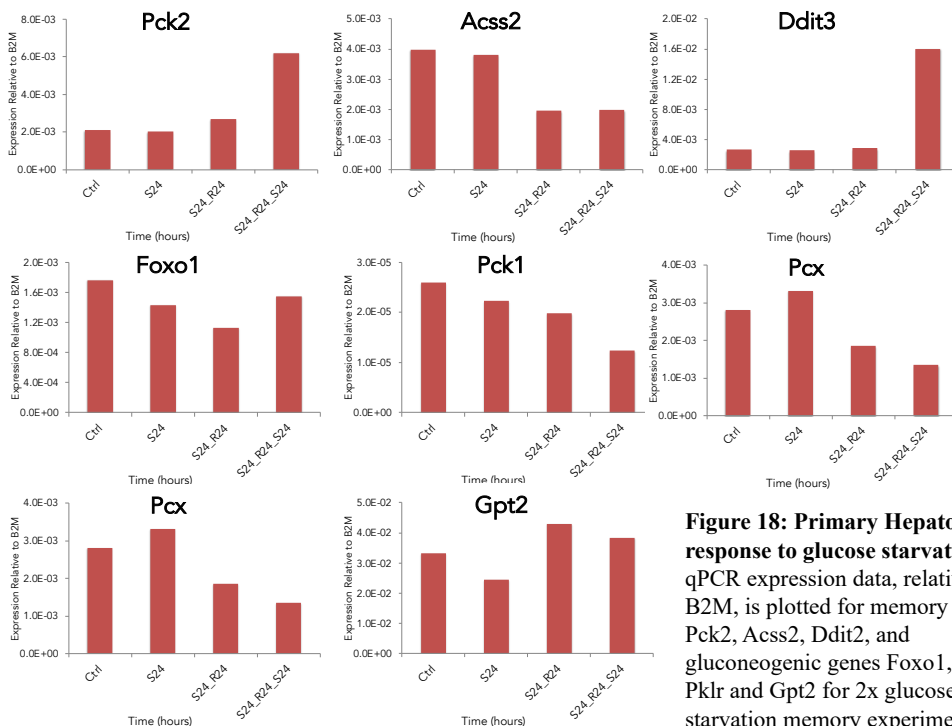


Figure 18: Primary Hepatocyte response to glucose starvation: qPCR expression data, relative to B2M, is plotted for memory genes, *Pck2*, *Acss2*, *Ddit2*, and gluconeogenic genes *Foxo1*, *Pck1*, *Pklr* and *Gpt2* for 2x glucose starvation memory experiment.

Hepatic glucose production is highly regulated by the peptide hormone glucagon (Sharabi, Tavares, and Puigserver 2019) which is involved in gluconeogenesis, glycogenolysis, glycogenesis, triglyceride storage, and other metabolic processes. Glucagon treatment has been shown to increase Pepck mRNA levels in cultured primary hepatocytes (Christ et al. 1988) therefore we treated our primary mouse hepatocyte cultures with glucagon.

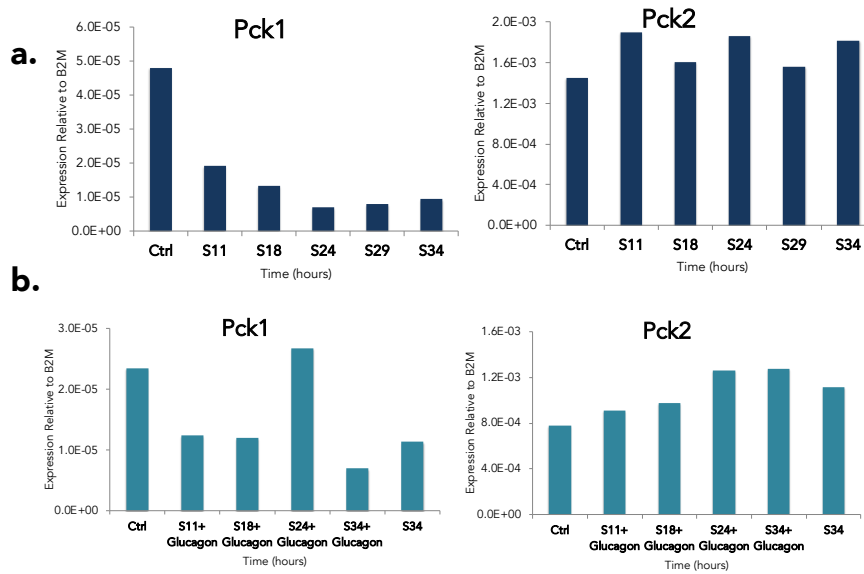


Figure 19: Glucagon treatment of Primary Hepatocyte response to glucose starvation: Primary hepatocytes were glucose starved (a) or starved and treated with 25mM glucagon (b) then tested with qPCR for Pck1 and Pck2 gene expression, data is relative to B2M.

We measured the expression of Pck1 and Pck2 of hepatocytes in conditions of no glucose (Fig 19a) at 11, 18, 24, 29, and 34 hours and cultured with no glucose and 25mM glucagon (Fig 19b), at the same time points. The response for hepatocytes cultured in no glucose or no glucose with glucagon in both Pck1 and Pck2 was not as we expected, and not easy to interpret. These results suggest our starvation conditions are not inducing a canonical gluconeogenesis transcriptional cascade and thus additional optimization would be required to properly investigate memory in primary hepatocytes.

2.3 ATF4 is Necessary for the Expression of a Subset of Memory Genes.

2.3.1 ATF4 Expression in Response to Starvation

Our above findings, that we do not observe the expected gluconeogenic transcriptional response, prompted us to further examine what pathways are overrepresented in our UU* memory groups (Fig 12a). If we combine the top hits, PERK regulation, tRNA aminoacylation, ATF4 activation in response to ER stress, amino acid transport, and unfolded protein response (UPR) with our TF overrepresentation data revealing the presence of ATF4 motifs only in the UU* memory groups and (Fig 13), suggesting an involvement of ATF4 in our memory model.

Of the 65 memory genes in the UU* group, many have reported interactions with ATF4 such as CHAC1, ASNS, AARS, TRIB3, DDIT3, CEBPG (Quiros et al. 2017) and PCK2. In fact, the gene encoding ATF4 is itself, categorized as a memory gene in UUN group in our RNA-Seq data (Fig 20a), though when we test it in additional starvation memory experiments, it had memory in only 1 of 4 experiments by qPCR (Fig 20b), and western blot (Fig 20c), though ATF4 expression always increases when glucose starved and returns to basal levels in the glucose refeeding.

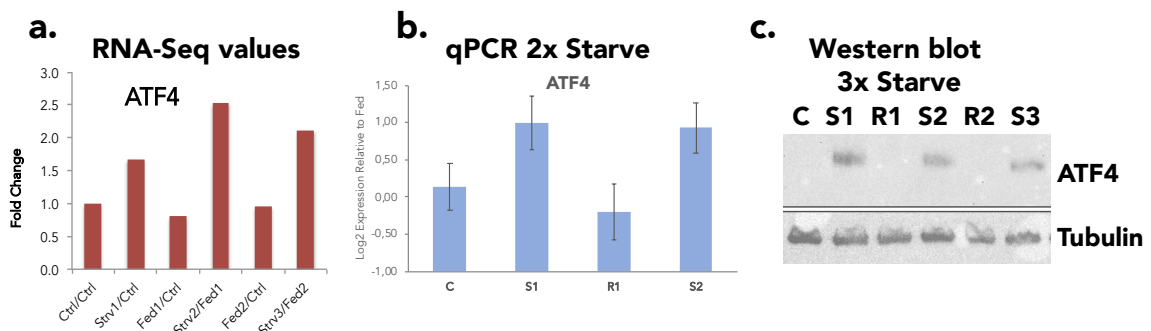


Figure 20: ATF4 Behavior in Glucose Starvation Memory: (a) RNA-Seq fold change of plotted reads, normalized by gene length compared to Control (b) qPCR (n=4) for 2x starvation, plotted log₂ expression relative to fed(R), error bars are standard deviation, and (c) Western blot detection for ATF4 for 3x starvation.

The kinetics of gene expression for ATF4 during the glucose starvation time course and refeeding with glucose are very similar to the kinetics observed with PCK2 during our experimental design optimization experiments. Since ATF4 is a transcription factor, we checked protein levels during glucose starvation, observing no ATF4 protein present at 1 hour but its appearance begins at 2 hours, following the mRNA kinetics (Fig 21a), with protein increasing up to 24, 36, 48, and 72 hours during glucose starvation (Fig 21b). Protein measured by immunofluorescence after 24 hours of glucose starvation shows ATF4 staining is localized in the nucleus (Fig 21c).

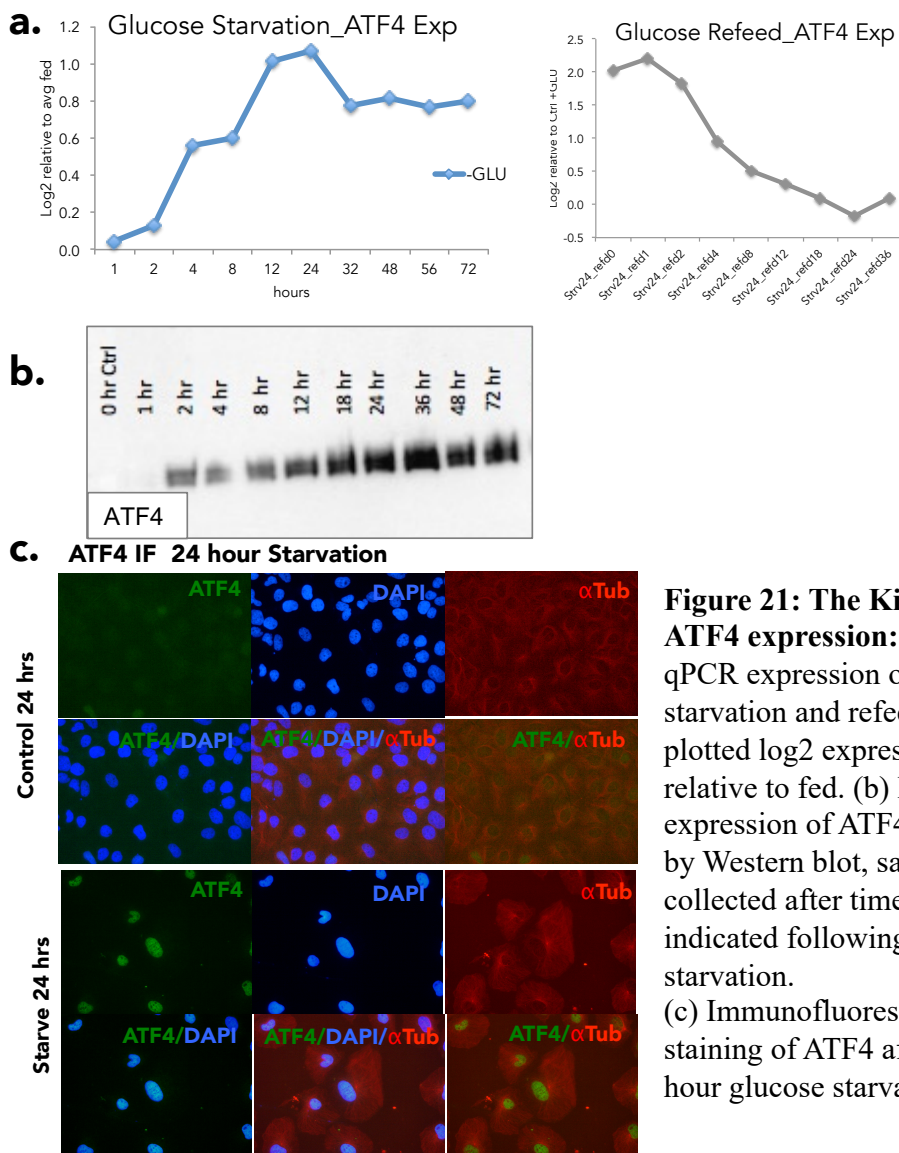


Figure 21: The Kinetics of ATF4 expression: (a) qPCR expression of glucose starvation and refeeding, plotted log₂ expression relative to fed. (b) Protein expression of ATF4 detected by Western blot, samples collected after time point indicated following glucose starvation. (c) Immunofluorescence staining of ATF4 after 24 hour glucose starvation.

2.3.2 siRNA Knockdown of ATF4

As mentioned previously (Quiros et al. 2017), ATF4 regulates several UU* memory genes response to stress to activate their transcription. We used siRNA to deplete ATF4 in Huh7 cells, in both fed and starved conditions to investigate the role of ATF4 in our system (Fig 22). We recorded a 97% knockdown in the fed condition and 99% knockdown in glucose starved cells in the siRNA treated cells. In the control scrambled siRNA treated cells, we detected a nearly 2 fold increase expression of ATF4 in starved cells while in the ATF4 siRNA treated cells, we saw no increase in expression, even though there were still a small percentage of ATF4 transcripts present. Next, we performed qPCR on our ATF4 knocked down samples for several memory genes. Gene expression of PCK2, ASNS, CHAC1, MTHFR2, and TRIB3 was lower in both the starved and fed conditions in ATF4 knocked down cells and is therefore dependent on the presence of the TF ATF4 for induction. In ASNS, CHAC1, and TRIB3 we do observe increased expression after 24 hours of starvation, however this can be attributed to an increase in the 3% of ATF4 expression remaining which are still able to regulate gene transcription, though binding of the small amount of ATF4 to ATF4 motifs. The memory gene DDIT3 does not show the same behavior and is not affected by knockdown of ATF4, at least not at the 24 hour time point measured in this time course.

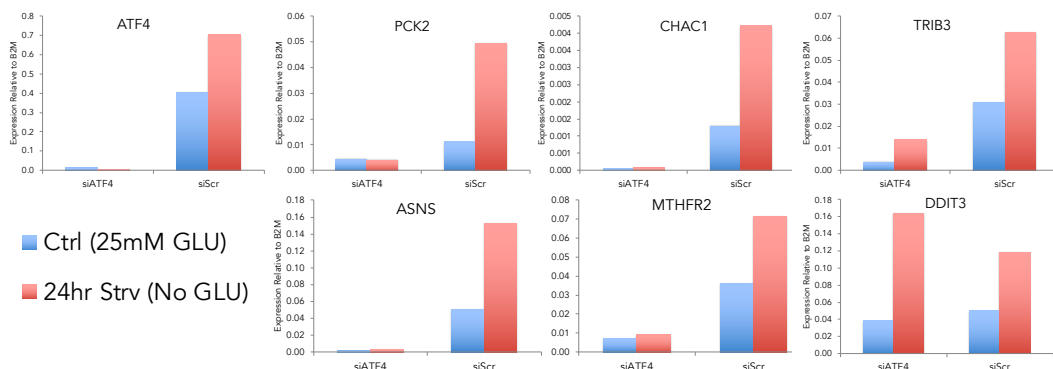


Figure 22: siRNA Knockdown of ATF4: qPCR expression, relative to B2M, in siRNA mediated knockdown in Ctrl (25mM glucose) and no-glucose media treated Huh7 cells after 24 hours, for ATF4 (siATF4) and scrambled control (siScr). ATF4 knockdown resulted in a 97% reduction of ATF4 transcripts and effected the expression of memory genes PCK2, CHAC1, TRIB3, ASNA,and MTHFR2, not did not affect DDIT3 expression.

2.3.3 ATF4 Inhibitor ISRIB

Our ATF4 knockdown experiments showed that the expression of many memory genes exhibits a dependence on ATF4, coinciding with the presence of ATF4 binding sites in the gene. The existence of an ATF4 specific small molecule inhibitor (Sidrauski et al. 2013; Sidrauski et al. 2015) allowed us to ask if we could specifically inhibit ATF4 binding at specific time points, thereby affecting transcriptional memory. First, we titrated the inhibitor, ISRIB, assessing gene transcription of ATF4 and memory genes PCK2 and ASNS to determine the optimal concentration to use in subsequent experiments. We tested 12 μ M concentration and halved the dilution up until 0.325 μ M, assaying for activity with minimal toxic effects on the Huh7 cells (Fig 23a). We observed an effect on the transcription of the memory genes PCK2 and ASNS when the cells were cultured in 0.325 μ M ISRIB in both 24 hour starved and glucose fed conditions, though less effect in fed cells, as compared to control cells. In these experiments, the ISRIB inhibitor is present in the media for the full 24 hours of the glucose starvation. We also tested its effects on cells starved for 18 hours, thereby highly expressing the genes, then treating them with the inhibitor while continuing the starvation to the full 24 hours (Fig 23b). The memory genes PCK2 and ASNS show very little effect of ATF4 inhibition on cells already starved for 18 hours, which at this point are nearly at their highest level of transcription.

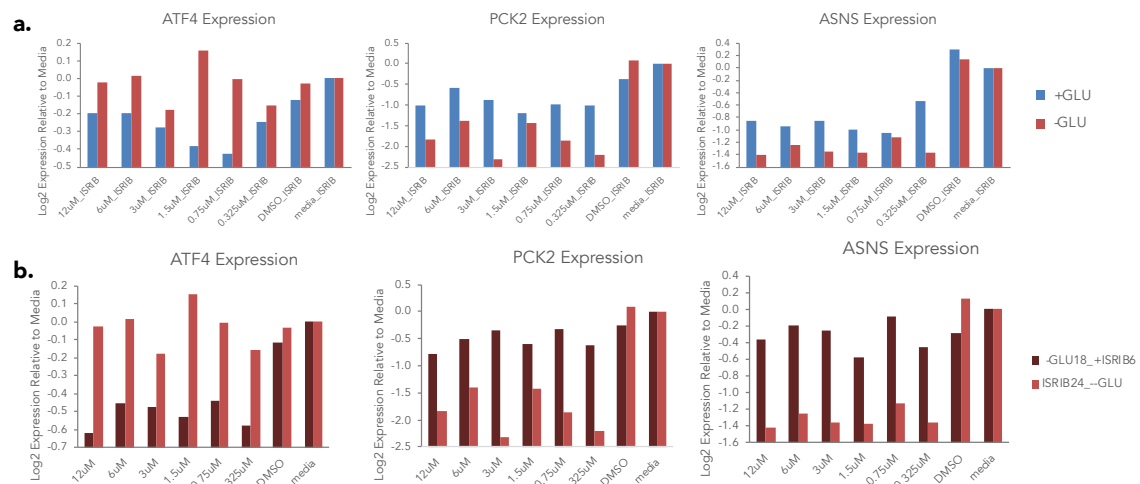


Figure 23: ATF4 inhibitor ISRIB: (a) Titration of ATF4 inhibitor ISRIB in 2 fold dilutions from 12uM to 0.325uM in glucose starved and glucose fed conditions and (b) treatment of ISRIB for 24 hours of starvation or for the final 6 hours of a 24 hour glucose starvation, qPCR results plotted Log2 expression relative to media control.

2.3.4 Gene Expression Kinetics for ATF4 Responsive Memory Genes

As illustrated by our siRNA knockdown and small molecule inhibition of ATF4, we have shown that several memory genes are dependent on ATF4 for their expression in response to glucose starvation. By examining these genes' expression kinetics with qPCR, we can observe that they closely follow ATF4 expression in response to glucose starvation (Fig 24). We observed a first response at 2 hours of starvation, followed by sizable increase in expression from 2 to 4 hours and increasing strongly from 8 to 12 hours. For the memory genes PCK2, SHMT2, AARS, and CEBPG, we observed a slight increase of expression at 4 hours, their expression steadily increased from 4 to 24 hours, displaying a slight lag time when compared to ATF4 expression, coinciding with the idea that ATF4 expression is necessary for the expression of these genes. Of the genes we investigated, DDIT3 is the exception as its kinetics showed a strong increase in expression between 1 hour and 2 hours, at which time it plateaus and remains highly expressed throughout the entirety of the time course. The difference in DDIT3 kinetics may explain why we do not detect an effect on its expression when ATF4 is depleted (Fig 22), though more experiments would be needed to confirm this.

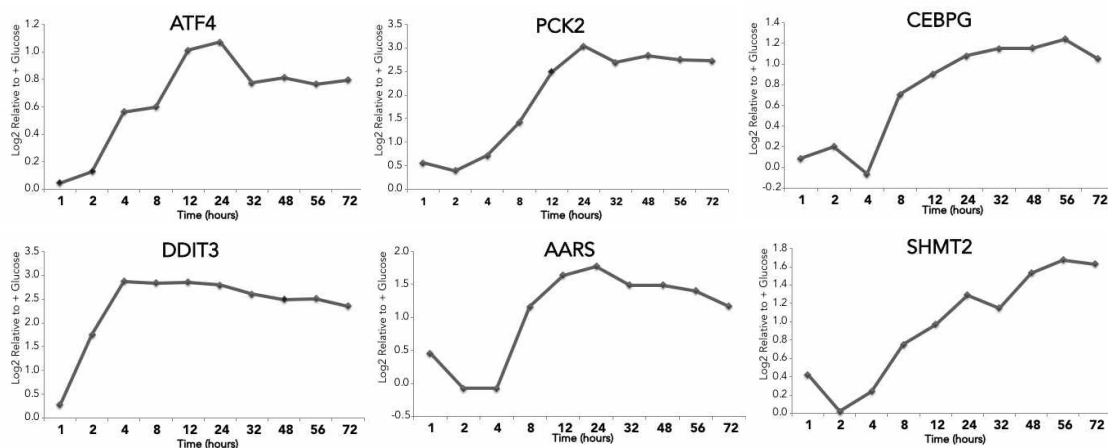


Figure 24: Kinetics of ATF4 responsive genes: qPCR results for the expression of select memory genes during 72 hour glucose starvation of Huh7 cells, qPCR results plotted Log₂ expression relative to Fed control.

2.3.5 Endoplasmic Reticulum (ER) Stress Effect on Memory

Next, we wanted to investigate whether the memory phenomena we observe is linked to an endoplasmic reticulum stress response. Several compounds can trigger ER stress in cells including tunicamycin and thapsigargin. Using previously reported concentrations and time of action for these compounds (Sidrauski et al. 2013) (Sidrauski et al. 2015), we tested the effect of ER stress induction in Huh7 cells. Initially we assessed ER stress induction and recovery short time course in presence of tunicamycin, 2ug/mL, or thapsigargin, 250nM (Fig 25). While we did not observe a major increase in expression of ATF4, PCK2, or DDIT3 in tunicamycin treated samples when compared to control, we did detect a noteworthy response in the thapsigargin treated cells.

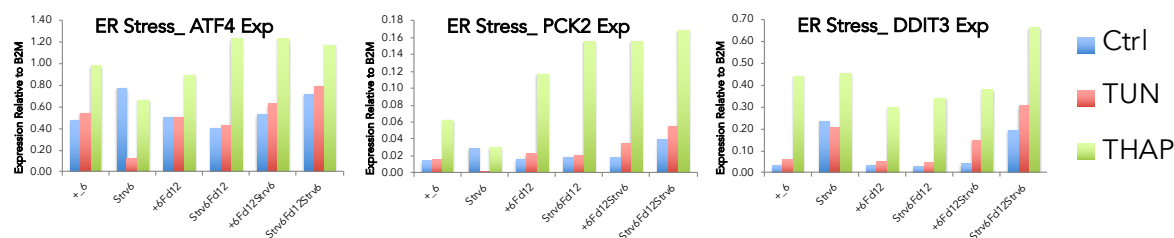


Figure 25: Testing of ER Stress inducers on Huh7 cells: qPCR expression, relative to B2M, for repeated induction of ER stress with tunicamycin, 2ug/mL (TUN) or thapsigargin, 250nM (THAP) or glucose starvation (Ctrl) of Huh7 cells.

We observed peak expression for ATF4, PCK2, and ASNS at 18 hours at both the 250 and 500 mM concentration (Fig 26a). Next, we performed an experiment to mimic memory using an 18 hour thapsigargin treatment, an 18 hour recovery and a second 18 hour thapsigargin treatment to test for “ER stress memory”. After 18 hour recovery from thapsigargin treatment ATF4, DDIT3, PCK2 or ASNS expression did not return to baseline (Fig 26b). We therefore decided on an 18 hour thapsigargin treatment (500mM) combined with a 78 hour recovery/fed to allow expression to return to basal expression (Fig 26c). In this experiment we did not observe an increase in the expression of the memory genes PCK2 and SHMT2 solely in response to ER stress.

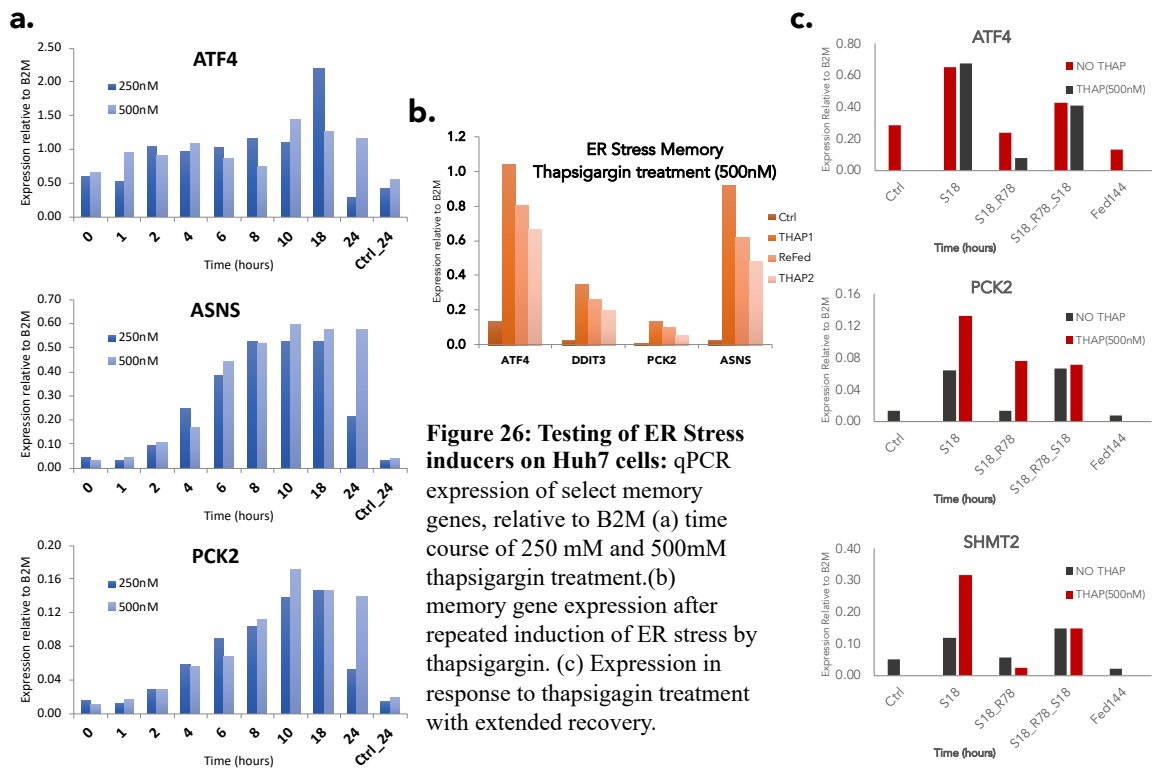


Figure 26: Testing of ER Stress inducers on Huh7 cells: qPCR expression of select memory genes, relative to B2M (a) time course of 250 mM and 500mM thapsigargin treatment. (b) memory gene expression after repeated induction of ER stress by thapsigargin. (c) Expression in response to thapsigargin treatment with extended recovery.

Aim III: Investigate the Mechanism Responsible for Transcriptional Memory

2.3.6 The Role of Transcription Factor CEBPG on the Expression of Memory Genes

In addition to ATF4, the binding site for the transcription factor CEBPG was also present in the promoters of many of the memory genes. Though not a statistically significant enrichment, literature searches have described an interaction between ATF4 and CEBPG (Huggins et al. 2015). Since CEBPG is also a memory gene, we chose to investigate the role of CEBPG in our starvation memory model. Preliminary experiments investigating the effect of siRNA mediated knockdown of CEBPG on memory gene expression in starved and fed cells showed that knockdown of CEBPG affected the expression of itself and of the memory genes PCK2 and CHAC1, with a small affect seen on the memory gene AARS (Fig 27). Interestingly, simultaneous knockdown of CEBPG and ATF4 had a greater effect on the expression of ATF4 alone and also a greater effect on the expression of PCK2, CHAC1, AARS, and ACSS2 than CEBPG depletion alone. These results suggest that ATF4 and CEBPG may play a combinatorial role in the expression of our memory genes. In the future, we hope to address this question by investigating whether CEBPG plays a role in dependence on ATF4 for memory gene expression by knocking down CEBPG in our memory experiments and performing ATF4 ChIP.

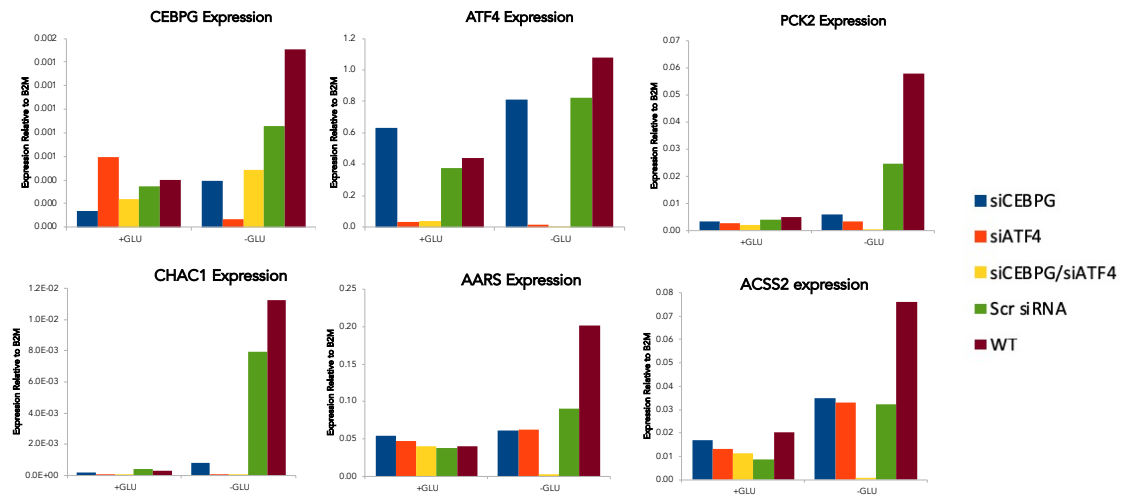


Figure 27: siRNA knockdown of CEBPG and ATF4: qPCR expression, relative to B2M, on select memory genes for Huh7 cells grown with glucose (+ GLU) and without glucose (-GLU) treated with siRNA for CEBP, ATF4, dual knockdown CEBPG and ATF4, scramble control (Scr siRNA), and untreated (WT) cells.

2.3.7 The Behavior of Pre-spliced, Nascent RNA During Glucose Starvation

One important aspect of our experiments is that all of our gene transcription data is exploring the behavior of full length polyA mRNA. While we clearly see a phenotype in our transcriptional memory experiments on mRNA expression, we should not overlook nascent, newly transcribed RNA, which has been shown to be implicated in transcriptional memory (Holoch and Moazed 2015; Palozola, Lerner, and Zaret 2019). To simplify this investigation, we first used existing RNA from our initial starvation time course to synthesize cDNA with Random primers and perform a run-on qPCR (Roberts et al. 2015; Elferink and Reiners 1996) to study pre-spliced RNA. We observed pre-spliced RNA for memory gene PCK2 at 2 hours, increasing at 4 and 8 hours, and plateauing at 12 hours, while mRNA levels have begun to increase transcription at 8 hours and steadily increased until peaking at 24 hours (Fig 28a). When we measure pre-spliced RNA in the first 3 glucose starvation, S1, S2, and S3, in our 5x starvation memory experiments (Fig 28b and c), we do not observe a difference in the level of expression at 24 hours (Fig 28c), though as the 48 hour starvation time course shows, the difference in the behavior of pre-spliced

RNA is its timing (Fig 28a). While we have shown above that mRNA kinetics do not change in the second starvation, we need to further investigate whether this is true for pre-spliced RNA.

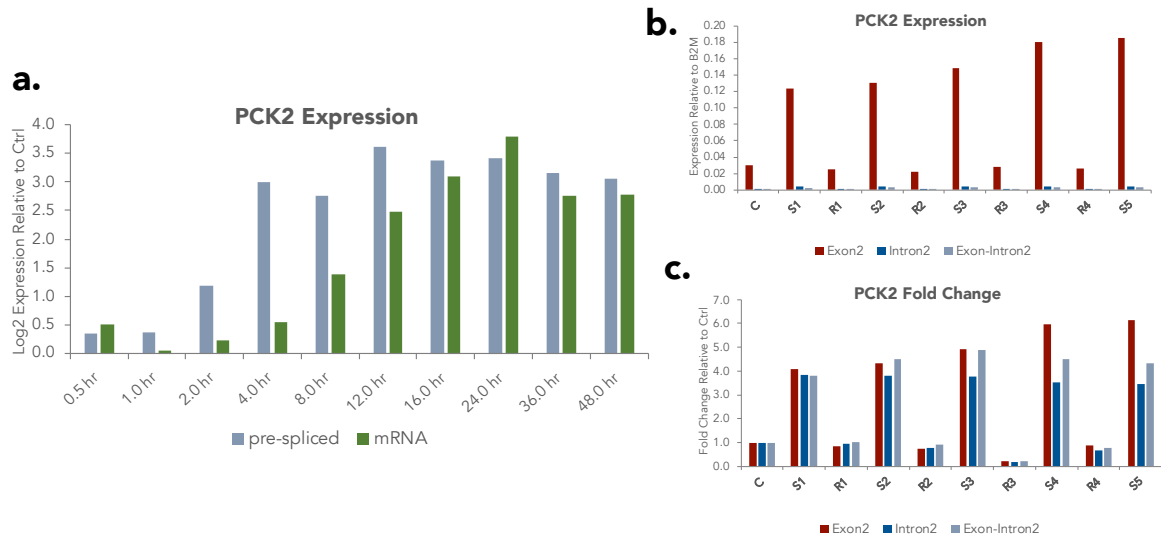


Figure 28: Run-On qPCR: Run-On qPCR expression on PCK2 on Huh7 cells (a) glucose starved for 72 hours, plotted by log2 expression relative to control, or on a 5x starvation time course plotted by (b) relative expression or (c) fold change from control .

2.3.8 Mass Spectrometry of Histone Modifications

Next, we investigated the effect of glucose starvation and feeding cycles on global histone modification levels by mass spectroscopy. Utilizing mass spectroscopy expertise within our group, we performed a 3 starvation memory time course followed by bottom up liquid chromatography mass spectrometry, LC-MS. After confirmation that our replicates were suitable (Fig 29a), we proceeded with the analysis. Globally we do not observe accumulation of histone modifications through repeated starvations (Fig 29b). Interestingly, global H3K9ac in our fed samples was higher than in the starve samples, contrary to the behavior of H3K9ac at promoters of active genes in Chromatin Immunoprecipitation (ChIP) experiments (Fig 29c and 34). Also, global H3K4me3 levels are higher in the starved samples compared to the fed. These LC-MS results confirm that

glucose starvation and feeding effect histone modifications on a global scale, however experiments targeting specific histone modifications must be performed.

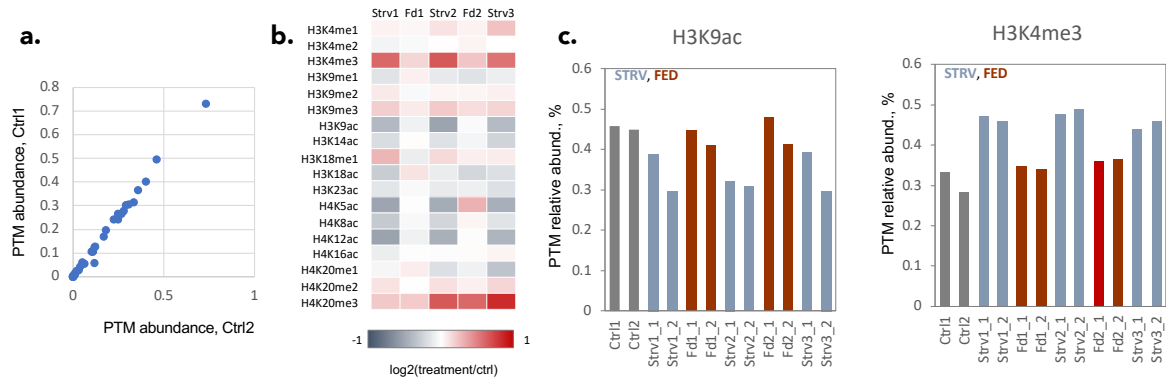


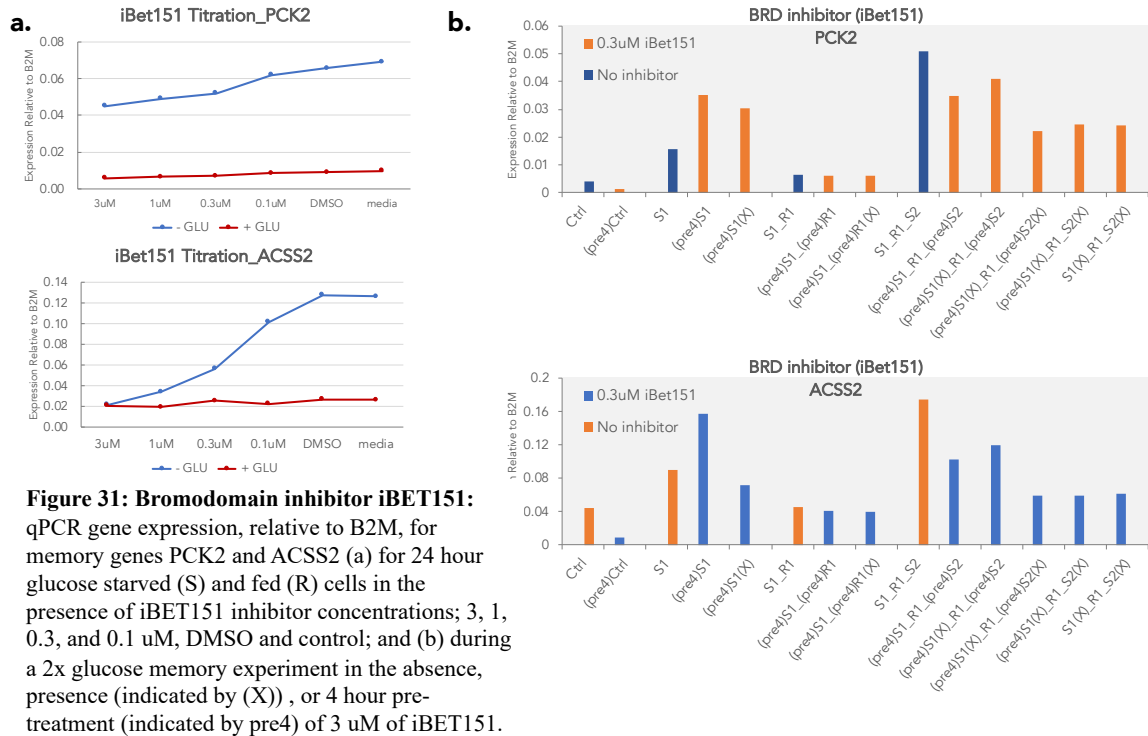
Figure 29: LC-MS on 3x Glucose starvation time course: Bottom up liquid chromatography mass spectrometry was performed in duplicated on snap frozen samples. Replicate quality was assessed (a) and histone modification log₂ treatment/control was plotted (b). Relative abundance of H3K9ac and H3K4me3 were calculated.

2.3.9 Modulation of Epigenetic Modifications by Small Molecules to Perturb

Memory.

Research has suggested that a less repressive chromatin state in the recovery phase of stimulated cells allows for their increased transcription in a second stimulation (Iberg-Badeaux et al. 2017; Natoli and Ostuni 2019; Lamke and Baurle 2017). Therefore, we wanted to investigate if a disruption of the repressive mark H3K27me₃ would disrupt the transcription of memory genes. We first titrated a small molecule inhibitor for EZH1/2 called UNC1999 on our Huh7 cells in glucose starved and fed conditions. EZH2 is the catalytic subunit of the Polycomb repressive complex2 (PRC2) that can repress gene expression through methylating H3K27 (Tan et al. 2014) and EZH1 is a noncanonical member of the PRC2 complex that has also shown to methylate H3K27 (Shen et al. 2008). We observed an effect on gene expression at our highest concentration, 3 μM, without an effect on cell viability, as observed by microscopy (Fig 30a). We then treated cells at each 24 hour starve or fed time point, in the presence of 3 μM UNC1999, with previous treatment with UNC1999 in an earlier time point, or without treatment, with an (X)

transcription by preventing histone acetylation and TF binding. The BET proteins, Brd2, Brd3, Brd4 and BrdT, are bromodomain containing epigenetic readers proteins that recognize acetylated lysine residues (Prinjha, Witherington, and Lee 2012). When we tested the iBET151 small molecule, we saw an effect on transcription of select memory genes at 0.3 μ M concentration and did not observe toxicity (Fig 31a), so we tested it further for effects on transcriptional memory. In previous studies used the iBET151 inhibitor to block transcription of affected genes after stimulation, they pre-treated the cells with inhibitor, therefore we also included this condition. However, pre-treatment of cells with compound does not alter the cells response, rather the presence or absence of inhibitor effects transcription, notably in the second starve. When iBET151 is present as indicated by and (X) after the condition, we observe lower expression when iBET151 is present when compared with no inhibitor or pretreated sample (Fig 31b).



Overall, the inhibitors do not provide a clear answer to the mode of regulation of memory genes, however they suggest that global blocking of epigenetics processes may

not be the best way to investigate our phenotype in an epigenetic context. The next step is to tease apart what is happening on the chromatin level at specific genes to gain more insight into how the DNA is behaving during our transcriptional memory time course.

2.3.10 Chromatin Immunoprecipitation to Profile Behavior at Memory Genes

To accomplish this, we performed a large scale Chromatin Immunoprecipitation sequencing (ChIP-seq) experiment for our 24 hour time course, and including several intermediate time points to investigate what is occurring during the initial 24 hour starvation by collecting an 8 hour starve time point prior to the starve1, 24 hour time point. We also included a 16 hour refeeding intermediate time point.

2.3.10.1 ChIP qPCR Optimization

The first step for the ChIP-Seq time course was to perform a ChIP qPCR to test conditions. Using suggested antibody concentrations and 60ug of chromatin, we tested the chromatin immunoprecipitation for histones H3, H3K4me3, H3K9ac, H3K27me3 and RNA Polymerase II (Pol II) C-terminal domain (CTD), RNA Pol II Serine 5 as a marker for transcriptional initiation and Serine 2 for transcriptional elongation. We observed significant enrichment for active genes B2M, PCK2 and ACSS2, for the histone marks H3K4me3 and H3K9ac (Fig 32a), and at lower levels for RNA Pol II, CTD, Pol II S5 and Pol II S2 for B2M (Fig 32b). We did not observe enrichment of H3K27me3 at B2M, PCK2 or ACSS2, however it was present at the HBB (hemoglobin) gene locus whose expression is repressed in Huh7 cells (Fig 32a). We also observed enrichment of H3K27ac at B2M and the memory gene STC2, with a higher signal in starved conditions (Fig 32c). Finally, we tested ChIP transcription factor ATF4 in our and observed binding at the TSS of memory genes PCK2 and ASNS (Fig 32d).

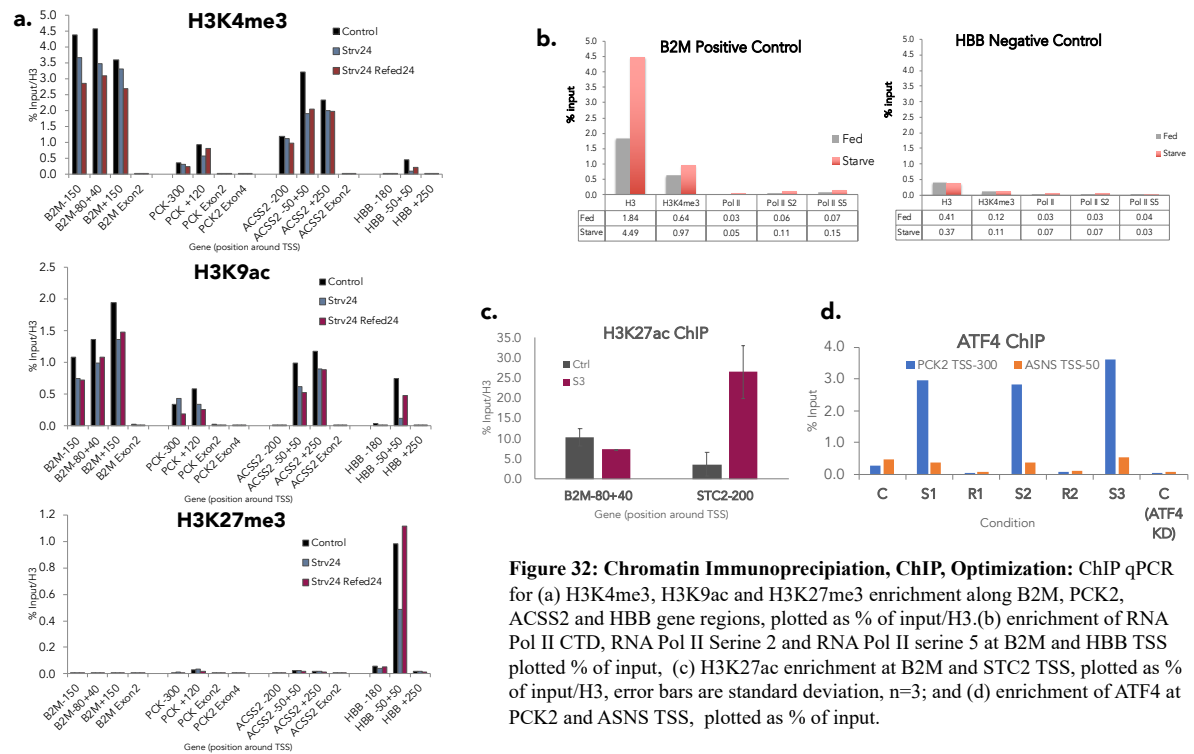
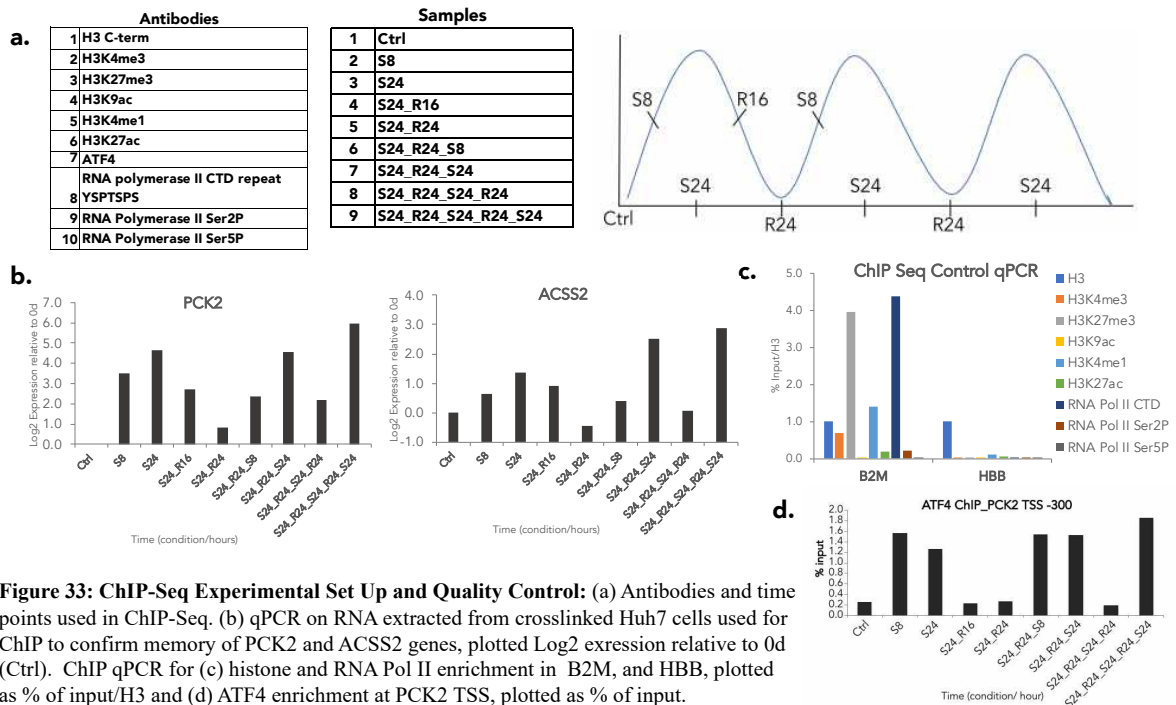


Figure 32: Chromatin Immunoprecipitation, ChIP, Optimization: ChIP qPCR for (a) H3K4me3, H3K9ac and H3K27me3 enrichment along B2M, PCK2, ACSS2 and HBB gene regions, plotted as % of input/H3. (b) enrichment of RNA Pol II CTD, RNA Pol II Serine 2 and RNA Pol II Serine 5 at B2M and HBB TSS plotted % of input. (c) H3K27ac enrichment at B2M and STC2 TSS, plotted as % of input/H3, error bars are standard deviation, n=3; and (d) enrichment of ATF4 at PCK2 and ASNS TSS, plotted as % of input.

2.3.10.2 ChIP- Seq Time Course

Once we determined the proper chromatin amount and antibody concentration for our IPs, we proceeded to perform our large scale ChIP-Seq experiment (Fig 33a). Samples were harvested daily, crosslinked with formaldehyde, centrifuged and frozen at -80°C until all samples were collected. At the time of collection, I removed 300 µl of crosslinked sample to process for RNA, cDNA synthesis and qPCR to confirm memory in our experiment (Fig 33b). We confirmed enrichments for all antibodies with qPCR (Fig 33c and 33d). We then submitted our ChIP'ed DNA to the IGBMC Sequencing facility for library preparation and 50 base paired end sequencing.



We received the aligned bam files from the sequencing platform along with a quality control and preliminary analysis of the experiment. While we included the intermediate time points starve 8 (S8), starve24_fed16 (S24_R16), and starve24_fed24_starve8 (S24_R24_S8), for our initial analysis we focused on the 24 hour time points for simplification of our initial analysis. We plotted profiles for the unnormalized, raw read counts we received from the sequencing facility around the TSS, focusing on the UUU, UUN, and NUU groups, while excluding the UUD group, since it only consists of 2 genes thereby skewing the visualization, and comparing them to NNN, UNN, and DNN as controls. Analysis of H3K4me3 distribution at gene promoters across the time points does not show major oscillations between starved and fed conditions, especially when compared to H3K9ac profiles which clearly oscillate and are highly enriched, in starved and observed at lower amount in fed conditions. We do not see any clear patterns between condition in H3K27me3 profiles, though there is a slight difference in the S24F24 condition, however this could be explained by the difference we observe in the S24F24 input profile (Fig 34).

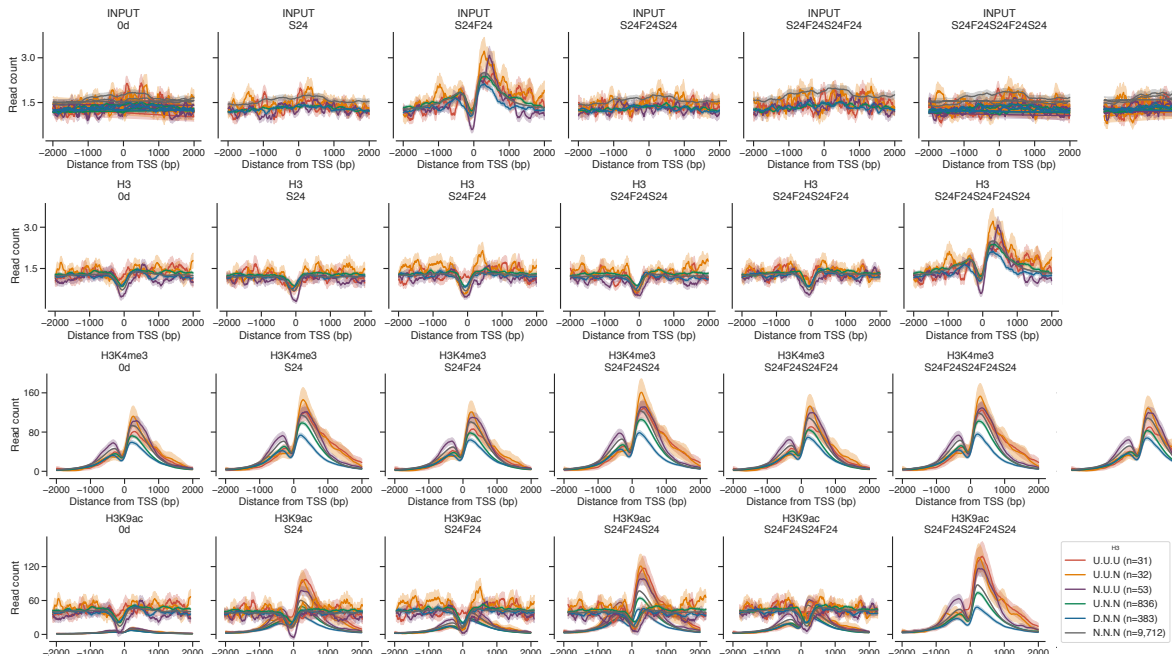


Figure 34: ChIP-Seq Results: Input, H3, H3K4me3, H3K9ac, and H3K27me3: Expression profiles of raw reads showing enrichment of input and indicated histone modification at indicated gene groups.

Since our transcriptional memory phenotype is stimulus-dependent and involves a robust transcriptional response, we also included the histone marks H3K4me1 and H3K27ac (Fig 35) which have been shown to be indicators of enhancer activity in our ChIP-Seq experiments. For H3K4me1, we observe a slight oscillation between starved and fed conditions, and also a slight increase in UUU and UUN genes when compared with the aforementioned controls. There is a clear oscillating pattern present for H3K27ac enrichments based on starved/fed state with a higher signal for UUU and UUN genes. Finally, we see a clear preferential binding for ATF4 in the UUU and UUN memory genes when compared with controls. These results, taken together, suggest that there may be memory related enhancer activity.

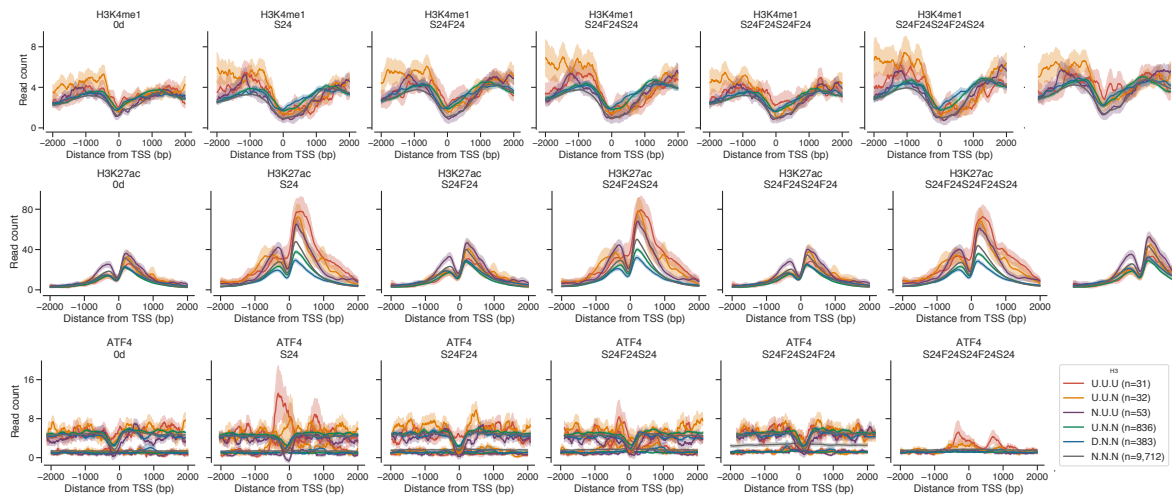


Figure 35: ChIP-Seq Results: H3K4me1, H3K27ac, and ATF4: Expression profiles of raw reads showing enrichment of indicated histone modification or TF at indicated gene groups.

Next, we examined our RNA Pol II CTD, RNA Pol II Serine 2, and RNA Pol II Serine 5 ChIP-seq data (Fig 36). Unfortunately, due to experimental issues, including low yield in the ChIP'ed material for our RNA Pol II samples, we did not get data for all antibodies at all time points in our time course. Preliminary analysis of the RNA Pol II data for RNA Pol II CTD and RNA Pol II Serine 5 exhibited enrichment at the TSS during starvation time points, notably in the UUU, UUN and NUU groups. We are currently repeating the experiments for RNA Pol II Serine 5.

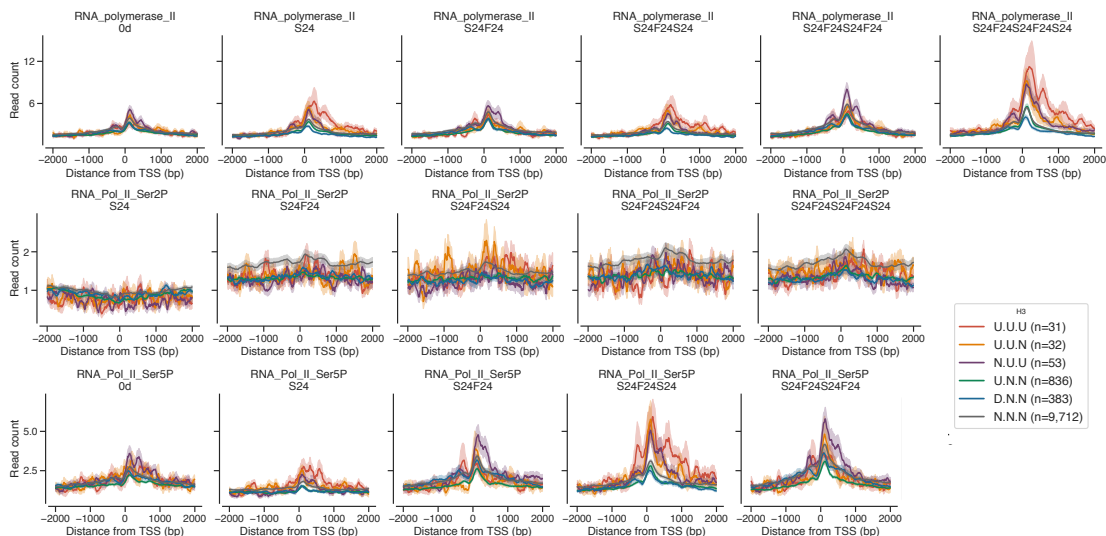


Figure 36: ChIP-Seq Results: RNA Polymerase II CTD, RNA Polymerase II Serine 2, RNA Polymerase II Serine 5 : Expression profiles of raw reads showing enrichment of indicated RNA Polymerase II variant at indicated gene groups.

2.3.10.3 The Role of Enhancers in Memory Gene Regulation

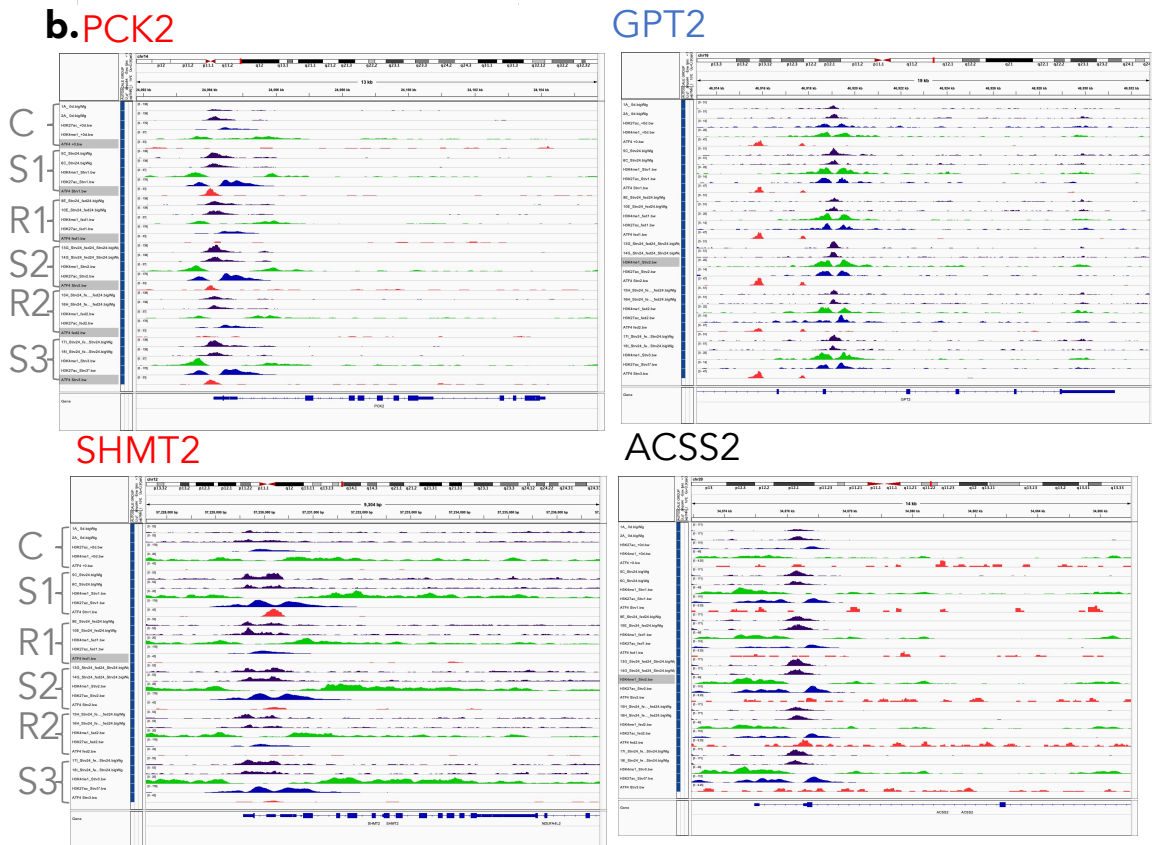
Distinct pattern of histone marks and transcription factor binding are associated with enhancers that regulate transcription (Carone et al. 2010). A poised enhancer state has been described in the memory systems in LPS stimulated macrophages at which H3K4me1 and H3K27ac marks are gained upon stimulation, along with specific TF binding and the H3K4me1 signal remains, even in the absence of stimulation (Ostuni et al. 2013). While several attempts to perform unbiased, top down analysis approaches were not successful to tease out the subtle phenotype of our memory genes, we instead chose to simplify my strategy. Therefore, we visualized ChIP enrichment for ATF4, H3K4me1, and H3K27ac along with ATAC-Seq signal for all memory genes with the Integrative Genomics Viewer (IGV) web browser (Robinson et al. 2011). We looked at all memory genes for a common pattern of expression and found that 29 of the 65 memory genes show a specific pattern of glucose starvation responsive enrichment of ATF4 and H3K27ac, with what appears to be a retention of H3K4me1 (Fig 37a and 37b). While these observations are preliminary, they provide a starting point for further analysis.

a. UUU/UUN/UUD

No Pattern	Primed /ATF4 at Strv	ATF4 bound	Not shown
ACLY	AARS	ASNSP1	RP1-228H13.5
ACSS2	ADM2	JDP2	RP11-42O15.3
ADGRD1	ASN5	LIPG	RP11-66O16.2
ALDH1L2	CARS	LPINT	
ALDOC	CEBPG	SNAI3-AS1	
ATF4	CHAC1	UNC93A	
CBS	DDIT3	WARS	
CTH	EIF4EBP1	XPOT	
DHCR7	GARS		
ENHO	INHBE		
EREG	MARS		
F7	MTHFD1L		
GLI1	MTHFD2		
GPT2	PKC2		
GRPEL2	PHGDH		
MTHFR	PSAT1		
RHBDD1	SARS		
SLC1A4	SEN2		
SLC3BA3	SH2B3		
SLC6A9	SHMT2		
SLC7A1	SLC17A2		
SLCO2A1	SLC3A2		
TUBE1	SLC43A1		
ULBP1	SLC7A11		
ZFP69B	SNTB1		
	STC2		
	TRIB3		
	UNC5B		
	YARS		

Figure 37: Manuel investigation of Memory gene Enhancer signatures using IGV browser: (a) Memory genes categorized by ATAC-Seq and enrichment of H3K4me1, H3K27ac and ATF4 (b) example of IGV tracks for select genes.

ATAC
H3K4me1
H3K27ac
ATF4



We also collaborated with Dr. Verena Heinrich from the group of Dr. Martin Vingron at the Department of Computational Molecular Biology at the Max Planck Institute for Molecular Genetics. Their group developed an enhancer prediction software called Condition-specific Regulatory Units Prediction (CRUP). The workflow consists of a novel pre-trained enhancer predictor that finds enhancers solely based on histone

modification ChIP-Seq data (Ramisch et al. 2019). Together, we have employed aspects of their CRUP analysis (data not shown), customized for our unique needs with the help of Dr. Heinrich. Once again, the large scale analysis of our data provided us with inconclusive results, however Dr. Heinrich developed a method to separate enhancers, identified by CRUP, into starvation responsive and non-starvation responsive. When we investigated the epigenetic profiles around these called enhancers, we see an enrichment of ATF4 and H3K27ac. The enrichment of ATF4 in the called enhancers is notable because they exclude promotor regions, where we have typically seen ATF4 bound. These interesting hints on ATF4 binding and enhancer further suggest that the ATF4 TF may be involved with enhancer activity along with additional cofactors we hope to uncover.

2.3.11 DNA Accessibility During Glucose Starvation by ATAC-Seq

To further investigate the behavior of Huh7 during our starvation time course, we performed an assay for transposable-accessible chromatin with high throughput sequencing, ATAC-Seq (Buenrostro et al. 2013; Buenrostro et al. 2015). With ATAC-Seq, we aimed to determine TFs binding, as well as using open DNA regions to improve our ability to study enhancers. We are currently analyzing our ATAC data, though in our initial analysis utilizing profile plots of ATAC signal, we observe some gene classifications that show increased openness compared others dependent on starved or fed state (Fig 38). In the UUU, UUN and NUU groups, we observe a starvation dependent increase in openness when compared to control or fed states. However, this analysis is very preliminary and we are currently exploring several analysis pipelines

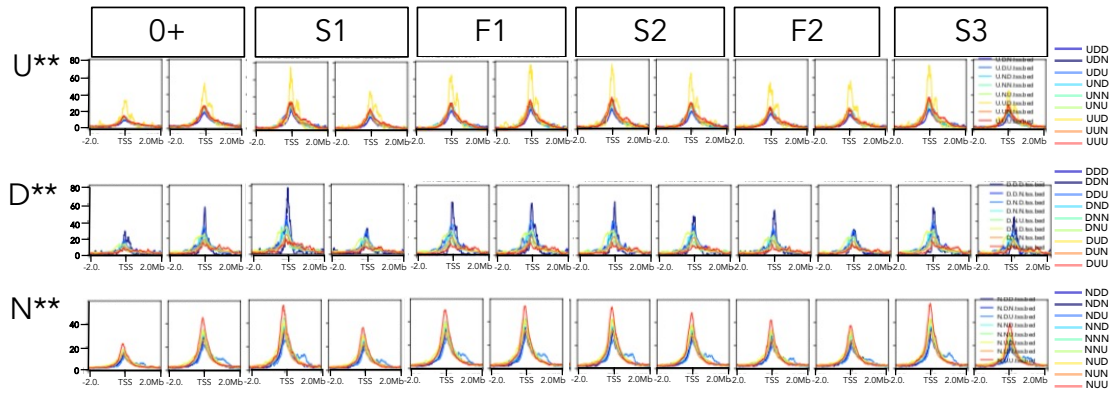


Figure 38: ATAC-Seq: Expression Profiles of raw reads from ATAC-Seq for indicated gene groups

3 Discussion

Overall, I have discovered a novel model of transcriptional memory triggered by glucose starvation in the Huh7 human liver hepatocarcinoma cells. Memory genes respond to starvation with an increase in expression, which is higher in a second, and sometimes third, starvation. These memory genes shared several characteristics, such as the requirement of transcription factors for their expression, glucose starvation dependent enrichment of ATF4, binding of RNA Pol II, and enrichment for the histone marks H3K9ac and H3K27ac at their promoters.

3.1 Notable Topics Concerning Memory Experimental Model

3.1.1 RNA Transcript Accumulation

After establishment of our glucose starvation memory time course, we used RNA-Seq to determine additional examples of transcriptional memory. Our preliminary, rather simple analysis using fold change differences, calculated with Excel, discovered about 75 genes, which exhibited a memory of higher expression in the second induction when compared to the first. The increase in mRNA levels in the second and third starves could be the result of a build-up or an absence of degradation of transcripts. When we determined memory genes using our decision tree model, we included an “accumulation effect” to monitor RNA build-up or lack of degradation. While we do witness some accumulation effects, we have confirmed by qPCR that this accumulation is not significant. It is worth noting that the RNA-Seq three starvation experiment was performed once in technical triplicates, therefore we rely on our repeated time course experiments as evidence that, in most cases, accumulation is not consistently observed in across multiple biological replicates.

3.1.2 Huh7 Cells have Incomplete Gluconeogenesis Machinery

Though PCK2 is known to be involved in gluconeogenesis, it is not the main isoform of PEPCCK involved in the process. The cytoplasmic isoform of PEPCCK gene is called PCK1 and is primarily responsible for gluconeogenic signaling in liver cells. Initially, we expected to find several gluconeogenesis enzymes, including PCK1, and related genes up regulated in response to glucose starvation. Surprisingly PCK1 had very little expression in our initial starvation time course, nor in our RNA-Seq data, especially when compared to the expression levels of PCK2, leading us to conclude that PCK2 is the primary gene regulating PEPCCK in Huh7 liver cells.

3.1.3 Correlating Memory Genes to Cell Cycle

Also using RNA-Seq, we investigated a potential role of cell cycle in our starvation memory time course. For this we investigated the expression of cell cycle related genes and detected no correlation with memory genes. However, we acknowledged this analysis may not be conclusive. Ideally, FACs sorting or other more robust methods of examining cell cycle regulation in Huh7 cells over the starvation would be more informative.

3.1.4 Additional Models for Studying Memory

Additional testing of primary hepatocytes would be worthwhile for drawing conclusions on whether the memory phenotype we see is liver specific, cancer specific, or possibly liver cancer specific. Though we performed preliminary experiments for primary mouse hepatocytes, we acknowledge that primary hepatocyte culture may not require the same conditions as liver cell lines, therefore errors may have been made in experimental design or execution. To more comprehensively address whether glucose starvation memory exists in other cell lines, we plan to test several additional cancer cell lines,

particular those with a high expression of PCK2 (Mendez-Lucas et al. 2014) (Leithner et al. 2015) (Zhao et al. 2017) (Vincent et al. 2015).

3.1.5 The Absence of Memory in our Experiments

Over the course of our experiments, we sometimes would perform a memory experiment and not see memory. For that reason, we always confirmed memory for the gene expression of PCK2 and at least one more memory gene before proceeding with our analysis. Over the course of many experiments, I would estimate a rate of about 1 out of 6 experiments did not exhibit a memory phenotype of higher expression in a second induction. Further investigation into this suggested that in our Huh7 cell lines, memory might change, namely if culture conditions are not ideal. Huh7 cells are highly proliferative and grow exponentially in culture, with no contact inhibition. Contact inhibition occurs in many cells in cultures when too many cells are in the plate and the cells will often quiesce and stop dividing. I tested Huh7 cells in culture and their proliferation is continuous and cells will even grow on top of each other when the plate is too full (data not shown). Along with this, Huh7 cells also grow very rapidly with a doubling of approximately every 12 hours and thereby depleting cell culture media quickly, as observed by the change of color or phenol containing media. While all of the Huh7 cells we use on our experiments are derived from one parental culture, over the course of this research, aliquots of cells have been frozen at various stages. It can be postulated that, at some point, a culture dish of cells was overgrown or the media was not changed promptly and the cells became starved by a depletion of glucose in the culture media. These cells were then propagated and frozen, and later when they were used for experiments, already had an altered physiological state affecting memory. We have experimentally shown a plateau of increased response after 3 starvations (Results-Fig 8a), we have not tested further starvations to investigate for how many more rounds of starving

and feeding the memory would be sustained. Finally, we have studied for how long the recovering feeding time between starvations can be extended and memory still be maintained. Preliminary results have shown that memory is maintained at least up to 96 hours. However, it is necessary to note the difficulty of running such experiments when keeping in mind the difficulty in culturing Huh cells at an optimal density and nutrient level, as mentioned above.

3.2 Starvation Response and Memory

3.2.1 The Role PEPCK in Cancer Cells

As introduced earlier, several groups have reported a role for gluconeogenic enzymes in cancer cell growth (Leithner et al. 2015) (Vincent et al. 2015; Balsa-Martinez and Puigserver 2015) (Montal et al. 2015) (Zhao et al. 2017). A recent editorial in FASEB journal, (Pederson 2016) cited these works in order to draw parallels between the cytoplasmic portion of the gluconeogenic reaction, which is essentially a reversal of glycolysis, to the process of aerobic glycolysis in cancer, commonly referred to as the Warburg effect, suggesting that these recent PEPCK regulated metabolic systems may provide insight into cancer cell metabolism. The Warburg effect of aerobic glycolysis occurs in cancer cells when glucose is converted to lactate in the presence of oxygen, in contrast to this, in most normal cells, glucose to lactate conversion occurs in oxygen limited conditions (Mayers and Vander Heiden 2015). In a recent review addressing the idea that gluconeogenesis may be repurposed to generate biosynthetic intermediates in starvation conditions in cancer cells, the importance of PEPCK encoding genes, PCK1 and PCK2 was emphasized (Grasmann et al. 2019) (Fig 1). Though we hypothesize a similar role for PCK2 as outlined in the review, we still have to confirm it experimentally. Ideally, we would like to profile the metabolomics on Huh7 cells during our starvation memory

time course by targeted metabolomics (Patti, Yanes, and Siuzdak 2012), tracking the carbon usage. However, due to the complexity of our time course, we first need to determine when to collect samples, depending on the metabolic state of our cells.

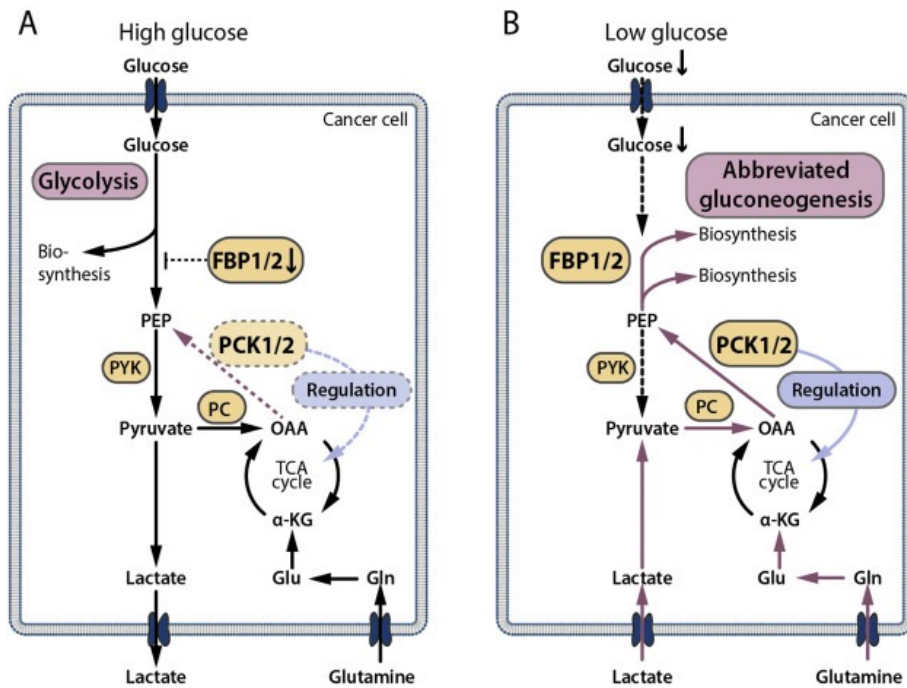


Figure 1: Model of Gluconeogenic pathways used by cancer cells in different nutrient conditions: Taken from Grasmann, G., et al. (2019). "Gluconeogenesis in cancer cells - Repurposing of a starvation-induced metabolic pathway?" *Biochim Biophys Acta Rev Cancer* 1872(1): 24-36.

3.2.2 Memory Genes Regulating Acetyl-CoA

To further explore the metabolic consequences of glucose starvation mediated memory, we checked our list of memory genes for further insight. Given the fact that we witness increased acetylation at many of our memory genes, as measured by H3K9ac and H3K27ac enrichment in ChIP-Seq, we noted that 2 memory genes, ACLY and ACSS2, are responsible for the generation of acetyl-coenzyme A (acetyl-CoA) for use in the TCA-cycle. Acetyl-CoA is an important molecule that plays a role in many metabolic processes, including as a precursor molecule fuels ATP production via the TCA cycle (Pietrocola et

al. 2015). In cells under normal fed conditions, acetyl-CoA is derived from citrate in the TCA cycle by the enzyme ATP citrate lyase, ACLY. However, in tumors and cancer cells (Comerford et al. 2014) and low oxygen, stressed conditions (Schug et al. 2015), acetyl-CoA is generated from cytosolic acetate by the enzyme acetyl-CoA synthetase, ACSS2. Highlighting the importance of the amount of acetyl-CoA available to fuel the TCA cycle, it is very interesting that both genes have transcriptional memory in response to starvation. It has also been shown that the levels of acetyl-CoA can be correlated to acetylation levels (Kinnaird et al. 2016). These findings suggest that the availability of acetyl-CoA during starvation could be useful in understanding whether the memory of ACSS2 and ACLY gene expression plays a role in memory or is a consequence of a metabolic disruption resulting from energy imbalance triggered by the glucose starvation. The exploration of these questions could also provide insight on whether the levels of acetyl CoA in our system have an effect on acetylation of histones.

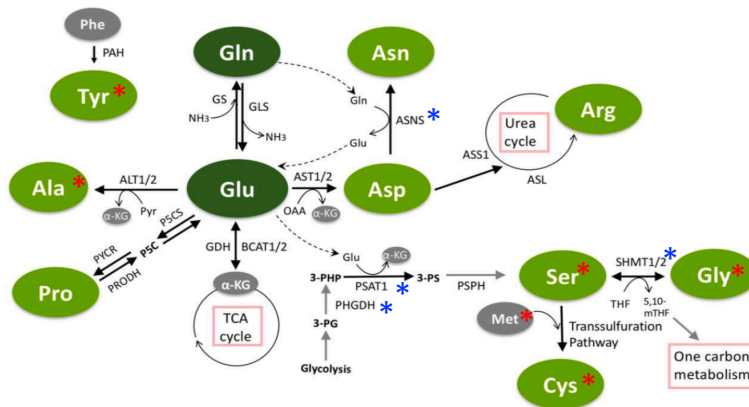
3.2.3 The Role of Amino Acid Metabolism in Memory

Upon further analysis of our memory gene groups, Gene Ontology (GO) analysis performed with the Enrichr database (Chen et al. 2013) provided insight onto other metabolic pathways that are affected. (Fig 2a). The most significantly enriched GO term was tRNA aminoacylation containing the genes CARS, YARS, WARS, MARS, SARS, GARS, and AARS. These genes encode for aminoacyl-tRNA synthetases, enzymes responsible for aminoacylation reaction, by covalently adding amino acids to tRNAs, in the first step of protein translation (Rajendran et al. 2018). Several of the amino acids that are reliant of these specific tRNA synthetases are involved non-essential amino metabolism, as well as other memory genes, ASNS, SHMT2, PSAT1, and PHGDH (Fig 2b and 2c).

a.

Term	P-value	Genes
tRNA aminoacylation (GO:0043039)	5.66E-11	CARS;YARS;WARS;MARS;SARS;GARS;AARS
tRNA aminoacylation for protein translation (GO:0043040)	1.56E-10	CARS;YARS;WARS;MARS;SARS;GARS;AARS
dicarboxylic acid metabolic process (GO:0043648)	9.26E-10	ACLY;MTHFD1L;MTHFD2;SHMT2;GPT2;MTHFR;ALDH1L2
foliac acid metabolic process (GO:0046655)	3.48E-09	MTHFD1L;SHMT2;MTHFD2;MTHFR;ALDH1L2
foliac acid-containing compound metabolic process (GO:0046656)	9.97E-09	MTHFD1L;SHMT2;MTHFD2;MTHFR;ALDH1L2
amino acid transport (GO:0006865)	1.17E-08	SLC43A1;SLC1A4;SLC3A2;SLC7A11;SLC38A3;SLC7A1
carboxylic acid transport (GO:0046942)	1.68E-08	SLC43A1;SLC1A4;SLC3A2;SLC7A11;SLC38A3;SLC7A1
L-serine metabolic process (GO:0006563)	4.93E-08	CBS;PSAT1;SHMT2;PHGDH
tetrahydrofolate metabolic process (GO:0046653)	7.10E-08	MTHFD1L;SHMT2;MTHFD2;MTHFR
serine family amino acid biosynthetic process (GO:0006564)	7.10E-08	CBS;PSAT1;CTH;PHGDH
nitrogen compound transport (GO:0071705)	1.57E-07	SLC43A1;SLC3A2;SLC1A4;SLC7A11;SLC38A3;SLC7A1
serine family amino acid metabolic process (GO:0006565)	2.34E-07	SHMT2;CBS;CTH;SARS
intrinsic apoptotic signaling pathway in response to DNA damage (GO:0006958)	1.22E-06	DDIT3;TRIB3;CHAC1;ATF4
L-amino acid transport (GO:0015807)	1.44E-06	SLC6A9;SLC1A4;SLC3A2;SLC38A3
neutral amino acid transport (GO:0015804)	1.44E-06	SLC6A9;SLC43A1;SLC1A4;SLC38A3
homocysteine metabolic process (GO:0050667)	2.71E-06	CBS;CTH;MTHFR
water-soluble vitamin metabolic process (GO:0006566)	5.45E-06	MTHFD1L;MTHFD2;SHMT2;MTHFR;ALDH1L2
PERK-mediated unfolded protein response (GO:0006959)	7.06E-06	DDIT3;ASNS;ATF4
translation (GO:0006412)	1.04E-05	CARS;YARS;WARS;MARS;SARS;GARS;AARS

b.



* Amino acid processed by tRNA synthetase memory gene

* Memory gene

c.

Amino Acid	Gene	Enzyme
alanine	AARS	alanyl-tRNA synthetase
* methionine	MARS	methionyl-tRNA synthetase
* glycine	GARS	glycyl-tRNA synthetase
* tyrosine	YARS	tyrosyl-tRNA synthetase
* serine	SARS	seryl-tRNA synthetase
* cysteine	CARS	cysteinyl-tRNA synthetase
tryptophan	WARS	tryptophanyl-tRNA synthetase

Figure 2: tRNA Aminoacylation genes are involved in glucose starvation memory. GO analysis of memory genes. (b) The pathway of non-essential amino acid metabolism, red * are amino acids from tRNA-synthetase that have memory and blue* denote other memory genes. *adapted from Choi, B. H. and J. L. Coloff, 2019. "The Diverse Functions of Non-Essential Amino Acids in Cancer." Cancers (Basel) 11(5).* (c) tRNA amino synthetase genes that exhibit memory

It has also been reported that ATF4 can regulate several of these tRNA synthetase genes through C/ebp-ATF4 response element (CARE) sequences, called CARE enhancers, at both the TSS but also at downstream location, where RNA Pol II enrichment is also found (Shan et al. 2016). The existence of an ATF4 mediated enhancer is a notion that is a very plausible regulator of memory and we have dedicated a considerable effort seeking such enhancers in our data analysis.

3.2.4 The Role of ATF4 in Memory

The transcription factor ATF4 plays a major role in the endoplasmic reticulum's (ER) response to stress. Disruption of the homeostasis of the ER leads to ER stress, and subsequently activates the unfolded protein response (UPR) program to re-establish normal function in the ER. Stressors include hypoxia, amino acid deprivation, and glucose starvation, all of which activate one or more of the 3 branches of the UPR response pathway (Corazzari et al. 2017). Glucose starvation activates the PERK-eIF2a-ATF4 branch of the UPR pathway in tumors (Wang and Kaufman 2014) and cancer cell lines (Mendez-Lucas et al. 2014). In addition to interacting directly with several memory genes, ATF4 expression is upregulated in response to PERK signaling, which is one of the major ER stress sensors involved in the UPR. (Hetz et al. 2011), further suggesting its possible importance to our memory phenotype. We expected that our ATF4 response to starvation is part of an ER mediated stress response, therefore we examined the expression of the gene responsible for PERK expression, as PERK is upstream to ATF4 in the ER stress response cascade. The gene expression of PERK oscillates slightly in response to glucose starvation, however its Log2 difference in gene expression is minor when compared with control, suggesting that PERK gene expression is not responding to glucose starvation in a time dependent manner thus PERK is not a direct member of our memory pathway.

3.3 Possible Mechanisms of Memory

3.3.1 Role of DNA Methylation

In addition to understanding the biological context of glucose starvation mediated memory in Huh7 cells, a main goal of our research is to unravel the mechanism mediating the transcriptional memory. A recent publication reported DNA hypermethylation at the promoter of memory gene ASNS in response to amino acid depletion of asparagine in

asparagine sensitive acute lymphatic leukemia (ALL) cells, resulting a lack of in an ATF4-dependent expression of ASNS. Hence, promoter hypomethylation is a prerequisite for ATF4 binding, however it is not sufficient for ASNS expression in the absence of ATF4 (Jiang et al. 2019). DNA methylation is a well characterized mechanism to transmit epigenetic memory to daughter cells (Bird 2002), therefore we are very curious to investigate DNA methylation at the promoters of memory genes. Additional implication of ATF4 on ASNS memory has been demonstrated in HepG2 cell deprived of amino acids. ATF4 has been shown to be required for expression of ASNS in HepG2 cells, coinciding with increased H3 occupancy at the promoter, even after cells are refed. (Balasubramanian, Shan, and Kilberg 2013)

3.3.2 Role of Histone Modifications in Memory

3.3.2.1 Data Analysis Strategy and Limitations

A main aim of our research is to characterize the epigenetic signature of the memory we observe in response to glucose starvation in Huh7 cells. For this reason, we performed a large scale ChIP-Seq for histone marks responsible for gene activation and repression, in transcriptional induction models. We were very interested in investigating the role of enhancers in memory and how repressive and active marks behaved in our memory system. We first approached our data analysis in an unbiased way to uncover histone modification signatures in our time points, with the assumption that a memory phenotype involving an enhancer-mediated memory would become apparent.

Unfortunately, after several iterations of data analysis with collaborators from the Institute of Computational Biology in the group of Dr. Maria Colomé-Tatché at Helmholtz Zentrum München, we were unsuccessful at uncovering a clear memory histone modification mechanism. Designing and executing data analyses for such complex data was one of the largest challenges of the project. We began our analysis using a top-down approach of

examining all the data together and looking for differences based on starvation conditions. However, it became evident after we validated our memory genes, that it is difficult to separate the robust expression response to starvation between the 835 UNN oscillating genes and the 65 memory genes. It was at this time that we took a more bottom up approach, by focusing on the characteristics of specific memory genes and comparing them to each other, as well as to differentiate them from the glucose responsive oscillating genes.

3.3.2.2 Enhancers

Despite our efforts to uncover a role for enhancers in the regulation of memory genes, we cannot provide concrete proof for, or against, their involvement. Ongoing analysis of our large scale NGS sequencing data sets are providing us with several options for studying enhancer function in our memory model. Combining the DNA-accessibility data from ATAC seq along with histone mark ChIP-Seq, we are exploring newly published analytical methods to investigate what role enhancers may play in the transcriptional regulation of memory genes.

3.4 Future Outlook

While we are still investigating the mechanism behind the regulation of our starvation-induced memory genes whose expression increases in response to subsequent starvations, we are also exploring what other information is contained in our large scale RNA-Seq, ChIP-Seq, ATAC-Seq and LC-MS data sets. In addition to the memory genes that increase their expression, we also have a list of genes that decrease their expression in response to starvations. Currently, our RNA-Seq analysis decision tree model is focused on the expression level changes of genes in response to starvation while using the recover/fed responses to determine as a baseline of expression for genes. We plan to create another

decision tree model in order to shift our memory focus to how genes respond in subsequent fed states, in response to starvation and study how these genes are regulated.

Additionally, we can use our large data set to gain insight into a more general response to glucose starvation in our Huh7 cells. In essence, the glucose starvation model we are using is a very reliable system of gene induction, thus we can use our data to categorize a more general gene induction in response to glucose in Huh7 cells and further explore our data to study transcription.

Overall, we have successfully identified and characterized a robust glucose starvation responsive transcriptional memory in human liver cancer cells. Next, we will determine if this memory is specific to liver cells or cancer cells and how it is established and maintained. The implications of this type of adaptive memory in cancer cells provides insight on cancer metabolism and may lead to novel approaches to cancer research through perturbations of this adaptation. It would also be interesting to explore whether other cellular stresses, such as amino acid deprivation or hypoxia, result in a similar transcriptional memory.

4 Materials and Methods

4.1 Cell Culture

4.1.1 Cell Line Culture

Human hepatocarcinoma cell line, Huh7, was cultivated in Dulbecco's Modified Eagle's Media (DMEM) – high glucose with 4500 mg/L (25mM) glucose and sodium bicarbonate, supplemented with L-glutamine, Penicillin-streptomycin, non-essential amino acids, and sodium pyruvate.

Human liver carcinoma cell line, HepG2 was cultivated in Eagle's Minimum Essential Medium, supplemented with L-glutamine, Penicillin-streptomycin, at 37 °C, 5% CO₂.

For glucose starvation experiments, Huh7 (or HepG2) cells are counted and plated, then cultured in 25mM glucose containing DMEM for 24 hours prior to the start of the experiments. Cells are washed 2 times with PBS and 0mM glucose containing DMEM media was added to the cells at time 0. For refeeding, 0 mM glucose DMEM media is removed and 25mM glucose DMEM is added to the plate.

4.1.2 Primary Hepatocyte Culture

Primary hepatocytes were isolated from C57BL/6NHsd male mice via collagenase perfusion as described previously (Zeigerer et al. 2012) . Cells were cultured in collagen gel-coated 24-well plates at 200,000 cells/well in WilliamsE medium; substituted with 10% FBS, 100 nM dexamethasone, and penicillin/streptomycin; and maintained at 37 °C, 5%CO₂. After 2 hours of attachment, cultures were washed with PBS. Thereafter cells were washed with PBS and coated with collagen. After 24 hours, hepatocytes were either starved from glucose, cells were washed 2 times with PBS, then DMEM with 0mM

glucose was added for time points indicated or for glucagon experiments, hepatocytes were for treated with 25mM glucagon for indicated time point.

4.1.3 siRNA Knockdown

For siRNA Transfections, cells were seeded to 60-80% Confluence, 1×10^5 in 6 well dish. For each reaction, 9 μ l Lipofectamine RNAiMAX Reagent was diluted in 150 μ l OptiMEM in a 1.5mL tube. In a separate tube, 6 μ l of 20uM stock of siRNA was diluted in 150 Opti-Mem Medium, mixed then added to the diluted Lipofectimine RNAiMAX tube and incubated at room temperature for 5 minutes. The siRNA-lipid complex is then added to the cells in the 6 well dish. Cells used for experiments after 24 hours of siRNA treatment.

4.2 Transcription

4.2.1 RNA Extraction

RNA extraction: 1×10^5 - 2×10^6 cells were either trypsinized and pelleted, or lysed directly in cell culture dish and processed according to manufacturer's directions with the Quick RNA Miniprep kit, including a 15 minute DNase treatment and eluted in 30 μ l RNase, DNase-free water. RNA is measured using Multiskan plate reader, uDrop microplate.

4.2.2 cDNA Synthesis

Using 150ng-1 μ g RNA, cDNA was prepared with RevertAid First Strand cDNA Kit with Oligo(dt) primer for gene expression Real Time qPCR and Random Primer for Nuclear Run-On (Nascent) RNA experiments according to manufacturer's instructions.

4.2.3 qPCR- Quantitative Real Time PCR

In a 25 μ l reaction volume, Absolute Blue qPCR SYBR Green 2x Mix (12.5 μ l), water (10.15 μ l), 50 μ M Primers, forward and reverse 1:1 mix (0.35 μ l) plus 2 μ l cDNA. Reaction was run in 96 well plates on the Roche LightCycler 480 or Roche 96 LightCycler Instrument Real-Time PCR Detection System

4.3 Fluidigm BioMark and Singular Single Cell qPCR

Transcriptional Profiling in Huh7 were sorted using a microfluidic chip (IFC, 10–17 mM) for in the Fluidigm C1 system. In brief, after trypsinization. Huh7 cells were washed by centrifugation with PBS to remove excess debris and loaded onto the IFC for single-cell sorting. After cell isolation, RNA was extracted and reverse transcribed using the C1 Single-Cell Auto Prep. Array for Pre-Amp.

qPCR was performed in the BioMark using the 96.96 IFC and Sample/Loading Kit for single cell and bulk population experiments using Delta gene custom expression assay. Analysis was performed with Singular Analysis Toolset 3.0, Graphpad Prism, and Microsoft Excel.

4.4 RNA-Seq

RNA samples were submitted to IGBMC Sequencing platform. For each condition, 3 technical replicates were sequenced. Libraries were prepared by platform for TruSeq Sample Prep Kit for stranded mRNA-seq and sequenced with single ended 50 base pair sequencing. Reads were mapped onto the hg38 assembly of human genome using Tophat (v2.0.14 2013) and bowtie2 (v2.1.0) aligner. For all conditions, total read count for individual samples were between 40 and 70 million reads with 92-95% aligned reads. Only transcripts that have greater than or equal to 10 counts in all conditions were analyzed.

Data normalization was performed using the TMM method (Robinson and Oshlack 2010) to correct for different library sizes and the quality of the data was checked by performing simple clustering, as well as principal component analysis. Limma analysis (Ritchie et al. 2015) was performed to determine memory genes, as described in the Results section-figure 9, only results with an output q-value greater or equal to 0.01 were deemed significant.

4.5 Protein

4.5.1 Protein Extraction

Scraped or trypsinized cells were centrifuged for at 1500 rpm for 5 min, and supernatant was removed. The pellet was resuspended 1ml PBS and transferred to 1.5 ml tube, spun at 1500 RPM and supernatant was removed. Cell pellet was stored at -80°C.

4.5.2 RIPA Extraction

The cell pellet was resuspended in 150-1000 µl RIPA Buffer plus Complete protease inhibitor then incubated on ice for 30 min, vortexed every 10min. The lysates were sonicated at 50% amplitude for 30sec ON, 30sec OFF for 5 min in the qSonica sonicator. The lysates were centrifuged at 14000 RPM at 4 °C for 15 min and the supernatant was transferred to new pre-cooled 1.5ml tube. The protein concentration was measured using the Pierce BCA Protein assay.

4.5.3 Western Blot

Proteins were loaded on an SDS Page Gel run at 180V for 60 min. The gel was transferred to nitrocellulose membrane for 1 hour at room temperature with ice insert at 250 mA. The transferred membrane was stained with Ponceau then blocked in 5% Milk TBS-tween20 (0.5%) for 1 hour, then the membrane was incubated with the primary antibody diluted in 5% BSA TBS-tween20 (0.5%) overnight at 4 °C. The next day the membrane was washed 3 times with TBS-tween20 (0.5%) for 10 min at room temperature on shaker. The membrane is then incubated with the species appropriate secondary antibody for 1 hour at room temperature on shaker, the washed 2 times with TBS-Tween20 and one time with TBS. Then the membrane is exposed with ECL reagent for 5 minutes and imaged on the BioRad Chemidoc Touch.

4.5.4 Fixation of Cells and Immunofluorescence

Cultured cells were fixed with paraformaldehyde (PFA) after cells were washed with cold PBS and 500 µl of 4% PFA was applied to the coverslips then incubated for 10 minutes at room temperature. The PFA was removed and coverslips were incubated with 500 µl ice cold 0.5% TritonX in PBS for 2 minutes at room temperature and at 4°C for 10 minutes. Coverslips were washed 2 times with cold PBS and stored at 4°C in PBS.

Immunofluorescence

Coverslips were blocked in 3ml 3% BSA/1X PBS-Tween20 (0.5%) (PBST) for 1 hour at room temperature on the shaker, then aspirated. Primary antibody was diluted in 3% BSA/1X PBST and applied to the coverslips for 1 hour in a wet chamber. Cells were washed 3 times with PBST for 15 min each wash on the shaker. Cells were incubated with

appropriate secondary antibody diluted in 3% BSA/1X PBST for 1 hour at room temperature in a wet chamber. Cells were washed 2 times with PBST, and 1 time with PBS for 15 min each wash on the shaker. Coverslip were mounter onto slides with Vector shield mounting media with DAPI (Vectorlabs).

4.6 Chromatin Immunoprecipitation (ChIP)

Huh7 cells were grown on 15cm² plate (~1e⁷ cells per 15cm² plate) and crosslinked at room temperature (RT), under fume hood with 1% formaldehyde (0.583ml of 37% formaldehyde solution in 21 ml cell culture media) for 10 min with intermittent agitation. The plates were quenched with 1.5 ml of 2.5M glycine for 5 minutes with intermittent agitation. The plates were aspirated and washed 2 times with 20 ml cold PBS. Cells were harvested with cell lifter in 5ml of Scraping buffer (PBS with NaBu and Complete protease inhibitor). For memory experiment, 300 µl of cells was removed for RNA extraction to test for induction. Cells were centrifuged at 1260g (2500rpm) in 4°C for 10min then the supernatant was aspirated and sample was frozen at -80°C until all time points we collected Add 12ul Complete, Frozen at -80 °C.

After all time points were collected, cell pellets were resuspended in 1ml Lysis Buffer 1 (L1) (plus NaBu and Complete) and incubated on ice for 5 min then spun down to pellet nuclei at 800 x g for 5 min at 4°C. Nuclei are resuspended in Lysis Buffer 2 (L2) (plus NaBu and Complete). The nuclei were divided into equal volumes of 300-600 µl per tube then sonicated at 80% amplitude for 20sec ON, 40sec OFF for 25 min in the qSonica sonicator. The sonicated samples were centrifuged for 10 minutes at 14 000 x g at 4°C to remove cell debris. Supernatant was transferred to a 1.5 ml tube and chromatin concentration was measured, 15µg of sonicated chromatin was tested for sonication quality by decrosslinking in a final volume of 500 µl DB buffer with 20 µl NaCl 5M (0.2M) at 65°C overnight on with shaking then the sample was purified using the QIAquick PCR

Purification kit and 10 μ l of sample was run on a 1.5% agarose gel to confirm sonicated DNA sizes between 100 and 600 base pairs.

To Pre-block protein A/G – sepharose beads, 500 μ l of Protein A – sepharose beads was mixed with 500 μ l of Protein G sepharose in a 2 mL centrifuge tube then centrifuged for 2 minutes at 4,000 rpm and the supernatant was discarded. The A/G beads mix was washed twice with 1 mL of TE (each time vortex and centrifuged as described) the resuspend in 1ml TE. For blocking, 100 μ l of BSA (10mg/ml) and 200 μ L of denature tRNA (95C for 5 minutes) (sigma) was added to. to the 1 ml bead mixture and incubated for 2 hours with rotation at 4°C. Blocked beads were washed with 1 ml TE, as above, and resuspended in 500 μ l TE. 60 μ g of chromatin was diluted in dilution buffer (DB) to a final volume of 500 μ l in DNA low binding tubes then pre-cleared with 30 μ l of clocked A/G beads for 1 hour at 4°C with overhead rotation then centrifuged for 1 min at 4000 rpm and supernatant was transferred to new 1.5ml. For Input control, 1% (0.6 μ g) chromatin was added to 300 μ l elution buffer (EB) and set aside.

For immunoprecipitation (IP), a pre-determined amount of antibody was added to the 60 μ g of pre-cleared chromatin and incubated overnight at 4°C with overhead rotation. The next day, 50 μ l pre-blocked Protein A/G - Sepharose beads were added and incubated 2h at 4°C with overhead shaking. The IP'ed chromatin was centrifuged for 1 min at 5000rpm RT and supernatant was discarded and the beads were resuspended in 1 ml Washing buffer and incubated at room temperature with overhead shaking then centrifuged for 5 min at 5000rpm at RT and supernatant was discarded. The wash was repeated 1 more time with Wash buffer and 1 time with Final wash buffer. IP'ed chromatin was eluted from the beads in 150 μ l EB, with a 10 min incubation at room temperature with overhead shaking then centrifuged for 5 min at 5000 rpm at RT and supernatant was transferred to a new tube, repeat for a final elution volume of 300 μ l. Next, samples were de-crosslinked with 12 μ l of 5M NaCl and 1.56 μ l of 10mg/ml RNase A and incubated at 37°C for 30

min then 1 μ l of 20mg/ml Proteinase K was added and incubated for 5-16 hours at 65°C with shaking. Samples were then purified using the QIAquick PCR Purification kit by diluting in 5 volumes (1500 μ l) of Binding buffer and ultimately eluted in 50 μ l Qiagen elution buffer. Samples are stored at -20°C or used in ChIP qPCR or for ChIP-Seq Library preparation.

4.6.1 ChIP-Seq Library Preparation

For Histone and RNA Pol II ChIP: ChIP samples were submitted to IGBMC Sequencing platform. Libraries were prepared by platform using Diagenode MicroPlex Library Preparation kit.

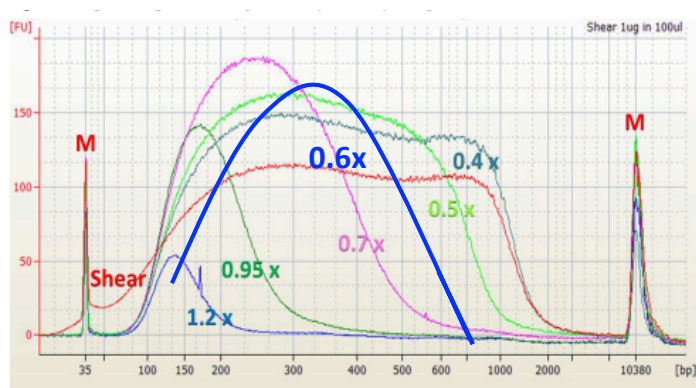
For ATF4 ChIP-Seq, ChIP'ed chromatin's quality was checked using the Qubit dsDNA HS Kit as per manufacturer's instructions. Library preparation for ChIP-Seq was done with the NEBNext Ultra II DNA Library Prep Kit for Illumina as per manufacturer's instructions, with supplementary notes for customization for our experiments (see following notes). ChIP-Seq libraries were prepared with 10ng ChIP sample diluted in 0.1X TE. Step 1, NEBNext End Prep was performed as per kit instructions. Step 2, Adaptor Ligation- NEBNext Adaptor for Illumina was diluted 10 fold (1:10 dilution) for a 1.5 μ M working adaptor concentration. Step 3B was performed, Cleanup of Adaptor-ligated DNA without Size Selection

PCR Enrichment of Adaptor-ligated DNA

For Step 4.1 PCR Amplification, we performed step 4.1.1A- for amplification when forward and reverse adaptor primers are in separate tubes in kit NEBNext Multiplex Oligos for Illumina. For step, 4.1.3. The cycling conditions for the PCR amplification were:

CYCLE STEP	TEMP	TIME	CYCLES
Initial Denaturation	98°C	30 seconds	1
Denaturation Annealing/ Extension	98°C 65°C	10 seconds 75 seconds	7
Final Extension	65°C	5 minutes	1
Hold	4°C	∞	

For the cleanup of PCR reaction, run the libraries from the final elution on the BioAnalyzer with a HS DNA chip to determine library size (optimal fragment size 200-600bp). Perform size selection to optimize library size for fragments between 200-600bp for a right size selection using the ratio SPRIselect volume of 0.6x (Fig 1).



M = upper and lower markers for High Sensitivity DNA chip.

Figure 1: Fragment Size Selection: BioAnalyzer track to highlight optimal size selection ratio of beads

30 μ l of Ampure beads (0.6x *50 μ l) were added to the ChIP-Seq libraries and mixed by pipetting up and down 10 times and samples were incubated at RT for at least 5 min. Tubes were placed on a magnetic rack when the beads settled against the wall of the tube, transfer the cleared supernatant to a new tube and the beads were discarded. To bind the size sized DNA, 45 μ l (0.9x) beads were added to the supernatant and mixed and incubated for 5 min at RT. The tubes were placed on the magnetic stand and the cleared supernatant was discarded. On the magnetic stand, the beads were washed twice with 80% freshly prepared ethanol and after the second wash, the residual liquid was removed and beads were dried for 5 min at RT. After the tube was removed from the magnetic rack, 21 μ l of

0.1X TE was used to elute the DNA from the beads by mixing and 2 minutes of incubation at RT. The tube was placed back on the magnetic rack and when supernatant cleared, transfer 20 μ l to a new tube. The sample for measured using the BioAnalyzer High Sensitivity chip to confirm 200-600 bp fragment.

Prepared ChIP libraries were submitted to Helmholtz Next Generation sequencing core facility for 50 bp paired end sequencing on the Illumina 4500. Sequence reads were mapped to reference genome hg38 using Bowtie (Langmead et al. 2009). Total reads ranged from 25 to 40 million reads with approximately 80% of reads mapped.

ChIP-Seq Analysis

For Histone and RNA Pol II ChIP-Seq processed by the IGBMC Sequencing platform, samples were sequenced by 50 bp paired end sequencing on the Illumina 4500. Total reads for individual samples ranged from approximately 60 to 115 million reads, with approximately 60 to 80% of reads mapped, and mapped to genome hg38. Alignment was performed using Bowtie 1.0.0 (Langmead et al. 2009) and quality control was performed using FastQC analysis tool ("FastQC" 2010).

For all ChIP-Seq samples, peak calling was performed using MACS-2 (Zhang et al. 2008) using standard parameters and calling narrow peaks. Peak location annotation was performed using ChipSeekr (Yu, Wang, and He 2015). Raw reads were used to plot expression across the TSS.

4.7 ATAC seq

For the cell lysis, Huh7 cells were trypsinized, counted and 50,000 cells in a volume of 50 μ l TE were transferred to a 1.5ml tube and centrifuged at 1200 rpm to pellet cells and supernatant was discarded. Lysis buffer (10 μ l of 1M Tris·Cl, pH 7.4 (final 10 mM), 2 μ l of 5M NaCl (final 10 mM), 3 μ l of 1M MgCl₂ (final 3 mM), 10 μ l of 10% NP-

40 (final 0.1% v/v), and 975 μ l nuclease-free H₂O) was freshly prepared, on ice and 50 μ l was added to cell pellet and pipetted up and down to resuspend cells. Lysed cells were centrifuged at 500 x g for 10 minutes at 4°C and supernatant (cytoplasm) was discarded, and pellet (nuclei) was kept.

For the transposition, transposition reaction mix was prepared using the Nextera DNA Library Prep. For volumes per sample of 50,000 cells, 50 μ l transposition reaction mix was prepared with 25 μ l of 2X TD Buffer, 2.5 μ l of Tn5 Transposase and 22.5 μ l of nuclease-free H₂O and added to pellet and mixed by pipetting up and down to resuspend nuclei then incubated at 37°C for 30 minutes. Next, the DNA is Purified using Qiagen MiniElute Reaction Cleanup Kit with the final elution of DNA in 10 μ l EB (Elution Buffer).

To generate the library, the DNA was amplified with indexed primers by combining 10 μ l of purified transposed DNA with 10 μ l of nuclease-free H₂O, 2.5 μ l of Ad1_noMX primer (25 μ M), 2.5 μ l of Ad2* (*depending on index number) indexing primer (25 μ M), and 25 μ l of NEBNext High-Fidelity 2X PCR Master Mix mixed in a PCR tube and amplified with the PCR program:

72°C	5 minutes	x5 cycles
98°C	30 seconds	
98°C	10 seconds	
63°C	30 seconds	
72°C	1 minute	

To determine how many more cycles of amplification is necessary, 5 μ l of the partially amplified library was removed and placed in a new tube.

Remove tubes from PCR machine and use 5 μ l of each partially-amplified library to perform qPCR to determine how many additional PCR cycles are needed. The goal is to stop amplification well prior to saturation to avoid variation among samples due to PCR bias. To this 5 μ l of partially-amplified library, 4.41 μ l of nuclease-free H₂O, 0.25 μ l of

Ad1_noMX primer, 0.25 μ l of Ad2* indexing primer, of 0.09 μ l 100X SYBR Green I, and 5 μ l of NEBNext High-Fidelity 2X PCR Master Mix were added to 96 well plate and mixed, then run in a qPCR machine for the program:

98°C	30 seconds	
98°C	10 seconds	x20 cycles
63°C	30 seconds	
72°C	1 minute	

In order to calculate the number of additional PCR cycles needed for each sample, we examined the plot of R vs Cycle Number and by determined the number of cycles needed to reach 1/3 of the maximum R. Using the remaining 45 μ l of the partially-amplified library run the PCR for the appropriate number (N) of cycles (in our experiment it was 7 additional cycles).

98°C	30 seconds	
98°C	10 seconds	xN cycles (7)
63°C	30 seconds	
72°C	1 minute	

To remove primer dimers, single left-sided bead purification was performed by adding 1.8X volume (81 μ l) of AMPure XP beads and mixed by pipetting up and down 10 times then incubated at room temperature for 10 minutes. The tubes were placed on the magnetic stand and the cleared supernatant was discarded. On the magnetic stand, the beads were washed twice with 80% freshly prepared ethanol and after the second wash, the residual liquid was removed and beads were dried for 5 min at RT. After the tube was removed from the magnetic rack 20 μ l nuclease-free H₂O was used to elute the DNA from the beads by mixing and 2 minutes of incubation at RT. The tube was placed back on the magnetic rack and when supernatant cleared, transfer 20 μ l to a new tube. Purified libraries can be stored at -20°C.

Before submitting for sequencing, the library quality was assessed by testing a 1:3 dilution of library in water on a Bioanalyzer DNA High Sensitivity chip and with the Qubit High Sensitivity DNA kit. ATAC libraries were submitted to Helmholtz Next Generation sequencing core facility for 50 bp paired end sequencing on the Illumina 4500. Sequence reads were mapped to reference genome hg38 using Bowtie2(Langmead et al. 2009). Peaks were called using MACS-2 (Zhang et al. 2008) and annotated using Homer (Heinz et al. 2010). Raw reads were used to plot expression across the TSS while downstream analysis investigating differentially accessible regions was performed by edgeR (Robinson, McCarthy, and Smyth 2010) though not shown.

Materials

4.8 Antibodies

Antibody	Species	Dilution WB	Company	Ordering info
Alpha Tubulin	mouse	WB 1:5000, IF 1:1000	Abcam	ab7291
ATF4 (D4B8)	rabbit	WB 1:500, IF 1:250, ChIP 3 μ l	Cell Signaling	11815
H3 C-term	rabbit	ChIP 2 μ L	Abcam	ab1791
H3K27ac	rabbit	ChIP 5 μ l	Abcam	ab4729
H3K27me3	rabbit	ChIP 5 μ l	Active Motif	39155
H3K4me1	rabbit	ChIP 2 μ l	Abcam	ab8895
H3K4me3	rabbit	ChIP 1 μ L	Millipore	17-614
H3K9ac - ChIP grade	rabbit	ChIP 5 μ L	Abcam	ab4441
PCK2	rabbit	WB 1:3000	Pierce (Thermo Scientific)	PA5-28078
RNA polymerase II CTD repeat YSPTSPS	mouse	ChIP 10 μ L	Abcam	ab817
RNA Polymerase II Ser2P	rat	ChIP 200 μ L	gift from lab of Dirk Eick	
RNA Polymerase II Ser5P	rat	ChIP 200 μ L	gift from lab of Dirk Eick	

4.9 Consumables

Product	Manufacturer
1.5ml Eppendorf tubes, safe lock cap	Eppendorf, Wesseling-Berzdorf, Germany
2.0ml Eppendorf tubes, safe lock cap	Eppendorf, Hamburg, Germany
2X ABsolute Blue qPCR SYBR Green Mix	Thermo Fisher Scientific, Waltham, USA
Acrylamide 40%	SERVA Electrophoresis, Heidelberg, Germany
Agarose	Carl Roth, Karlsruhe, Germany
Agencourt AMPure XP magnetic beads (Beckman Coulter)	Agilent Technologies, Waldbronn
Agilent High Sensitivity DNA Bioanalysis Kit	Agilent Technologies, Waldbronn
Ammonium persulfate (APS)	Carl Roth, Karlsruhe, Germany
Ampicillin (1000x stock at 50 mg/mL)	Carl Roth, Karlsruhe, Germany
BCA Protein Assay Kit (Pierce)	Thermo Fisher Scientific, Waltham, USA
Beta-mercaptoethanol	Carl Roth, Karlsruhe, Germany
Bovine Serum Albumin Fraction V	Carl Roth, Karlsruhe, Germany
C1™ Single-Cell Preamp IFC, 10–17 µm	Fluidigm, San Francisco, USA
Cell culture dish 100 mm	Greiner Bio One Frickenhausen, Germany
Cell culture dish 60 mm	Greiner Bio One Frickenhausen, Germany
cOmplete EDTA-free protease inhibitor cocktail	Roche, Basel, Switzerland
Coomassie brilliant blue	Carl Roth, Karlsruhe, Germany
Corning cell lifter	Sigma-Aldrich, St. Louis, USA
Coverslips	Thermo Fisher Scientific, Waltham, USA
Delta Gene™ Assays	Fluidigm, San Francisco, USA
Dexamethasone	Sigma-Aldrich, St. Louis, USA

Product	Manufacturer
Dimethyl sulfoxide (DMSO)	Carl Roth, Karlsruhe, Germany
DMEM (Dulbecco's Modified Eagle Medium), no glucose (GIBCO)	Thermo Fisher Scientific, Waltham, USA
DMEM Dulbecco's Modified Eagle's Medium - high glucose With 4500 mg/L glucose and sodium bicarbonate	Sigma-Aldrich, St. Louis, USA
Eagle's Minimum Essential Medium	Sigma-Aldrich, St. Louis, USA
ECL detection reagent	Bio-Rad Laboratories, München, Germany
Ethanol (EtOH) 100%	Carl Roth, Karlsruhe, Germany
Ethylenediaminetetraacetic acid (EDTA)	Carl Roth, Karlsruhe, Germany
Fetal bovine serum (FBS) (GIBCO)	Thermo Fisher Scientific, Waltham, USA
Formaldehyde 37%	Sigma-Aldrich, St. Louis, USA
GE 96.96 Dynamic Array DNA Binding Dye Sample & Assay Loading Reagent Kit	Fluidigm, San Francisco, USA
Glycerol	Carl Roth, Karlsruhe, Germany
Glycine	Carl Roth, Karlsruhe, Germany
Hydrochloric acid (HCl)	Carl Roth, Karlsruhe, Germany
IGEPAL CA-630®	Sigma-Aldrich, St. Louis, USA
L Glutamine 200 mm	Sigma-Aldrich, St. Louis, USA
L-glutamine solution	Sigma-Aldrich, St. Louis, USA
Lipofectamine RNAiMAX Reagent (GIBCO)	Thermo Fisher Scientific, Waltham, USA
Magnesium chloride (MgCl ₂)	Carl Roth, Karlsruhe, Germany
MEM Non-essential Amino Acid Solution 100X	Sigma-Aldrich, St. Louis, USA
MicroPlex Library Preparation Kit v3	Diagenode Inc., Denville, USA

Product	Manufacturer
MinElute Reaction Cleanup Kit	Qiagen, Hilden, Germany
NEBNext High-Fidelity 2X PCR Master Mix	New England Biolabs, Frankfurt a.M., Germany
NEBNext Multiplex Oligos for Illumina	New England Biolabs, Frankfurt a.M., Germany
NEBNext Ultra II DNA Library Prep Kit for Illumina	New England Biolabs, Frankfurt a.M., Germany
Nextera DNA Library Prep Kit	Illumina Inc., San Diego, USA
NP40	Sigma-Aldrich, St. Louis, USA
Opti-MEM™ I Reduced Serum Medium (GIBCO)	Thermo Fisher Scientific, Waltham, USA
Paraformaldehyde	Sigma-Aldrich, St. Louis, USA
PBS: Dulbecco's phosphate buffered saline	Sigma-Aldrich, St. Louis, USA
Penicillin-Streptomycin	Sigma-Aldrich, St. Louis, USA
Ponceau Red S	Sigma-Aldrich, St. Louis, USA
Powdered milk, blotting grade	Carl Roth, Karlsruhe, Germany
Proteinase K	Sigma-Aldrich, St. Louis, USA
Qubit dsDNA HS Assay Kit	Thermo Fisher Scientific, Waltham, USA
Quick-RNA Miniprep Kit	Zymo, Freiburg, Germany
RevertAid First Strand cDNA Kit	Thermo Fisher Scientific, Waltham, USA
RNAse A	Sigma-Aldrich, St. Louis, USA
Sodium bicarbonate (NaHCO ₃)	Carl Roth, Karlsruhe, Germany
Sodium Butyrate (NaBU)	Alfa Aesar, Haverhill, USA
Sodium chloride (NaCl)	Carl Roth, Karlsruhe, Germany
Sodium deoxycholate (NaDOC)	Sigma-Aldrich, St. Louis, USA

Product	Manufacturer
Sodium dihydrogen phosphate (NaH ₃ PO ₄)	Carl Roth, Karlsruhe, Germany
Sodium dodecyl sulfate (SDS)	Carl Roth, Karlsruhe, Germany
Sodium hydroxide (NaOH)	Carl Roth, Karlsruhe, Germany
Sodium Pyruvate Solution	Sigma-Aldrich, St. Louis, USA
SYBR Green I	Thermo Fisher Scientific, Waltham, USA
Tetramethylethylenediamine (TEMED)	Carl Roth, Karlsruhe, Germany
Tris-Base	Sigma-Aldrich, St. Louis, USA
Tris-HCl	Sigma-Aldrich, St. Louis, USA
Triton X-100	Carl Roth, Karlsruhe, Germany
TruSeq Stranded mRNA Library Prep	Illumina Inc., San Diego, USA
Trypan blue	Thermo Fisher Scientific, Waltham, USA
Trypsin-EDTA solution	Sigma-Aldrich, St. Louis, USA
Tween-20	Sigma-Aldrich, St. Louis, USA
Vector mounting media with DAPI	Vector Laboratories, Burlingame, USA
William's Medium E, w: L-Glutamine, w: 2.24 g/L	PAN-Biotech, Aidenbach, Germany
NaHCO ₃	

4.10 Buffers

Name	Composition
1x Phosphate-Buffered Saline (PBS)	10mM Na ₂ HPO ₄ 2mM KH ₂ PO ₄ 2.7mM KCl 137mM NaCl (adjust to pH 7.2)
1x Phosphate-Buffered Saline Tween (PBST)	10mM Na ₂ HPO ₄ 2mM KH ₂ PO ₄ 2.7mM KCl 137mM NaCl (adjust to pH 7.2) 0,5% Tween-20
1x Tris-Buffered Saline Tween (TBST)	150mM NaCl 50mM Tris-HCl pH 8 0,2% Tween-20
1x Tris-EDTA (TE)	10mM Tris-HCl (pH 8.0) 1mM EDTA (pH 8.0)
4x Laemmli Loading buffer	250mM Tris-HCl (pH 6.8) 20% `Beta-mercaptoethanol 2% SDS 0.1% Bromphenol blue 40% Glycerol

Name	Composition
10x Glycine transfer buffer (Western blot)	247mM Tris-HCl 1.9M Glycine
10x SDS running buffer (Western blot)	247mM Tris-HCl 1.9M Glycine 0.5% SDS
Cell Lysis (ATAC-Seq)	10mM Tris·Cl, pH 7.4 10mM NaCl 3mM MgCl ₂ 0.1% NP-40
Dilution Buffer (ChIP)	1% Triton X-100 2mM EDTA (pH 8.0) 150mM NaCl 20mM Tris-HCl (pH8.0)
Elution Buffer (ChIP)	100mM NaHCO ₃ 1%SDS
Final wash buffer (ChIP)	0.1% SDS 0.5% NP40 2mM EDTA 500mM NaCl 20mM Tris-HCl (pH 8.0)
L1 lysis buffer (ChIP)	50mM Tris-HCl (pH 8.0) 2mM EDTA (pH 8.0) 0.1% NP40 10% Glycerol

Name	Composition
L2 lysis buffer (ChIP)	1% SDS 10mM EDTA 50mM Tris-HCl (pH 8.0)
Ponceau S staining solution	0.5% (w/v) Ponceau S 1% Acetic acid
RIPA Buffer	0.2% SDS 1% Triton-X 1mM EDTA 150mM NaCl 50mM Tris-HCl pH8 0.5% NaDOC
SDS running gel (Western blot)	6 to 18.7% Acrylamide 375mM Trip-HCl (pH 8.8) 0.1% SDS
SDS stacking gel (Western blot)	5% Acrylamide 125mM Trip-HCl (pH 6.8) 0.1% SDS
Wash buffer (ChIP)	0.1% SDS 0.5% NP40 2mM EDTA 150mM NaCl 20mM Tris-HCl (pH 8.0)

4.11 Primers

4.11.1 Human Expression Primers

Name	5'-3' sequence
AARS_15/16_F	GGCTCCCTGACTTCTGTTGA
AARS_15/16_R	CTTCTTCCGTCACGATCACA
ACSS2_14/15 F	ACGAACGCTTTGAGACAACC
ACSS2_14/15 R	ATCAATCCTGCCAGTGATCC
ASNS_7/8_F	AAGACAGCCCCGATTTACTG
ASNS_7/8_R	AGAGCCTGAATGCCTTCCTC
CHAC1_1/2_F	CTACAGCCGCCGTTTCTG
CHAC1_1/2_R	GATCTTCAAGGAGCGTCACC
hATF4_1/2 F	CTGTGGATGGGTTGGTCAGT
hATF4_1/2 R	GCATCCAAGTCGAACTCCTT
hATG7_11/12 F	ACCTTGGGTTGCAATGTAGC
hATG7_11/12 R	CTGCCTCACAGGATTGGAGT
hB2M F	TGAAGCTGACAGCATTCGG
hB2M R	CTGCTGGATGACGTGAGTAAA
hCEBPG Ex1 F	TGGTTCACAAAACACCTCA
hCEBPG Ex1 R	TGCTGTGGACGACTCAAGTT
hCREBH F	AGCTGGTGCTCACCGAGGAT
hCREBH R	TGCTTTCTTGCGCCGACTGC

Name	5'-3' sequence
hDDIT3_3/4_01 F	GGGGGTACCTATGTTTCACCT
hDDIT3_3/4_01 R	CTCCTCCTCAGTCAGCCAAG
hFBP1_6/7 F	ATGGCCTACGTCATGGAGAA
hFBP1_6/7 R	GCCCTCTGGTGAATGTCTGT
hGOT1_2/3 F	GGAGCTGTGCTTCTCGTCTT
hGOT1_7/8 F	CAGGGTTAGAGAGGGTGCTG
hLC3a_2/3 F	CGACCGCTGTAAGGAGGTA
hLC3a_2/3 R	CAGCTGCTTCTCACCTTGT
hPC_15/16 F	GTGGGCTACACCAACTACCC
hPC_15/16 R	TTGAGGGAGTCAAACACACG
hPCK1_5/6 F	GTGCTTTGCTCTCAGGATGG
hPCK1_5/6 R	CCGCCAGGTA CTTCTTCTCA
hPCK2_5/6 F	CCCTACGCATCGCCTCTC
hPCK2_5/6 F	CCCTACGCATCGCCTCTC
hPCK2_5/6 R	TGCCACATAGCGCTTCTTC
hPCK2_5/6 R	TGCCACATAGCGCTTCTTC
hPCK2_preSlc_ Ex2b F	CCACTGGCATTTCGAGATTTT
hPCK2_preSlc_ Ex2b R	TCTCAGCCTCAGTTCCATCA
hPCK2_preSlc_ Int-Ex2a F	CAGCCCAAGCTTTCTGTCTC
hPCK2_preSlc_ Int-Ex2a R	CCCATGCCAGTTAAGCCTAT
hPCK2_preSlc_ Int2a F	AGGTCTCCGCATATCCTCCT
hPCK2_preSlc_ Int2a R	CTGCTGCCTCTCGAAGTACC
hPFKL_16/17 F	TCCGACACTGCTGTAAATGC
hPFKL_16/17 R	GTCTCCACGATGAACACACG

Name	5'-3' sequence
hSHMT2_4/5 F	AGCCCTTCTGCAACCTCAC
hSHMT2_4/5 R	GTGGCTGATATCCGCTTGAC
hULK1_25/26 F	GTGCCATCGACCAGATCC
hULK1_25/26 R	GCTGGCCTTGTACAGCTCAT
STC2_2/3_F	GGCTTACATGGGATTTGCAT
STC2_2/3_R	AGCGTGGGCCTTACATTTTC

4.11.2 Mouse Expression Primers

Name	5'-3' sequence
mAcss2_13/14 F	GCCTGCAATCCTGAATGAGT
mAcss2_13/14 R	CCATAGACTGTGCGCATGAT
mB2m F	AGA CTG ATA CAT ACG CCT GCA
mB2m R	GCA GGT TCA AAT GAA TCT TCA G
mDdit3_3/4_1 F	GGAGGTCCTGTCCTCAGATG
mDdit3_3/4_1 R	GGACGCAGGGTCAAGAGTAG
mFoxo1_2 F	CTTCAAGGATAAGGGCGACA
mFoxo1_2 R	TCCTTCATTCTGCACTCGAA
mGpt2_10/11 F	GTATGCGTTCCTCGGATT
mGpt2_10/11 R	TCCAGGAGCTTCATGCAGTA
mPck1_6/7 F	GATGACATTGCCTGGATGAA
mPck1_6/7 R	CTTCACTGAGGTGCCAGGAG
mPck2_8_9 F	AGCACCAGAAGGTGTCCCTA
mPck2_8_9 R	CATGGCGCTACCTACAAACA

mPcx_14/15 F	GTGGGCTACACCAACTACCC
mPcx_14/15 R	AAAGACTCGGAAGACGTCCA
mPklr_7_8 F	GGCTCAGAAGATGATGATTGG
mPklr_7_8 R	CGAGTTGGTCGAGCCTTAGT

4.11.3 Human ChIP Primers

Name	5'-3' sequence
ChIP_hACSS2_Exon2 F	CCCATTCCTTCGGTACAACCT
ChIP_hACSS2_Exon2 R	TCATGGACATTTTCGATCCAG
ChIP_hACSS2_TSS-200bp F	CCCAACCCCTTATCTGTCCAC
ChIP_hACSS2_TSS-200bp R	TGGAGTGATGGGGAGTAACC
ChIP_hACSS2_TSS-50+50bp F	CCCTTCTGCTTTCACTCGAC
ChIP_hACSS2_TSS-50+50bp R	GAGGTTGGCAAGGACAGAAA
ChIP_hACSS2_TSS+250bp F	ACTTGACGTGATGGGGCTTC
ChIP_hACSS2_TSS+250bp R	CTCCGGCTCCAGCTTCCT
ChIP_hASNS TSS -50 F	TTCCCGAAGAACAACCAAG
ChIP_hASNS TSS -50 R	CAGTGCGCCTGTTTAAGGAT
ChIP_hB2M_Exon2 F	TTTCATCCATCCGACATTGA
ChIP_hB2M_Exon2 R	CCAGTCCTTGCTGAAAGACA
ChIP_hB2M_TSS-80+40bp R	GCGACGCCTCCACTTATATT
ChIP_hB2M_TSS+150bp F	GAGGCTATCCAGCGTGAGTC
ChIP_hB2M_TSS+150bp R	GAAGTCACGGAGCGAGAGAG
ChIP_hHBB_TSS-180bp F	TGGTATGGGGCCAAGAGATA
ChIP_hHBB_TSS-180bp R	GATGACAGCCGTACCTGTCC

Name	5'-3' sequence
ChIP_hHBB_TSS-50+50bp F	AGTCAGGGCAGAGCCATCTA
ChIP_hHBB_TSS-50+50bp R	CTCAGGAGTCAGATGCACCA
ChIP_hHBB_TSS+250bp F	TTGGACCCAGAGGTTCTTTG
ChIP_hHBB_TSS+250bp R	CTTTCTTGCCATGAGCCTTC
ChIP_hPCK2_Exon2 F	CCACTGGCATTTCGAGATTTT
ChIP_hPCK2_Exon2 R	TGGCAGTATTCTCAGCCTCA
ChIP_hPCK2_Exon4 F	GCACCATGTATGTGCTTCCA
ChIP_hPCK2_Exon4 R	GCCACCACATAGGCTGAGTC
ChIP_hPCK2_TSS-300bp F	GAGGAACTGGAAAGGCAATG
ChIP_hPCK2_TSS-300bp R	AGGTGGCAAACAAGCTAGGA
ChIP_hPCK2_TSS+120bp F	GTTTGGAGGCAGGGGTTG
ChIP_hPCK2_TSS+120bp R	TAGGGCTGGCACTAGCTTTC

4.11.4 ATAC-Seq Primers

Name	5'-3' sequence
Ad1_noMX	AATGATACGGCGACCACCGAGATCTACACTCGTCGGCAGCGTCAGATGTG
Ad2.1_TAAGGCGA	CAAGCAGAAGACGGCATAACGAGATTCGCCTTAGTCTCGTGGGCTCGGAGATGT
Ad2.2_CGTA TAG	CAAGCAGAAGACGGCATAACGAGATCTAGTACGGTCTCGTGGGCTCGGAGATGT
Ad2.3_AGGCAGAA	CAAGCAGAAGACGGCATAACGAGATTTCTGCCTGTCTCGTGGGCTCGGAGATGT
Ad2.4_TCCTGAGC	CAAGCAGAAGACGGCATAACGAGATGCTCAGGAGTCTCGTGGGCTCGGAGATGT
Ad2.5_GGACTCCT	CAAGCAGAAGACGGCATAACGAGATAGGAGTCCGTCTCGTGGGCTCGGAGATGT
Ad2.6_TAGGCATG	CAAGCAGAAGACGGCATAACGAGATCATGCCTAGTCTCGTGGGCTCGGAGATGT
Ad2.7_CTCTCTAC	CAAGCAGAAGACGGCATAACGAGATGTAGAGAGGTCTCGTGGGCTCGGAGATGT

Name	5'-3' sequence
Ad2.8_CAGAGAGG	CAAGCAGAAGACGGCATAACGAGATCCTCTCTGGTCTCGTGGGCTCGGAGATGT
Ad2.9_GCTACGCT	CAAGCAGAAGACGGCATAACGAGATAGCGTAGCGTCTCGTGGGCTCGGAGATGT
Ad2.10_CGAGGCTG	CAAGCAGAAGACGGCATAACGAGATCAGCCTCGGTCTCGTGGGCTCGGAGATGT
Ad2.11_AAGAGGCA	CAAGCAGAAGACGGCATAACGAGATTGCCTCTTGTCTCGTGGGCTCGGAGATGT
Ad2.12_GTAGAGGA	CAAGCAGAAGACGGCATAACGAGATTCTCTACGTCTCGTGGGCTCGGAGATGT
Ad2.13_GTCGTGAT	CAAGCAGAAGACGGCATAACGAGATATCACGACGTCTCGTGGGCTCGGAGATGT
Ad2.14_ACCACTGT	CAAGCAGAAGACGGCATAACGAGATACAGTGGTGTCTCGTGGGCTCGGAGATGT
Ad2.15_TGGATCTG	CAAGCAGAAGACGGCATAACGAGATCAGATCCAGTCTCGTGGGCTCGGAGATGT
Ad2.16_CCGTTTGT	CAAGCAGAAGACGGCATAACGAGATACAAACGGGTCTCGTGGGCTCGGAGATGT
Ad2.17_TGCTGGGT	CAAGCAGAAGACGGCATAACGAGATACCCAGCAGTCTCGTGGGCTCGGAGATGT
Ad2.18_GAGGGGTT	CAAGCAGAAGACGGCATAACGAGATAACCCCTCGTCTCGTGGGCTCGGAGATGT
Ad2.19_AGGTTGGG	CAAGCAGAAGACGGCATAACGAGATCCCAACCTGTCTCGTGGGCTCGGAGATGT
Ad2.20_GTGTGGTG	CAAGCAGAAGACGGCATAACGAGATCACCACACGTCTCGTGGGCTCGGAGATGT
Ad2.21_TGGGTTTC	CAAGCAGAAGACGGCATAACGAGATGAAACCCAGTCTCGTGGGCTCGGAGATGT
Ad2.22_TGGTCACA	CAAGCAGAAGACGGCATAACGAGATTGTGACCAGTCTCGTGGGCTCGGAGATGT
Ad2.23_TTGACCCT	CAAGCAGAAGACGGCATAACGAGATAGGGTCAAGTCTCGTGGGCTCGGAGATGT
Ad2.24_CCACTCCT	CAAGCAGAAGACGGCATAACGAGATAGGAGTGGGTCTCGTGGGCTCGGAGATGT

Abbreviations

Abbreviation	Definition
IGBMC	Institut de génétique et de biologie moléculaire et cellulaire
polyA	poly-adenylated
2x	2 times
3x	3 times
AARE	amino acid response element
ac	acetylated
acetyl-CoA	Acetyl-coenzyme A
ADLOB	aldolase B
ALL	lymphatic leukemia cells (ALL)
ATAC-Seq	assay for transposable-accessible chromatin with high throughput sequencing
ATF4	Activating transcription factor 4
BET	Bromodomain and Extra-Terminal motif
bp	base pair
BSA	Bovine albumin serum
CBP/p300	co-activators- CREB-binding protein/ EP300
CEBPG	gene responsible for CCAAT Enhancer Binding Protein Gamma
ChIP	Chromatin Immunoprecipitation
ChIP-Seq	Chromatin Immunoprecipitation sequencing
ChREBP	Carbohydrate-responsive element-binding protein
CpG	Cytosene (phosphodiesterbond) guanine
CREBH	(cAMP)-responsive element-binding protein H
CRTC2	CREB Regulated Transcription Coactivator 2
CTD	C-terminal domain
CTD	C-terminal domain
dATF2	Drosophila Activating transcription factor 2
DMEM	Dulbecco's Modified Eagle's Medium
DNA	Deoxyribonucleic acid
DNMT	DNA methyltransferase enzyme
eIF2a	eukaryotic initiation factor 2 alpha

Abbreviation	Definition
ER	endoplasmic reticulum
EZH2	Enhancer Of Zeste 2
F1,6P	fructose 1,6-biphosphate
F6P	fructose-6-phosphate
FACs	fluorescence activated cell sorting
FBP1	fructose 1,6 bisphosphatase
FBS	Fetal Bovine Serum
FLC	Flowering Locus C
FOXO1	Forkhead box protein O1
G6P	glucose-6-phosphate
G6PC	glucose-6-phosphatase
Gpt2	glutamic pyruvate transaminase2
H1	histone 1
H2A	histone 2A
H2B	histone 2B
H3	histone 3
H3.3	histone variant 3.3
H4	histone 4
hr	hour
IFN- γ	interferon- γ
IGV	Integrative Genomics Viewer
IP	immunoprecipitation
iPS	on induced pluripotent stem
ISRIB	integrated stress response inhibitor
K	lysine
Kb	kilo bases
KHK	fructokinase
LC-MS	liquid chromatography mass spectrometry
Log ₂ (FC)	the Log ₂ fold change
LPS	lipopolysaccharide
LSD1	Lysine-specific histone demethylase 1
me	methylated
min	minute

Abbreviation	Definition
mM	millimolar
N/A	non-affected
NaBu	sodium butyrate
NaPyr	sodium pyruvate
NEAA	non-essential amino acids
NRO-RNA	nuclear run on -RNA
NT	nuclear transfer
OAA	oxaloacetate
°C	degrees Celsius
p	phosphorylated
P-TEFb	positive transcription elongation factor b
PBS	Phosphate-buffered saline
PBST	PBS-Tween20
PC	pyruvate carboxylase
PCA	principle component analysis
PCR	polymerase chain reaction
PcG	Polycomb-group proteins
PCK1	gene for cytosolic phosphoenolpyruvate carboxylase
PCK2	gene for mitochondrial phosphoenolpyruvate carboxylase
Pcx	gene responsible for pyruvate carboxylase
pen/strep	penicillin / streptomycin
PEP	phosphoenolpyruvate
PEPCK	phosphoenolpyruvate carboxylase
PEPCK-C	cytosolic phosphoenolpyruvate carboxylase
PEPCK-M	mitochondrial phosphoenolpyruvate carboxylase
PERK	protein kinase R (PKR)-like endoplasmic reticulum kinase
PFA	Paraformaldehyde
PIC	pre-initiation complex
Pklr	gene responsible for pyruvate kinase
PRC1	Polycomb repressive complex 1
PRC2	Polycomb repressive complex 2
PTM	posttranslational modification
qPCR	quantitative polymerase chain reaction

Abbreviation	Definition
R	arginine
RNA	Ribonucleic acid
RNA Pol II	enzyme RNA polymerase II
RNA-Seq	RNA sequencing
rpm	Revolutions per minute
RT	room temperature
S	serine
siRNA	small interfering RNA
SREBP	Sterol regulatory element-binding protein
TBS	Tris-buffered saline
TCA cycle	tricarboxylic acid cycle
TF	Transcription Factor
TFIIH	Transcription factor II Human
THAP	thapsigargin
tRNA	transfer ribonucleic acid
trxG	trithorax
TSS	transcription start site
TUN	tunicamycin
ug	microgram
ul	microliter
uM	micromolar
UPR	unfolded protein response
x g	relative centrifugal force (RCF)

Bibliography

- Allis, C. D., and T. Jenuwein. 2016. 'The molecular hallmarks of epigenetic control', *Nat Rev Genet*, 17: 487-500.
- Allis, C. David, Marie-Laure Caparros, Thomas Jenuwein, and Danny Reinberg. 2015. *Epigenetics* (CSH Press, Cold Spring Harbor Laboratory Press: Cold Spring Harbor, New York).
- Amente, S., L. Lania, and B. Majello. 2013. 'The histone LSD1 demethylase in stemness and cancer transcription programs', *Biochim Biophys Acta*, 1829: 981-6.
- Baird, T. D., and R. C. Wek. 2012. 'Eukaryotic initiation factor 2 phosphorylation and translational control in metabolism', *Adv Nutr*, 3: 307-21.
- Balasubramanian, M. N., J. Shan, and M. S. Kilberg. 2013. 'Dynamic changes in genomic histone association and modification during activation of the ASNS and ATF3 genes by amino acid limitation', *Biochem J*, 449: 219-29.
- Balsa-Martinez, E., and P. Puigserver. 2015. 'Cancer Cells Hijack Gluconeogenic Enzymes to Fuel Cell Growth', *Mol Cell*, 60: 509-11.
- Bantignies, F., and G. Cavalli. 2006. 'Cellular memory and dynamic regulation of polycomb group proteins', *Curr Opin Cell Biol*, 18: 275-83.
- Barnes, C. E., D. M. English, and S. M. Cowley. 2019. 'Acetylation & Co: an expanding repertoire of histone acylations regulates chromatin and transcription', *Essays Biochem*, 63: 97-107.
- Bastow, R., J. S. Mylne, C. Lister, Z. Lippman, R. A. Martienssen, and C. Dean. 2004. 'Vernalization requires epigenetic silencing of FLC by histone methylation', *Nature*, 427: 164-7.
- Berger, S. L. 2002. 'Histone modifications in transcriptional regulation', *Curr Opin Genet Dev*, 12: 142-8.
- Bird, A. 2002. 'DNA methylation patterns and epigenetic memory', *Genes Dev*, 16: 6-21.

- Brickner, J. H. 2009. 'Transcriptional memory at the nuclear periphery', *Curr Opin Cell Biol*, 21: 127-33.
- Buenrostro, J. D., P. G. Giresi, L. C. Zaba, H. Y. Chang, and W. J. Greenleaf. 2013. 'Transposition of native chromatin for fast and sensitive epigenomic profiling of open chromatin, DNA-binding proteins and nucleosome position', *Nat Methods*, 10: 1213-8.
- Buenrostro, J. D., B. Wu, H. Y. Chang, and W. J. Greenleaf. 2015. 'ATAC-seq: A Method for Assaying Chromatin Accessibility Genome-Wide', *Curr Protoc Mol Biol*, 109: 21 29 1-9.
- Campos, E. I., J. M. Stafford, and D. Reinberg. 2014. 'Epigenetic inheritance: histone bookmarks across generations', *Trends Cell Biol*, 24: 664-74.
- Carone, B. R., L. Fauquier, N. Habib, J. M. Shea, C. E. Hart, R. Li, C. Bock, C. Li, H. Gu, P. D. Zamore, A. Meissner, Z. Weng, H. A. Hofmann, N. Friedman, and O. J. Rando. 2010. 'Paternal induced transgenerational environmental reprogramming of metabolic gene expression in mammals', *Cell*, 143: 1084-96.
- Catarino, R. R., and A. Stark. 2018. 'Assessing sufficiency and necessity of enhancer activities for gene expression and the mechanisms of transcription activation', *Genes Dev*, 32: 202-23.
- Chen, E. Y., C. M. Tan, Y. Kou, Q. Duan, Z. Wang, G. V. Meirelles, N. R. Clark, and A. Ma'ayan. 2013. 'Enrichr: interactive and collaborative HTML5 gene list enrichment analysis tool', *BMC Bioinformatics*, 14: 128.
- Choi, B. H., and J. L. Coloff. 2019. 'The Diverse Functions of Non-Essential Amino Acids in Cancer', *Cancers (Basel)*, 11.
- Christ, B., A. Nath, H. Bastian, and K. Jungermann. 1988. 'Regulation of the expression of the phosphoenolpyruvate carboxykinase gene in cultured rat hepatocytes by glucagon and insulin', *Eur J Biochem*, 178: 373-9.

- Comerford, S. A., Z. Huang, X. Du, Y. Wang, L. Cai, A. K. Witkiewicz, H. Walters, M. N. Tantawy, A. Fu, H. C. Manning, J. D. Horton, R. E. Hammer, S. L. McKnight, and B. P. Tu. 2014. 'Acetate dependence of tumors', *Cell*, 159: 1591-602.
- Corazzari, M., M. Gagliardi, G. M. Fimia, and M. Piacentini. 2017. 'Endoplasmic Reticulum Stress, Unfolded Protein Response, and Cancer Cell Fate', *Front Oncol*, 7: 78.
- D'Urso, A., and J. H. Brickner. 2014. 'Mechanisms of epigenetic memory', *Trends Genet*, 30: 230-6.
- . 2017. 'Epigenetic transcriptional memory', *Curr Genet*, 63: 435-39.
- Daxinger, L., and E. Whitelaw. 2012. 'Understanding transgenerational epigenetic inheritance via the gametes in mammals', *Nat Rev Genet*, 13: 153-62.
- DeNicola, G. M., and L. C. Cantley. 2015. 'Cancer's Fuel Choice: New Flavors for a Picky Eater', *Mol Cell*, 60: 514-23.
- Ding, Y., M. Fromm, and Z. Avramova. 2012. 'Multiple exposures to drought 'train' transcriptional responses in Arabidopsis', *Nat Commun*, 3: 740.
- Elferink, C. J., and J. J. Reiners, Jr. 1996. 'Quantitative RT-PCR on CYP1A1 heterogeneous nuclear RNA: a surrogate for the in vitro transcription run-on assay', *Biotechniques*, 20: 470-7.
- "FastQC." In. 2010. edited by S. Andrews.
<http://www.bioinformatics.babraham.ac.uk/projects/fastqc/>.
- Foster, S. L., D. C. Hargreaves, and R. Medzhitov. 2007. 'Gene-specific control of inflammation by TLR-induced chromatin modifications', *Nature*, 447: 972-8.
- Francis, N. J., and R. E. Kingston. 2001. 'Mechanisms of transcriptional memory', *Nat Rev Mol Cell Biol*, 2: 409-21.
- Gerstein, M. B., A. Kundaje, M. Hariharan, S. G. Landt, K. K. Yan, C. Cheng, X. J. Mu, E. Khurana, J. Rozowsky, R. Alexander, R. Min, P. Alves, A. Abyzov, N. Addleman,

- N. Bhardwaj, A. P. Boyle, P. Cayting, A. Charos, D. Z. Chen, Y. Cheng, D. Clarke, C. Eastman, G. Euskirchen, S. Fietze, Y. Fu, J. Gertz, F. Grubert, A. Harmanci, P. Jain, M. Kasowski, P. Lacroute, J. J. Leng, J. Lian, H. Monahan, H. O'Geen, Z. Ouyang, E. C. Partridge, D. Patacsil, F. Pauli, D. Raha, L. Ramirez, T. E. Reddy, B. Reed, M. Shi, T. Slifer, J. Wang, L. Wu, X. Yang, K. Y. Yip, G. Zilberman-Schapira, S. Batzoglou, A. Sidow, P. J. Farnham, R. M. Myers, S. M. Weissman, and M. Snyder. 2012. 'Architecture of the human regulatory network derived from ENCODE data', *Nature*, 489: 91-100.
- Grant, C. E., T. L. Bailey, and W. S. Noble. 2011. 'FIMO: scanning for occurrences of a given motif', *Bioinformatics*, 27: 1017-8.
- Grasmann, G., E. Smolle, H. Olschewski, and K. Leithner. 2019. 'Gluconeogenesis in cancer cells - Repurposing of a starvation-induced metabolic pathway?', *Biochim Biophys Acta Rev Cancer*, 1872: 24-36.
- Hahn, S. 2004. 'Structure and mechanism of the RNA polymerase II transcription machinery', *Nat Struct Mol Biol*, 11: 394-403.
- Heinz, S., C. Benner, N. Spann, E. Bertolino, Y. C. Lin, P. Laslo, J. X. Cheng, C. Murre, H. Singh, and C. K. Glass. 2010. 'Simple combinations of lineage-determining transcription factors prime cis-regulatory elements required for macrophage and B cell identities', *Mol Cell*, 38: 576-89.
- Hetz, C., F. Martinon, D. Rodriguez, and L. H. Glimcher. 2011. 'The unfolded protein response: integrating stress signals through the stress sensor IRE1alpha', *Physiol Rev*, 91: 1219-43.
- Holoch, D., and D. Moazed. 2015. 'RNA-mediated epigenetic regulation of gene expression', *Nat Rev Genet*, 16: 71-84.
- Huggins, C. J., M. K. Mayekar, N. Martin, K. L. Saylor, M. Gonit, P. Jailwala, M. Kasoji, D. C. Haines, O. A. Quinones, and P. F. Johnson. 2015. 'C/EBPgamma Is a Critical

- Regulator of Cellular Stress Response Networks through Heterodimerization with ATF4', *Mol Cell Biol*, 36: 693-713.
- Iberg-Badeaux, A., S. Collombet, B. Laurent, C. van Oevelen, K. K. Chin, D. Thieffry, T. Graf, and Y. Shi. 2017. 'A Transcription Factor Pulse Can Prime Chromatin for Heritable Transcriptional Memory', *Mol Cell Biol*, 37.
- Jenuwein, T., and C. D. Allis. 2001. 'Translating the histone code', *Science*, 293: 1074-80.
- Jiang, J., S. Srivastava, G. Seim, N. N. Pavlova, B. King, L. Zou, C. Zhang, M. Zhong, H. Feng, R. Kapur, R. C. Wek, J. Fan, and J. Zhang. 2019. 'Promoter demethylation of the asparagine synthetase gene is required for ATF4-dependent adaptation to asparagine depletion', *J Biol Chem*, 294: 18674-84.
- Kamada, R., W. Yang, Y. Zhang, M. C. Patel, Y. Yang, R. Ouda, A. Dey, Y. Wakabayashi, K. Sakaguchi, T. Fujita, T. Tamura, J. Zhu, and K. Ozato. 2018. 'Interferon stimulation creates chromatin marks and establishes transcriptional memory', *Proc Natl Acad Sci U S A*, 115: E9162-E71.
- Khan, A., O. Fornes, A. Stigliani, M. Gheorghe, J. A. Castro-Mondragon, R. van der Lee, A. Bessy, J. Cheneby, S. R. Kulkarni, G. Tan, D. Baranasic, D. J. Arenillas, A. Sandelin, K. Vandepoele, B. Lenhard, B. Ballester, W. W. Wasserman, F. Parcy, and A. Mathelier. 2018. 'JASPAR 2018: update of the open-access database of transcription factor binding profiles and its web framework', *Nucleic Acids Res*, 46: D1284.
- Kim, M., and J. Costello. 2017. 'DNA methylation: an epigenetic mark of cellular memory', *Exp Mol Med*, 49: e322.
- Kinnaird, A., S. Zhao, K. E. Wellen, and E. D. Michelakis. 2016. 'Metabolic control of epigenetics in cancer', *Nat Rev Cancer*, 16: 694-707.
- Kouzarides, T. 2007. 'Chromatin modifications and their function', *Cell*, 128: 693-705.

- Kundu, S., and C. L. Peterson. 2009. 'Role of chromatin states in transcriptional memory', *Biochim Biophys Acta*, 1790: 445-55.
- Lambert, S. A., A. Jolma, L. F. Campitelli, P. K. Das, Y. Yin, M. Albu, X. Chen, J. Taipale, T. R. Hughes, and M. T. Weirauch. 2018. 'The Human Transcription Factors', *Cell*, 172: 650-65.
- Lamke, J., and I. Baurle. 2017. 'Epigenetic and chromatin-based mechanisms in environmental stress adaptation and stress memory in plants', *Genome Biol*, 18: 124.
- Langmead, B., C. Trapnell, M. Pop, and S. L. Salzberg. 2009. 'Ultrafast and memory-efficient alignment of short DNA sequences to the human genome', *Genome Biol*, 10: R25.
- Lawrence, M., S. Daujat, and R. Schneider. 2016. 'Lateral Thinking: How Histone Modifications Regulate Gene Expression', *Trends Genet*, 32: 42-56.
- Leithner, K., A. Hrzenjak, M. Trotsmuller, T. Moustafa, H. C. Kofeler, C. Wohlkoenig, E. Stacher, J. Lindenmann, A. L. Harris, A. Olschewski, and H. Olschewski. 2015. 'PCK2 activation mediates an adaptive response to glucose depletion in lung cancer', *Oncogene*, 34: 1044-50.
- Li, B., M. Carey, and J. L. Workman. 2007. 'The role of chromatin during transcription', *Cell*, 128: 707-19.
- Longo, V. D., and S. Panda. 2016. 'Fasting, Circadian Rhythms, and Time-Restricted Feeding in Healthy Lifespan', *Cell Metab*, 23: 1048-59.
- Lu, P. D., H. P. Harding, and D. Ron. 2004. 'Translation reinitiation at alternative open reading frames regulates gene expression in an integrated stress response', *J Cell Biol*, 167: 27-33.
- Mayers, J. R., and M. G. Vander Heiden. 2015. 'Famine versus feast: understanding the metabolism of tumors in vivo', *Trends Biochem Sci*, 40: 130-40.

- Medzhitov, R. 2007. 'TLR-mediated innate immune recognition', *Semin Immunol*, 19: 1-2.
- Mendez-Lucas, A., J. A. Duarte, N. E. Sunny, S. Satapati, T. He, X. Fu, J. Bermudez, S. C. Burgess, and J. C. Perales. 2013. 'PEPCK-M expression in mouse liver potentiates, not replaces, PEPCK-C mediated gluconeogenesis', *J Hepatol*, 59: 105-13.
- Mendez-Lucas, A., P. Hyrossova, L. Novellademunt, F. Vinals, and J. C. Perales. 2014. 'Mitochondrial phosphoenolpyruvate carboxykinase (PEPCK-M) is a pro-survival, endoplasmic reticulum (ER) stress response gene involved in tumor cell adaptation to nutrient availability', *J Biol Chem*, 289: 22090-102.
- Montal, E. D., R. Dewi, K. Bhalla, L. Ou, B. J. Hwang, A. E. Ropell, C. Gordon, W. J. Liu, R. J. DeBerardinis, J. Sudderth, W. Twaddel, L. G. Boros, K. R. Shroyer, S. Duraisamy, R. Drapkin, R. S. Powers, J. M. Rohde, M. B. Boxer, K. K. Wong, and G. D. Girnun. 2015. 'PEPCK Coordinates the Regulation of Central Carbon Metabolism to Promote Cancer Cell Growth', *Mol Cell*, 60: 571-83.
- Nakabayashi, H., K. Taketa, K. Miyano, T. Yamane, and J. Sato. 1982. 'Growth of human hepatoma cells lines with differentiated functions in chemically defined medium', *Cancer Res*, 42: 3858-63.
- Natoli, G., and R. Ostuni. 2019. 'Adaptation and memory in immune responses', *Nat Immunol*, 20: 783-92.
- Ng, R. K., and J. B. Gurdon. 2008. 'Epigenetic memory of an active gene state depends on histone H3.3 incorporation into chromatin in the absence of transcription', *Nat Cell Biol*, 10: 102-9.
- Oh, K. J., H. S. Han, M. J. Kim, and S. H. Koo. 2013. 'Transcriptional regulators of hepatic gluconeogenesis', *Arch Pharm Res*, 36: 189-200.
- Ohm, J. E., K. M. McGarvey, X. Yu, L. Cheng, K. E. Schuebel, L. Cope, H. P. Mohammad, W. Chen, V. C. Daniel, W. Yu, D. M. Berman, T. Jenuwein, K. Pruitt, S. J. Sharkis, D. N. Watkins, J. G. Herman, and S. B. Baylin. 2007. 'A stem cell-

- like chromatin pattern may predispose tumor suppressor genes to DNA hypermethylation and heritable silencing', *Nat Genet*, 39: 237-42.
- Ostuni, R., V. Piccolo, I. Barozzi, S. Polletti, A. Termanini, S. Bonifacio, A. Curina, E. Prosperini, S. Ghisletti, and G. Natoli. 2013. 'Latent enhancers activated by stimulation in differentiated cells', *Cell*, 152: 157-71.
- Palozola, K. C., J. Lerner, and K. S. Zaret. 2019. 'A changing paradigm of transcriptional memory propagation through mitosis', *Nat Rev Mol Cell Biol*, 20: 55-64.
- Patti, G. J., O. Yanes, and G. Siuzdak. 2012. 'Innovation: Metabolomics: the apogee of the omics trilogy', *Nat Rev Mol Cell Biol*, 13: 263-9.
- Pederson, T. 2016. 'Fueling Cancer: Glucose, Again', *FASEB J*, 30: 1377-9.
- Pietrocola, F., L. Galluzzi, J. M. Bravo-San Pedro, F. Madeo, and G. Kroemer. 2015. 'Acetyl coenzyme A: a central metabolite and second messenger', *Cell Metab*, 21: 805-21.
- Prinjha, R. K., J. Witherington, and K. Lee. 2012. 'Place your BETs: the therapeutic potential of bromodomains', *Trends Pharmacol Sci*, 33: 146-53.
- Puschendorf, M., R. Terranova, E. Boutsma, X. Mao, K. Isono, U. Brykczynska, C. Kolb, A. P. Otte, H. Koseki, S. H. Orkin, M. van Lohuizen, and A. H. Peters. 2008. 'PRC1 and Suv39h specify parental asymmetry at constitutive heterochromatin in early mouse embryos', *Nat Genet*, 40: 411-20.
- Quiros, P. M., M. A. Prado, N. Zamboni, D. D'Amico, R. W. Williams, D. Finley, S. P. Gygi, and J. Auwerx. 2017. 'Multi-omics analysis identifies ATF4 as a key regulator of the mitochondrial stress response in mammals', *J Cell Biol*, 216: 2027-45.
- Rajendran, V., P. Kalita, H. Shukla, A. Kumar, and T. Tripathi. 2018. 'Aminoacyl-tRNA synthetases: Structure, function, and drug discovery', *Int J Biol Macromol*, 111: 400-14.

- Ramisch, A., V. Heinrich, L. V. Glaser, A. Fuchs, X. Yang, P. Benner, R. Schopflin, N. Li, S. Kinkley, A. Romer-Hillmann, J. Longinotto, S. Heyne, B. Czepukojc, S. M. Kessler, A. K. Kiemer, C. Cadenas, L. Arrigoni, N. Gasparoni, T. Manke, T. Pap, J. A. Pospisilik, J. Hengstler, J. Walter, S. H. Meijssing, H. R. Chung, and M. Vingron. 2019. 'CRUP: a comprehensive framework to predict condition-specific regulatory units', *Genome Biol*, 20: 227.
- Rechavi, O., L. Hourri-Ze'evi, S. Anava, W. S. S. Goh, S. Y. Kerk, G. J. Hannon, and O. Hobert. 2014. 'Starvation-induced transgenerational inheritance of small RNAs in *C. elegans*', *Cell*, 158: 277-87.
- Reddy, M. A., E. Zhang, and R. Natarajan. 2015. 'Epigenetic mechanisms in diabetic complications and metabolic memory', *Diabetologia*, 58: 443-55.
- Ritchie, M. E., B. Phipson, D. Wu, Y. Hu, C. W. Law, W. Shi, and G. K. Smyth. 2015. 'limma powers differential expression analyses for RNA-sequencing and microarray studies', *Nucleic Acids Res*, 43: e47.
- Roberts, T. C., J. R. Hart, M. U. Kaikkonen, M. S. Weinberg, P. K. Vogt, and K. V. Morris. 2015. 'Quantification of nascent transcription by bromouridine immunocapture nuclear run-on RT-qPCR', *Nat Protoc*, 10: 1198-211.
- Robinson, J. T., H. Thorvaldsdottir, W. Winckler, M. Guttman, E. S. Lander, G. Getz, and J. P. Mesirov. 2011. 'Integrative genomics viewer', *Nat Biotechnol*, 29: 24-6.
- Robinson, M. D., D. J. McCarthy, and G. K. Smyth. 2010. 'edgeR: a Bioconductor package for differential expression analysis of digital gene expression data', *Bioinformatics*, 26: 139-40.
- Robinson, M. D., and A. Oshlack. 2010. 'A scaling normalization method for differential expression analysis of RNA-seq data', *Genome Biol*, 11: R25.
- Roeder, R. G. 1996. 'The role of general initiation factors in transcription by RNA polymerase II', *Trends Biochem Sci*, 21: 327-35.

- Ronningen, T., A. Shah, A. H. Reiner, P. Collas, and J. O. Moskaug. 2015. 'Epigenetic priming of inflammatory response genes by high glucose in adipose progenitor cells', *Biochem Biophys Res Commun*, 467: 979-86.
- Rui, L. 2014. 'Energy metabolism in the liver', *Compr Physiol*, 4: 177-97.
- Santos, A., R. Wernersson, and L. J. Jensen. 2015. 'Cyclebase 3.0: a multi-organism database on cell-cycle regulation and phenotypes', *Nucleic Acids Res*, 43: D1140-4.
- Savvidis, C., and M. Koutsilieris. 2012. 'Circadian rhythm disruption in cancer biology', *Mol Med*, 18: 1249-60.
- Schuettengruber, B., M. Ganapathi, B. Leblanc, M. Portoso, R. Jaschek, B. Tolhuis, M. van Lohuizen, A. Tanay, and G. Cavalli. 2009. 'Functional anatomy of polycomb and trithorax chromatin landscapes in *Drosophila* embryos', *PLoS Biol*, 7: e13.
- Schug, Z. T., B. Peck, D. T. Jones, Q. Zhang, S. Grosskurth, I. S. Alam, L. M. Goodwin, E. Smethurst, S. Mason, K. Blyth, L. McGarry, D. James, E. Shanks, G. Kalna, R. E. Saunders, M. Jiang, M. Howell, F. Lassailly, M. Z. Thin, B. Spencer-Dene, G. Stamp, N. J. van den Broek, G. Mackay, V. Bulusu, J. J. Kamphorst, S. Tardito, D. Strachan, A. L. Harris, E. O. Aboagye, S. E. Critchlow, M. J. Wakelam, A. Schulze, and E. Gottlieb. 2015. 'Acetyl-CoA synthetase 2 promotes acetate utilization and maintains cancer cell growth under metabolic stress', *Cancer Cell*, 27: 57-71.
- Seok, S., T. Fu, S. E. Choi, Y. Li, R. Zhu, S. Kumar, X. Sun, G. Yoon, Y. Kang, W. Zhong, J. Ma, B. Kemper, and J. K. Kemper. 2014. 'Transcriptional regulation of autophagy by an FXR-CREB axis', *Nature*, 516: 108-11.
- Seong, K. H., D. Li, H. Shimizu, R. Nakamura, and S. Ishii. 2011. 'Inheritance of stress-induced, ATF-2-dependent epigenetic change', *Cell*, 145: 1049-61.
- Shan, J., F. Zhang, J. Sharkey, T. A. Tang, T. Ord, and M. S. Kilberg. 2016. 'The *C/ebp*-*Atf* response element (CARE) location reveals two distinct *Atf4*-dependent,

- elongation-mediated mechanisms for transcriptional induction of aminoacyl-tRNA synthetase genes in response to amino acid limitation', *Nucleic Acids Res*, 44: 9719-32.
- Sharabi, K., C. D. J. Tavares, and P. Puigserver. 2019. 'Regulation of Hepatic Metabolism, Recent Advances, and Future Perspectives', *Curr Diab Rep*, 19: 98.
- Shen, X., Y. Liu, Y. J. Hsu, Y. Fujiwara, J. Kim, X. Mao, G. C. Yuan, and S. H. Orkin. 2008. 'EZH1 mediates methylation on histone H3 lysine 27 and complements EZH2 in maintaining stem cell identity and executing pluripotency', *Mol Cell*, 32: 491-502.
- Shlyueva, D., G. Stampfel, and A. Stark. 2014. 'Transcriptional enhancers: from properties to genome-wide predictions', *Nat Rev Genet*, 15: 272-86.
- Sidrauski, C., D. Acosta-Alvear, A. Khoutorsky, P. Vedantham, B. R. Hearn, H. Li, K. Gamache, C. M. Gallagher, K. K. Ang, C. Wilson, V. Okreglak, A. Ashkenazi, B. Hann, K. Nader, M. R. Arkin, A. R. Renslo, N. Sonenberg, and P. Walter. 2013. 'Pharmacological brake-release of mRNA translation enhances cognitive memory', *Elife*, 2: e00498.
- Sidrauski, C., A. M. McGeachy, N. T. Ingolia, and P. Walter. 2015. 'The small molecule ISRIB reverses the effects of eIF2alpha phosphorylation on translation and stress granule assembly', *Elife*, 4.
- Sims, R. J., 3rd, R. Belotserkovskaya, and D. Reinberg. 2004. 'Elongation by RNA polymerase II: the short and long of it', *Genes Dev*, 18: 2437-68.
- Stark, R., and R. G. Kibbey. 2014. 'The mitochondrial isoform of phosphoenolpyruvate carboxykinase (PEPCK-M) and glucose homeostasis: has it been overlooked?', *Biochim Biophys Acta*, 1840: 1313-30.
- Stern, S., Y. Fridmann-Sirkis, E. Braun, and Y. Soen. 2012. 'Epigenetically heritable alteration of fly development in response to toxic challenge', *Cell Rep*, 1: 528-42.

- Stockwell, S. R., C. R. Landry, and S. A. Rifkin. 2015. 'The yeast galactose network as a quantitative model for cellular memory', *Mol Biosyst*, 11: 28-37.
- Tan, J. Z., Y. Yan, X. X. Wang, Y. Jiang, and H. E. Xu. 2014. 'EZH2: biology, disease, and structure-based drug discovery', *Acta Pharmacol Sin*, 35: 161-74.
- Tian, Y., G. Garcia, Q. Bian, K. K. Steffen, L. Joe, S. Wolff, B. J. Meyer, and A. Dillin. 2016. 'Mitochondrial Stress Induces Chromatin Reorganization to Promote Longevity and UPR(mt)', *Cell*, 165: 1197-208.
- Turner, B. M. 2002. 'Cellular memory and the histone code', *Cell*, 111: 285-91.
- Venkatesh, S., and J. L. Workman. 2015. 'Histone exchange, chromatin structure and the regulation of transcription', *Nat Rev Mol Cell Biol*, 16: 178-89.
- Vincent, E. E., A. Sergushichev, T. Griss, M. C. Gingras, B. Samborska, T. Ntimbane, P. P. Coelho, J. Blagih, T. C. Raissi, L. Choiniere, G. Bridon, E. Loginicheva, B. R. Flynn, E. C. Thomas, J. M. Tavaré, D. Avizonis, A. Pause, D. J. Elder, M. N. Artyomov, and R. G. Jones. 2015. 'Mitochondrial Phosphoenolpyruvate Carboxykinase Regulates Metabolic Adaptation and Enables Glucose-Independent Tumor Growth', *Mol Cell*, 60: 195-207.
- Waddington, C. H. 1942. 'Canalization of development and the inheritance of acquired characters', *Nature*, 150: 563-65.
- . 2012. 'The epigenotype. 1942', *Int J Epidemiol*, 41: 10-3.
- Wang, M., and R. J. Kaufman. 2014. 'The impact of the endoplasmic reticulum protein-folding environment on cancer development', *Nat Rev Cancer*, 14: 581-97.
- Wortel, I. M. N., L. T. van der Meer, M. S. Kilberg, and F. N. van Leeuwen. 2017. 'Surviving Stress: Modulation of ATF4-Mediated Stress Responses in Normal and Malignant Cells', *Trends Endocrinol Metab*, 28: 794-806.
- Yang, J., S. C. Kalhan, and R. W. Hanson. 2009. 'What is the metabolic role of phosphoenolpyruvate carboxykinase?', *J Biol Chem*, 284: 27025-9.

- Yu, G., L. G. Wang, and Q. Y. He. 2015. 'ChIPseeker: an R/Bioconductor package for ChIP peak annotation, comparison and visualization', *Bioinformatics*, 31: 2382-3.
- Zeigerer, A., J. Gilleron, R. L. Bogorad, G. Marsico, H. Nonaka, S. Seifert, H. Epstein-Barash, S. Kuchimanchi, C. G. Peng, V. M. Ruda, P. Del Conte-Zerial, J. G. Hengstler, Y. Kalaidzidis, V. Koteliensky, and M. Zerial. 2012. 'Rab5 is necessary for the biogenesis of the endolysosomal system in vivo', *Nature*, 485: 465-70.
- Zhang, D., Z. Tang, H. Huang, G. Zhou, C. Cui, Y. Weng, W. Liu, S. Kim, S. Lee, M. Perez-Neut, J. Ding, D. Czyz, R. Hu, Z. Ye, M. He, Y. G. Zheng, H. A. Shuman, L. Dai, B. Ren, R. G. Roeder, L. Becker, and Y. Zhao. 2019. 'Metabolic regulation of gene expression by histone lactylation', *Nature*, 574: 575-80.
- Zhang, F., X. Xu, B. Zhou, Z. He, and Q. Zhai. 2011. 'Gene expression profile change and associated physiological and pathological effects in mouse liver induced by fasting and refeeding', *PLoS One*, 6: e27553.
- Zhang, Y., T. Liu, C. A. Meyer, J. Eeckhoute, D. S. Johnson, B. E. Bernstein, C. Nusbaum, R. M. Myers, M. Brown, W. Li, and X. S. Liu. 2008. 'Model-based analysis of ChIP-Seq (MACS)', *Genome Biol*, 9: R137.
- Zhao, J., J. Li, T. W. M. Fan, and S. X. Hou. 2017. 'Glycolytic reprogramming through PCK2 regulates tumor initiation of prostate cancer cells', *Oncotarget*, 8: 83602-18.

Appendix

Acknowledgements

First, I would like to express my deepest gratitude to my parents, Robert and Mary Ann, for their support along this long and bumpy PhD journey and to my brothers Mike and Steve, along with all my New York, Kentucky, Strasbourg, and Munich friends and family for their help and encouragement.

I would like to thank my PhD supervisor Dr. Robert Schneider for the opportunity to work in his lab, as well as the support, and freedom to pursue my project. I also would like to thanks Dr. Sylvain Daujat, Dr. Hei Sook Sul, Dr. Till Bartke, and Dr. Kurt Schmoller for helpful discussion. I would also like to recognize the members of my thesis committee, Dr. Andrew Pospisilik, Dr. Stefan Stricker, and Dr. Romeo Ricci for insightful discussion and technical help.

I also would like to extend thanks to the past and present members of the Schneider lab, especially soon-to-be-Dr. Lara Zorro Shahidian for keeping it fun in the lab (and all the scientific and thesis preparation help), Dr. Saulius Lukauskas and Roberto Olayo Alarcon for helpful discussions and computational contributions, and Asieh Shahjahanpour for her help with experiments. I would also like to recognize my collaborators Dr. Verena Heinrich and Akshaya Ramakrishnan for help with data analysis.

A special thanks to Dr. Uwe Schaefer for his help and support throughout my scientific journey!